Model Scale Tunnel Fire Tests- Point extraction ventilation

Haukur Ingason, Ying Zhen Li

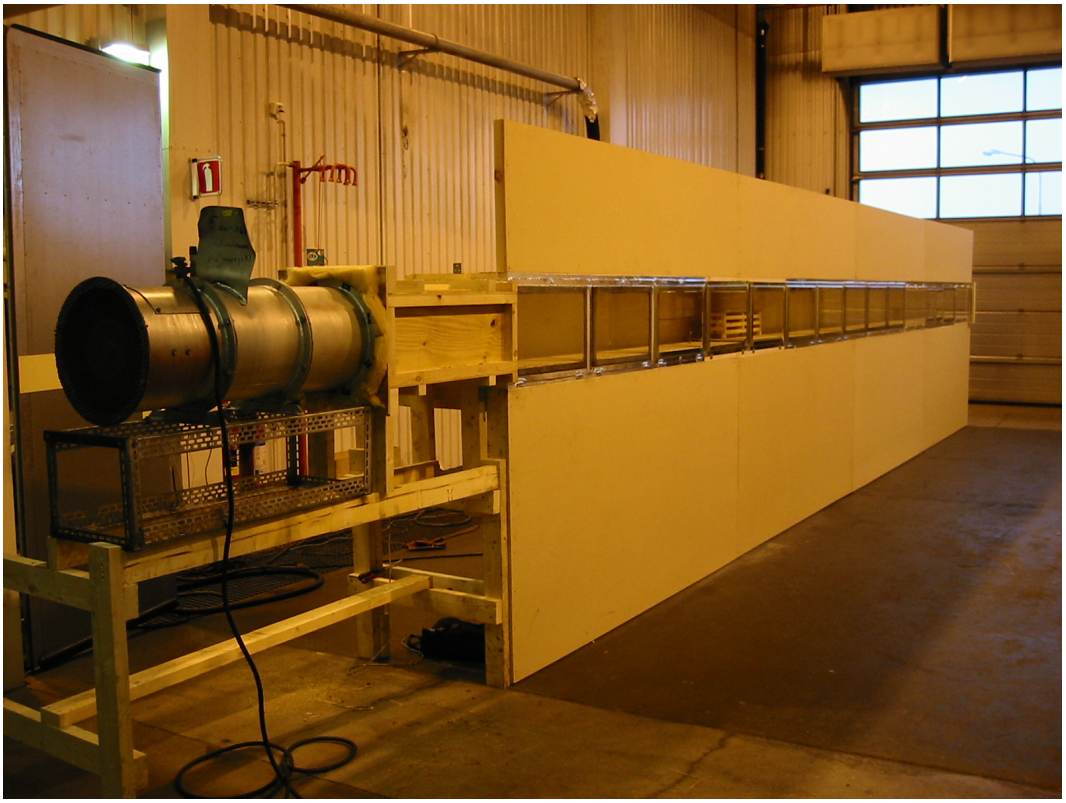

SP Technical Research Institute of Sweden

Fire Technology

SP Report 2010:03

Haukur Ingason, Ying Zhen Li

Abstract

Model Scale Tunnel Fire Tests with Point Extraction Ventilation

Theoretical and experimental results from a series of tests in a model scale tunnel (1:23) with point extraction ventilation systems are presented. The point extraction ventilation system was tested under different fire and flow conditions using either forced longitudinal ventilation or natural ventilation. The study focuses on single and two point extraction systems. Wood crib piles were used to simulate the fire source, which was designed to correspond to a HGV (Heavy Goods Vehicle) fire load in large scale. The parameters tested were the number of wood cribs, the longitudinal ventilation velocity and the arrangement of the extraction vent openings and the exhaust capacity. The fire spread between wood cribs with a free distance corresponding to 15 m in large scale was tested. The maximum heat release rate, fire growth rate, maximum temperature rise beneath the ceiling, flame length and heat flux were plotted using relationships obtained from theoretical considerations. The data were found to correlate well with empirical correlations that were established. Comparison was made with large-scale data wherever possible.

Key words: model scale, tunnel fire, point extraction vent, fire spread, longitudinal ventilation, extraction ventilation

SP Sveriges Provnings- och Forskningsinstitut
SP Rapport 2010:03
ISBN 978-91-86319-38-0
ISSN 0284-5172
Borås 2009

SP Swedish National Testing and Research Institute
SP Report 2010:03

Postal address:
PO Box 857,
SE-501 15 BORÅS, Sweden
Telephone: +46 33 16 50 00
Telex: 36252 Testing S
Telefax: +46 33 13 55 02
E-mail: info@sp.se

Table of Content

	Abstract	**2**
	Table of Content	**3**
	Preface	**4**
1	**Introduction**	**7**
2	**Theoretical considerations**	**10**
2.1	Scaling theory	10
2.2	Determination of heat release rate	10
3	**Experimental Setup**	**13**
3.1	Fire load	14
3.2	Instrumentation	15
4	**Test procedure**	**17**
5	**Test results**	**19**
5.1	Heat release rate	19
5.2	Gas temperatures	19
5.3	Total heat flux	19
5.4	Flame length	21
5.5	Flame spread	21
6	**Discussion of results**	**22**
6.1	Heat release rate	22
6.2	Maximum gas temperature rise below the ceiling	25
6.3	Flame length	26
6.4	Total Heat flux	30
6.5	Fire spread	32
6.6	Single point extraction system	35
6.7	Two point extraction system	42
7	**Conclusions**	**45**
8	**References**	**47**
Appendix A	**Test Results – Extraction ventilation**	**49**

Appendix A – Test Results with extraction ventilation

Preface

This project was sponsored by the Swedish Fire Research Board (BRANDFORSK) and the SP Tunnel and Underground Safety Centre.

The technicians Michael Magnusson, Joel Blom, Lars Gustafsson and Ari Palo-Oja at SP Fire Technology are acknowledged for their valuable assistance during performance of the tests. They were also responsible for the construction of the test rig.

The advisory group to the project is thanked for their contribution. The advisory group consisted of Johan Hedenfalk (SL), Lars Aidanpää (LKAB), Magnus Lindström (Brandkonsulten), Per Walmerdahl (FOI), Staffan Bengtson (Brandskyddslaget), Anders Walling (Brandforsk), Jan Blomqvist (Cerberus), Anders Berqvist (Stockhol Fire Brigade), Ovind Engdahl (Norsk Brannvern), Bernt Freiholtz (Vägverket), Odd Lyng, Gunnar Spång (SL), Christer Lindeman (SL), Jenette Stenman (Banverket), Bo Wahlström (Brandskyddslaget), Katarina Kieksi (Banverket) and Omar Harrami (SRV).

Summary

Fire tests were carried out in a 1:23 model scale tunnel. Fire loads corresponding to a HGV trailer were simulated using wood cribs of two different sizes. Point extraction ventilation systems were tested under different fire and flow conditions. The parameter tested were the number of wood cribs, the longitudinal ventilation velocity, ceiling height and the arrangement of the point extraction openings and the exhaust capacity. The fire spread between wood cribs, with a free distance corresponding to 15 m in large scale, was tested. The heat release rate, the fire growth rate, fire spread, flame length, and gas temperatures beneath tunnel ceiling were also investigated.

Longitudinal ventilation was established using an electrical fan attached to the entrance of the model tunnel. The tunnel was 10 m long, 0.4 m wide and 0.2 m high. The corresponding large-scale dimensions are 230 m long, 9.2 m wide and 4.6 m. The total flow rate through the extraction vents used was 0.06 m^3/s, 0.09 m^3/s and 0.14 m^3/s which corresponds to 152 m^3/s, 228 m^3/s and 355 m^3/s, respectively, in large scale. The number of exhaust openings that were used in the tests with lower ceiling height (0.2 m) varied between 1 and 4. The area of the openings was 0.026 m^2 or 0.052 m^2, which corresponds to 13.75 m^2 and 27.5 m^2, respectively, in large scale.

The model scale trials show that point extraction vents at ceiling level provide very effective control of smoke in the case of a very large fire in a tunnel. These openings should be provided at regular intervals in the tunnel roof. The distance between the extraction openings depends on what size of smoke zone that can be accepted. The extraction vent flows and the inward air flows produced by exhaust fans and jet fans are able to constrain the smoke within the zone between the fire source and the extraction vent of a single extraction system, or between two opened extraction vents. These results suggest that a very large fire, i.e. a HGV fire, can be controlled by appropriate use of point extraction ventilation systems.

The principle of an effective extraction system is that sufficient fresh air flows should be supplied from two sides. This must be done in order to confine the fire and smoke to the zone between the fire source and the vent of a single extraction system, or between two exhaust extraction vents. The fire and smoke flow cannot be confined if the flow rate in the extraction vents is the only parameter to be controlled. The confined longitudinal ventilation velocity on both sides must be controlled as well.

For a single point extraction ventilation system, fire and smoke flows upstream and downstream of the fire source can be fully controlled. Although this can only be the case if the longitudinal ventilation velocity upstream of the fire source is at least 0.6 m/s (2.9 m/s in large scale), and the longitudinal ventilation velocity downstream of the extraction vent is larger than 0.8 m/s (3.8 m/s in large scale). This is valid for a HGV fire or even several HGVs with heat release rates up to about 500 MW. Under these conditions, the mass flow rate through the extraction vent is about 0.134 kg/s, corresponding to 340 kg/s in large scale. This, in turn, corresponds to a volumetric flow rate of 284 m^3/s for fresh air in large scale.

In a two point extraction system, the longitudinal ventilation velocity on each side should be greater than approximately 0.6 m/s (2.9 m/s in large scale) in order to completely confine the fire and smoke flow to the zone between two extraction vents.

The point extraction system will also significantly reduce the risk of the fire spreading outside the fire and smoke zone. This is due to the effective removal of the visible flames and the heat transportation into the extraction vents. However, the fire spread cannot be

prevented in the near field of the fire due to high heat flux levels from the flames. Fire spread to a neighbouring wood crib occurs when the gas temperature beneath the ceiling and above the wood crib rises up to approximately 600 °C. Experimental data suggest that in a real tunnel, a vehicle 15 m behind a (simulated) burning HGV would catch fire in about nine minutes, and a third vehicle 15 m further behind the second vehicle would catch fire after a further delay of only approximately three minutes, mainly due to heat from the first vehicle. These numbers only give an indication of the order of magnitude as the thermal radiation thermal response of the ignited material does not scale very well. The experiments clearly show, however, that the fire spread rate increases as the numbers of wood cribs are increased. The fire spread rate is in quite good agreement with the Runehamar tunnel trials, where 'targets' were placed 15 m from the fire in order to simulate the effects of possible spread of the fire to further vehicles in the tunnel.

The heat release rate, the fire growth rate, the maximum temperature rise beneath the ceiling, the flame length and the heat flux were investigated. A stoichiometric line correlates well with the experimental data of the fuel mass loss rate per unit fuel surface area when the ventilation velocity is less than 0.4 m/s, and fuel mass loss rate per unit fuel surface area is not sensitive to the ventilation velocity for higher ventilation velocity. This means there is an upper limit to when the fire becomes fuel controlled. The fire growth rate is found to increase linearly with the ventilation velocity. The fire growth rate is nearly 3 times larger than that in free burn tests, when the ventilation velocity equals to 1m/s. This corresponds to 4.8 m/s in large scale. The dimensionless maximum temperature rise lies mainly in a range of 2.9 to 3.75, corresponding to the maximum temperature rise of 850 °C to 1100 °C. It seems that the maximum gas temperature beneath the tunnel ceiling is a weak function of the heat release rate and the ventilation velocity for the maximum heat release rates obtained here. The flame length is proven to be a weak function of the ventilation velocity, and experimental data correlate well with a dimensionless heat release rate. The peak total heat flux can be estimated using average temperature well. Finally, another correlation using gas temperature beneath the tunnel ceiling is also presented.

1 Introduction

Interest in fire safety issues in tunnels has increased dramatically owing to numerous catastrophic tunnel fires and the extensive monitoring by media. A common feature in all of these fires has been the influence of the fire load and ventilation on the growth of the fire. In several of the fires, the type of load being carried by heavy goods vehicles played an important part in determining the severity of the fire. The main reasons for this are that the heavy goods vehicles (HGVs) consist of highly flammable organic materials (not specifically hazardous material), and that the fire spreads very rapidly due to the longitudinal ventilation in the tunnel.

Most of our knowledge about smoke and fire spread in tunnels has generally been obtained from large scale testing. Large scale testing is, however, expensive, time consuming and logistically complicated to perform. The information obtained is often incomplete due to the limited number of tests and lack of instrumentation. Large scale testing is, however, necessary to obtain acceptable verification of model scale results or modelling in a realistic scale. Model scale tests can be used as a complement to large scale testing. They can provide information which is difficult to obtain otherwise and lend themselves to parameter studies which large scale tests do not. The tests presented here were performed in November 2002, in part to design the large scale experiments carried out in Runehamar tunnel September 2003 [1-3]. The part of model scale test programme that was carried out with longitudinal ventilation only has been reported by Ingason [4]. The part presented here concerning point extraction ventilation systems combined with longitudinal and natural flows has not been presented previously.

Urban twin-tube road tunnels often become congested with vehicles due to heavy traffic. The most common fire safety design concept today is to install jet fans in the ceiling in order to create longitudinal ventilation. This design concept assumes that the traffic is stopped upstream of a fire and that the tunnel ventilation ensures that upstream of the fire the tunnel is free of smoke. Vehicles downstream of the fire are assumed to continue driving out of the tunnel. The design of such a system assumes that the fire brigade shall be able to attack the fire from the smoke-free upstream side. However, in urban areas, where there are very likely queues in the tunnel this assumption fails. Consequently, people in the cars and buses trapped in traffic queues downstream of the fire source may not be able to escape from the fire and smoke quickly by driving their cars away from the seat of the fire, and the fire brigade may not be able to reach the fire and vehicles downstream of the fire due to congestion, resulting in a large number of people being put in jeopardy.

One way of solving this is to install an extraction system with large extraction points located close to the seat of the fire. Since the fire may develop at any location in the tunnel, extraction points at the ceiling must be provided throughout its length. The extraction ventilation system must then be powerful enough to create longitudinal flows from two directions. In some cases, jet fans in the ceiling or inflow of air at floor level may be needed to balance the longitudinal flow and obtain satisfactory flow conditions. With this type of ventilation system, people stuck in a queue will be much better protected from smoke and the fire brigade will be able to attack the fire from both sides. This design concept is useful for railway tunnel too. In the experiments presented in this report, this type of extraction system has been tested by using different fire loads and by combining it with longitudinal ventilation.

The extraction system can be categorized into single point extraction system, two point extraction system, three points extraction system, etc., by the number of opened extraction vents during a fire. Figure 1 and Figure 2 show the diagrams of a single point

extraction system and a two point extraction system, when the smoke flow was confined in an acceptable zone. The configurations of these systems is different, however, it is clear that the concept is essentially the same that incoming air flows with sufficiently large ventilation velocity should be supplied from both sides of these systems. These extraction systems can be used in a tunnel with a semi-transverse ventilation system or a transverse ventilation system. In a tunnel with transverse ventilation system, supply vents should be closed during a fire because if the supply vents are opened the extraction system must extract a higher gas flow, which obviously decreases the efficiency of the extraction system. Given that the fire and smoke flow will spread further, if more extraction vents with the same interval distance between two extraction vents are used at a given total exhaust flow rate, and it is easier to control the extraction system with fewer extraction vents, the single point extraction system and the two point extraction system are proposed and focused on here.

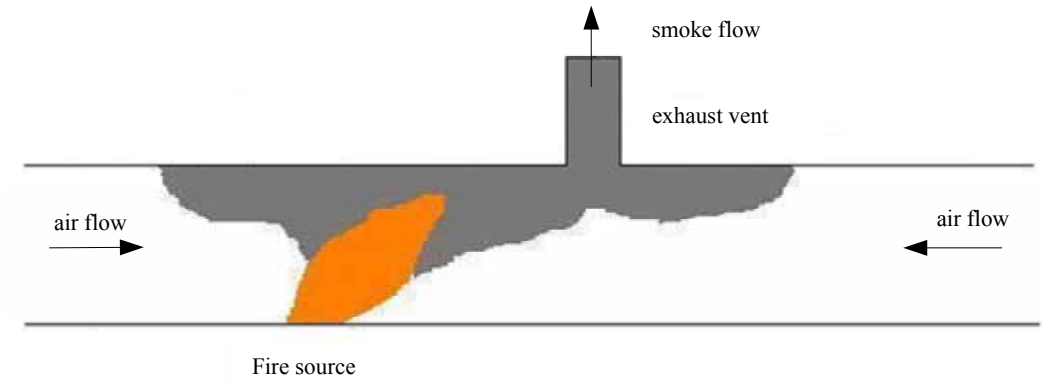

Figure 1 Diagram of single point extraction system

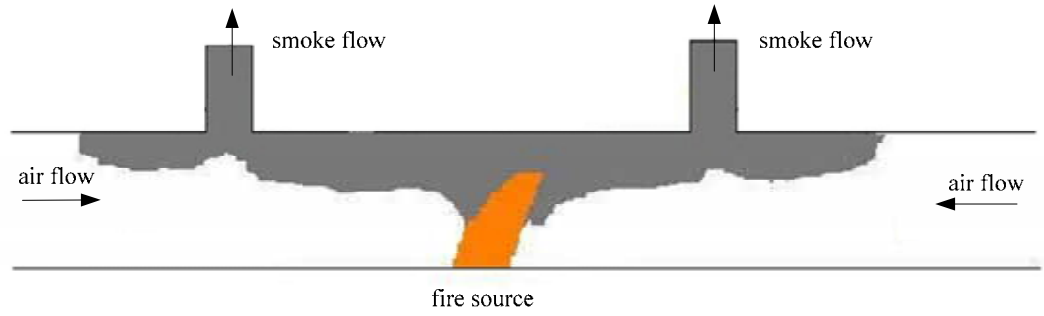

Figure 2 Diagram of two point extraction system

Vauquelin *et al.* [5][6] carried out a series of experiments in an isothermal model scale test-rig, to investigate the extraction capability of a two point extraction system and the efficiency of the extraction system. The symmetrical two point extraction system was used in their experiments, ignoring the probable ventilation velocity across the fire site. They noted that when a total exhaust volumetric flow rate is up to 370 m^3/s in large scale, smoke flow was just prevented from spreading across the extraction vents and completely controlled for a heat release rate of 10 MW in a tunnel with a height of 5 m and width of 10 m in large scale. For a heat release rate of 4 MW the corresponding exhaust volumetric flow rate is 279 m^3/s. They also proposed that the total exhaust volumetric flow rate can be much smaller if it is sufficient that the smoke flow is confined to an acceptable zone, downstream of the vents. The ventilation velocity induced by extraction, which is necessary to prevent the smoke layer development after the last extraction vent has been activated, was defined as the "confinement velocity". The total exhaust volumetric flow rate was 201 m^3/s, corresponding to a confinement velocity of 2.01 m/s, for a heat release

rate of 10 MW and 161 m^3/s, corresponding to a confinement velocity of 1.61 m/s, for a heat release rate of 4 MW. The smoke flow was confined between the portal and the exhaust point when the total exhaust volumetric flow rate was 337 m^3/s (4 times the smoke flow rate of the fire source) for a heat release rate of 20 MW. In other works, by extrapolating the experimental data the total exhaust volumetric flow rate should exceed 485 m^3/s, to completely control the smoke flow development, for a heat release rate of 20 MW.

According to these data, it seems to be impossible to prevent the smoke flow from spreading downstream of the extraction vents, using the two point extraction system, for a large fire, i.e., a HGV or several HGVs fire with a heat release rate more than 100 MW, even 300 MW. However, the method of cold gas entrainment, i.e. mixture of helium and nitrogen, which uses the density difference to model a fire instead of the temperature difference, induces an extra gas flow rate and ultimately induces experimental inaccuracy. In practice, the smoke flow rate mainly consists of air entrained in the process of fuel combustion and smoke spread, however, the smoke flow is introduced directly by the fire source in an isothermal model using the method of cold gas. In Vauquelin *et al.*'s experiments, a gas mixture of helium and air with a volumetric flow rate of up to 45.4 m^3/s and 84.3 m^3/s was introduced into the system as the fire source, for heat release rates of 10 MW and 20 MW, respectively, in large scale. Obviously, the extra gas flow thus introduced is very large, compared with the total exhaust volumetric flow rate. This measure makes the extraction system more difficult to control or confine the smoke flow, and the experimental error increases with the heat release rate.

In these experiments, the interval distance between two extraction vents, the geometry of extraction vents, the extraction flow rate of the extraction vents, and different ventilation system are taken into account.

The main objective of this report is to confirm whether a large tunnel fire involving a HGV fire or several HGVs, with heat release rate more than 100 MW, up to 300 MW, can be controlled or confined in an acceptable zone, using a point extraction ventilation system, and how to control it if possible in combination with longitudinal flow. In addition, the maximum heat release rate, the fire growth rate, the maximum temperature rise below the ceiling and the fire spread to other neighbouring wood cribs were also investigated in the model scale tests with extraction ventilation.

2 Theoretical considerations

2.1 Scaling theory

The model was built in scale 1:23, which means that the size of the tunnel is scaled geometrically according to this ratio. We neglect the influence of the thermal inertia of the involved material, the turbulence intensity and radiation but we scale the heat release rate, the time, flow rates, the energy content and mass. Information concerning different scaling theories can be obtained from for example references [7-10]. A summary of the scaling models applied in this project is provided in Table 1.

Table 1 A list of scaling correlations for the model tunnel.

Type of unit	Scaling model	Eq. number
Heat Release Rate (HRR) (kW)	$Q_F = Q_M \left(\frac{L_F}{L_M} \right)^{5/2}$	Eq. (1)
Volumetric flow (m3/s)	$\dot{V}_F = \dot{V}_M \left(\frac{L_F}{L_M} \right)^{5/2}$	Eq. (2)
Velocity (m/s)	$V_F = V_M \left(\frac{L_F}{L_M} \right)^{1/2}$	Eq. (3)
Time (s)	$t_F = t_M \left(\frac{L_F}{L_M} \right)^{1/2}$	Eq. (4)
Energy (kJ)	$E_F = E_M \left(\frac{L_F}{L_M} \right)^{3} \frac{\Delta H_{c,M}}{\Delta H_{c,F}}$	Eq. (5)
Mass (kg)	$m_F = m_M \left(\frac{L_F}{L_M} \right)^{3}$	Eq. (6)
Temperature (K)	$T_F = T_M$	Eq. (7)

L is the length scale. Index M is related to the model scale and index F to full scale (L_M=1 and L_F=23 in our case).

2.2 Determination of heat release rate

The heat release rate, Q (kW), which is directly proportional to the fuel mass loss rate, $\dot{m}_f$ (kg/s), can be calculated using the following equation:

$$Q = \dot{m}_f \chi H_T \qquad (8)$$

where H_T is the net heat of complete combustion (kJ/kg). The fuel mass loss rate, $\dot{m}_f$, is determined by the weight loss. In fires the combustion of fuel vapours is never complete, and thus the effective heat of combustion (H_c) is always less than the net heat of complete combustion (H_T). Further, χ, is the ratio of the effective heat of combustion to net heat of

complete combustion, i.e., $\chi = H_c / H_T$ [11] (Tewarson calls the 'effective heat of combustion' the 'chemical heat of combustion').

The actual heat release rate, Q (kW), at a measurement point can be obtained by the use of the following equation (without correction due to CO production) using oxygen consumption calorimetry [12, 13]:

$$Q = 14330 \dot{m}_a \left(\frac{X_{0,O_2}(1 - X_{CO_2}) - X_{O_2}(1 - X_{0,CO_2})}{1 - X_{O_2} - X_{CO_2}} \right) \qquad (9)$$

where X_{0,O_2} is the volume fraction of oxygen in the incoming air (ambient) or 0.2095 and X_{0,CO_2} is the volume fraction of carbon dioxide measured in the incoming air or $X_{0,CO_2} \approx 0.00033$. X_{O_2} and X_{CO_2} are the volume fractions of oxygen and carbon dioxide downstream of the fire measured by a gas analyser (dry).

If X_{CO_2} has not been measured equation (9) can be used by assuming X_{CO_2} =0. This will simplify equation (9) and usually the error will not be greater that 10 % for most fuel controlled fires. In the derivation of equation (9) it is assumed that $\dot{m}_a = \rho_a V A$ and that 13100 kJ/kg is released per kg of oxygen consumed. It is also assumed that the relative humidity (RH) of incoming air is 50%, the ambient temperature is 15°C, CO_2 in incoming air is 330 ppm (0.033 %) and the molecular weight of air, M_a, is 0.02895 kg/mol and of oxygen, M_{O2}, is 0.032 kg/mol. Further, ρ_a is the ambient air density, u is the ventilation velocity upstream the fire in m/s and A is the cross-sectional area of the tunnel in m^2 at the same location as the ventilation velocity measurement.

The total air mass flow rate, $\dot{m}$, inside the tunnel (and in the exhaust duct) can be determined both on the upstream ($\dot{m}_{us}$) and downstream side ($\dot{m}_{ds}$), based on the measured centre line velocity, u_c. The general equation for the air mass flow rate is:

$$\dot{m} = \zeta \frac{T_0 \rho_0}{T} u_c A \qquad (10)$$

Actually the average ventilation velocity can be expressed as $V = \xi u_c$ in most cases for the temperature at the measurement point equals to the ambient temperature. The theoretically determined mass flow correction factor (ratio of mean to maximum velocity), ζ , is dependent on the temperature and velocity over the cross-section of the the exhaust duct or the tunnel. In the calculations of the air mass flow rates, a theoretical value of ζ =0.817 was used [14].

The gas velocity was determined using the measured pressure difference, Δp, for each bi-directional probe [15] and the corresponding gas temperature. The diameter of the probes, D, used was 16 mm and the probe length, L, was 32 mm. The velocity was obtained from Equation (11):

$$u_c = \frac{1}{k}\sqrt{\frac{2\Delta pT}{\rho_0 T_0}} \qquad (11)$$

where k was a calibration coefficient equal to 1.08. The ambient values used in equation (11) were T_0 = 293 K and ρ_0 =1.2 kg/m^3.

The O_2, CO and CO_2 was measured at two heights: 0.88 × H and 0.5 × H, where the tunnel height H was 0.2 m.

3 Experimental Setup

A total of 12 tests with point extraction ventilation systems were carried out. The fire load was simulated using wood cribs. Extraction ventilation was tested with different ventilation conditions, natural and forced longitudinal ventilation. The parameters tested were the longitudinal ventilation rate, the arrangement of the exhaust openings and the exhaust capacity. Moreover, the fire spread between wood cribs with a free distance of 0.65 m (about 15 m in large scale) was tested.

Figure 3 A photo of a model-scale tunnel used by Ingason [4] for tests with longitudinal ventilation. A fan was attached to the tunnel entrance and windows were put on one side in order to observe the smoke flow.The tunnel was modified in order to carry out the tests with point extraction ventilation system.

Longitudinal ventilation was established using an electrical axial fan attached to the entrance of the model tunnel, as shown in Figure 3. The fan it self was 0.95 m long with an inner diameter of 0.35 m and 0.8 HP motor yielding a maximum capacity of 2000 m^3/h (at 1400 rpm and 7.5 mmH_2O). The rotation speed, and thereby the capacity, could be controlled by an electrical device coupled to the motor. Between the fan and the tunnel entrance a 0.8 m long rectangular plywood box with the dimensions 0.4 wide and 0.3 m high, was mounted to create a uniform flow at the entrance of the tunnel. The swirls created by the axial fan, were hampered by filling the plywood box with straw fibres. Longitudinal wind velocities of 0 m/s and 0.62 m/s were used in the test series. According to Equation (3), the corresponding large scale velocity is 0 and 3 m/s, respectively.

The tunnel itself was 10 m long, 0.4 m wide and 0.2 m high, as shown in Figure 4. The corresponding large scale dimensions were 230 m long, 9.2 m wide and 4.6 m high. The extraction ventilation channel, with a height of 0.1 m and the same width as the tunnel, was above the ceiling, as shown in Figure 5. The total flow rate through the extraction vents used were 0.06 m^3/s, 0.10 m^3/s and 0.15 m^3/s which according to equation (2) corresponds to about 150 m^3/s, 250 m^3/s and 380 m^3/s respectively, at large scale. The number of exhaust openings that were used in the tests was varied between 1 and 2. In other words, in these tests a single point extraction system and two point extraction system was studied. The area of the openings were 0.026 m^2 and 0.052 m^2, respectively, which corresponds to 13.75 m^2 and 27.5 m^2 in large scale.

The model was constructed using non-combustible, 15 mm thick, boards (Promatect H). The density of the boards was 870 kg/m^3, the heat capacity was 1.13 kJ/kg·K and heat conduction was 0.19 W/m·K. The floor, ceiling and one of the vertical walls were built in Promatect H boards while the front side of the tunnel was covered with a fire resistance window glaze. The 5 mm thick window glaze (0.6 m wide and 0.35 m high) was mounted in steel frames which measured 0.67 m by 0.42 m, see figures 4 and 5.

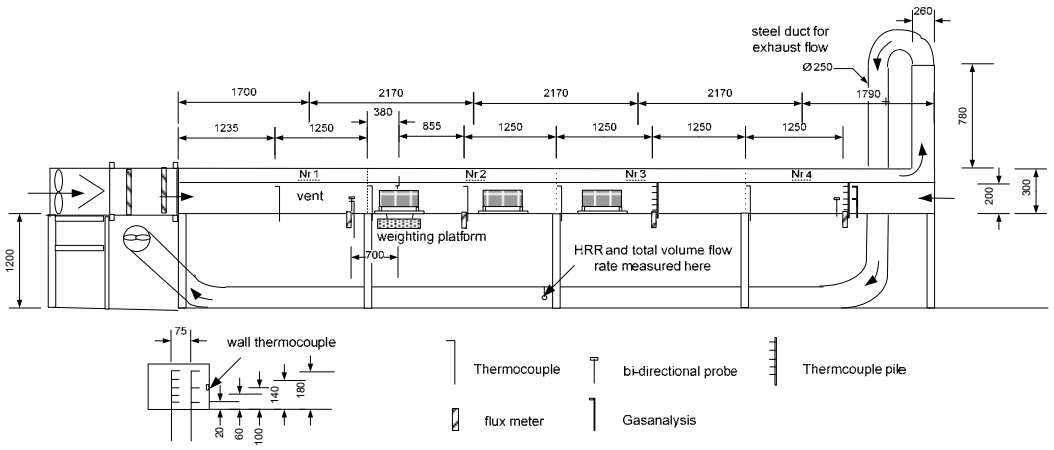

Figure 4 A schematic of the model-scale test-rig with extraction system.

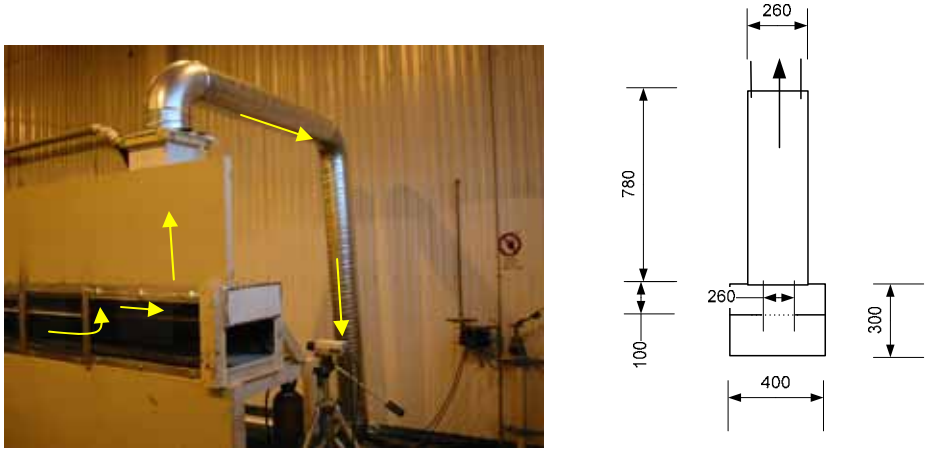

Figure 5 A schematic drawing of the model tunnel used for extraction ventilation.

3.1 Fire load

The fire load consisted of a wood crib (pine). In the longitudinal ventilation study two different types of wood cribs were used: wood crib A and wood crib B, respectively. In the present study only the wood crib B was used. A detailed description of wood crib B is given in Figure 6. More detailed information about the wood cribs for each test is given in Table 2. The total weight of wood crib B ranged from 0.91 kg to 1.24 kg. The total fuel surface area of wood crib B was estimated to be 0.56 m^2.

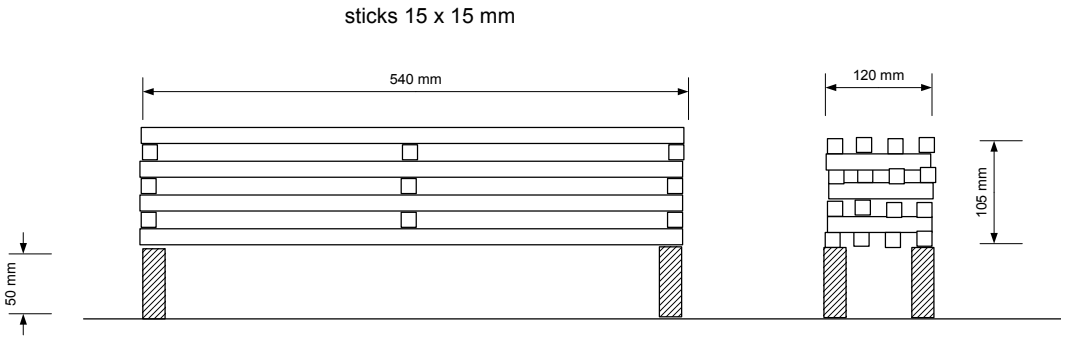

Figure 6 Detailed drawing of the wood crib (wood crib B).

3.2 Instrumentation

Various measurements were conducted during each test. The first wood crib was placed on a weighing platform (W), consisting of a scale attached by four steel rods to a free floating dried Promatect H board measuring 0.65 m long, 0.35 m wide and 0.12 m thick. In the case when more than one wood cribs was used in the tests, only the first wood crib was weighted, and the total heat release rate was measured using oxygen calorimetry technology in the exhaust duct. The weighing platform was connected to a data logging system recording the weight loss every second. The centre of the weighing platform was 2.87 m from the tunnel entrance (x=0) and the accuracy of the weighing platform was +/- 0.1 g.

The temperatures were measured with welded 0.25 mm type K thermocouples (TC). The locations of the thermocouples are shown in Figure 4, and the channel numbers and the identification of the instruments used are presented in Figure 7. Most of the thermocouples were placed 0.02 m below the ceiling along the tunnel centre line. A pile of thermocouples was placed 6.22 m (pile A in Figure 7) and 8.72 m from the inlet opening (pile B in Figure 7), respectively. The thermocouples of pile A and B were place in the centre of the tunnel and 0.02 m, 0.06 m, 0.10 m, 0.14 m and 0.18 m above the floor, respectively. Additional thermocouples were placed at a distance of 0.075 m from the tunnel wall at pile B and at heights of 0.02 m, 0.10 m and 0.18 m, respectively, above the floor level. A thermocouple was attached to the side wall 0.10 m above the floor and 8.72 m from the tunnel entrance.

A bi-directional [15] probe (BD) was placed at the centreline of the tunnel 8.72 m from the inlet (at pile B). Another bi-directional probe was placed upstream of the fire at the centre of the cross-section and 1.15 m from the inlet. The pressure difference was measured with a pressure transducer with a measuring range of +/-20 Pa. A hot-wire anemometer was also used to measure the velocities at the portals of the model tunnel.

At three locations and flush to the floor board, water-cooled heat flux meters, of type Schmidt-Boelter, were placed to record the total heat flux. The locations were 3.72 m (Flux 1), 6.22 m (Flux 2) and 8.72 m (Flux 3) from the tunnel entrance (x=0) in Test 7 and 8. During other tests the meter at 6.22 m (Flux 2) was moved upstream of the fire to location 2.165 m. The flux meters at 3.72 m (Flux 1) and 8.72 m (Flux 3). In tests 7 and 8 the location of the meters was the same as in the first case, i.e. 3.72 m (Flux 1), 6.22 m (Flux 2) and 8.72 m (Flux 3).

The gas concentrations (O_2, CO_2 and CO) were measured 8.72 m from the entrance (at pile B) using two measuring probes consisting of open copper tubes (Ø 6 mm). They were located at two different heights, 0.10 m and 0.175 m above the floor. The oxygen

was measured with an M&C Type PMA 10 (0 – 21 %) and the CO_2 (0 –10%) and CO (0 – 3 %) was measured with Siemens Ultramat 22.

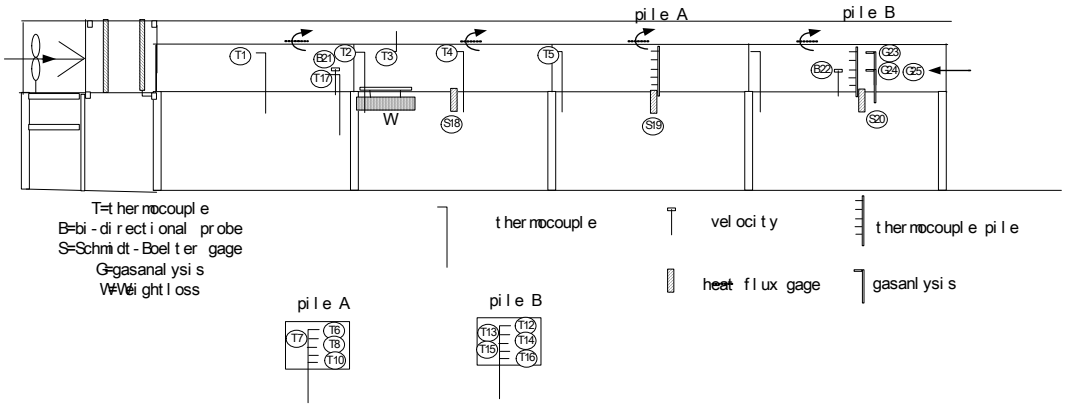

Figure 7 The channel number and identification of all the instruments.

A bi-directional probe and an oxygen probe were mounted in the centre of the 0.25 m diameter steel exhaust duct on the floor, see Figure 4.

The weighing platform, the thermocouples, the pressure transducers, the gas analysers and flux meters were all connected to IMP 5000 KE Solotron loggers. The data were recorded on a laptop computer at a rate of about one scan per second.

4 Test procedure

The wood cribs used in each test were dried over a night in a furnace with 60 ºC (<5% moisture). The first wood crib was placed on the weighing platform at a height 50 mm above floor. A cube of fibreboard (measuring 0.03 m, 0.03 m and 0.024 m) was soaked in heptane (9 mL) and placed on the weighing platform board at the upstream edge of the wood crib as shown in Figure 8. At 2 minutes from starting the logging system, this cube was ignited.

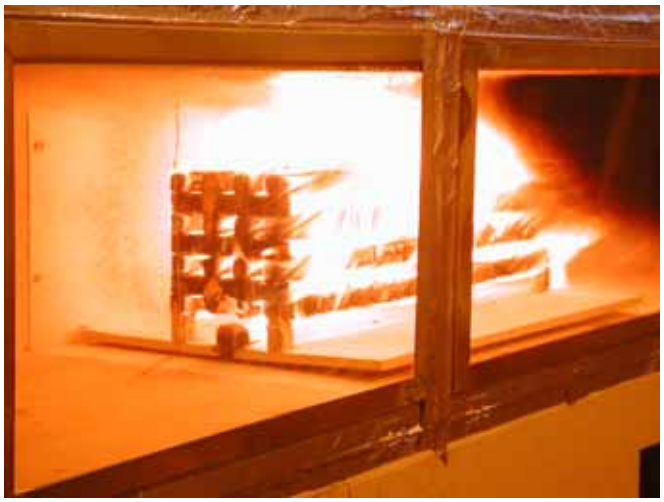

Figure 8 A photo showing a fully developed fire (Test 5 in Ingason's tests[4]). The ignition source consisted of a fibreboard cube placed on the weighing platform board at the upstream edge of the wood crib.

In Table 2, detailed information on each test carried out is presented. A total of 12 tests were carried out, including eight tests with the single point extraction system (Test 1 ~ Test 8), three tests with the two point extraction system (Test 9 ~ Test11) and one test with a three points extraction system (Test 12).

These tests were carried out with the same tunnel width and ceiling height, 0.4 m and 0.2 m, respectively, and type of wood crib but varying numbers of wood cribs and extraction vent openings in the ceiling. In tests with more than one wood crib, the free distance between the cribs was 0.65 m. This means that the centre to centre distance between the cribs was 1.19 m. An extra Promatect H board was placed under wood crib Nr 2 and wood crib Nr 3 in order to maintain the same distance between the top of the wood crib and the ceiling.

The centre of the ceiling openings (vents) were placed with an equal distance of 2.17 m, which corresponds to 50 m in large scale. The distance from the tunnel entrance (x=0) to the centre of the opening Nr 1 was 1.7 m (see Figure 4). The size of the openings varied during the tests: 0.026 m^2 and 0.052 m^2, respectively. The width of the openings was kept the same during all tests, 0.026 m, while the length (in the x-direction) was varied: 0.1 m and 0.2 m, respectively. The size of the openings corresponds to 13.75 m^2 and 27.5 m^2 in large scale, respectively. The steel duct was connected to the central ventilation system used to ventilate the fire test hall. The flow rate was determined before each test by regulating a valve between the steel duct and the central ventilation system. The total exhaust airflow in the steel duct was 0.06 m^3/s, 0.10 m^3/s, and 0.15 m^3/s, respectively, corresponding to about 150 m^3/s, 250 m^3/s, 380 m^3/s, respectively, in large scale.

Table 2 Summary of tests carried out with extraction ventilation

Test nr	T_o	Initial average longitudinal ventilation	Number of wood cribs	Wood crib Nr - weight	Arrangement of wood cribs – free distance	Open vents Nr	Area of open vents
	ºC	m/s		kg	m		m^2
1	20.6	0.60	1	1.048	–	Nr 4	0.052
2	19.8	0	1	1.060	–	Nr 2	0.026
3	21.0	0	1	1.002	–	Nr 1	0.026
4	21.5	0	2	1.114	0.65	Nr 2	0.052
5	22.2	0	1	1.046	–	Nr 1	0.026
6	21.2	0.60	1	1.138	–	Nr 2	0.026
7	21.7	0.60	2	Nr 1-1.128 Nr 2-1.142	Serie– 0.65	Nr 4	0.052
8	20.7	0.60	3	Nr 1-1.158 Nr 2-1.052 Nr 3-1.236	Serie– 0.65	Nr 4	0.052
9	21.1	0	1	1.106	–	Nr 1、Nr 2	0.026
10	20.9	0	1	0.960	–	Nr 1、Nr 2	0.026
11	20.1	0	2	0.906	Serie– 0.65	Nr 1、Nr 2	0.052
12	22.0	0	1	1.028	–	Nr 2、Nr3、Nr 4	0.026

5 Test results

A presentation of the test results is given in this chapter. All the detailed test results for each test are given in Appendix A. The heat release rate was measured both by measuring the weight loss and using the oxygen calorimeter technique. Note that only the weight loss of the first wood crib was measured. In the tests involving several wood cribs, the total heat release rate was measured using the oxygen calorimetry in the exhaust duct.

5.1 Heat release rate

In Table 3 the main test results related to the air flow conditions and the heat release rates are given. The test number is given in the first column. The second and third column contain the average velocities, V_{us} and V_{right}, measured near the left portal and right portal respectively. The fourth column shows the measured total volumetric flow rate measured in the extraction vents, $\dot{V}_{ex}$. The fifth column shows the fuel mass burning rate, $\dot{m}_f$, at the maximum heat release rate. The sixth column shows the maximum heat release rate based on equation (8). In the calculations, a combustion efficiency of χ=0.9 was applied. This value was multiplied by the heat of combustion of 16.7 MJ/kg obtained from the free burn test. The parameter $t_{\max}$ is the time in minutes from ignition when the maximum heat release rate occurs. The linear fire growth rate, $\Delta Q / \Delta t$, is taken from the time when the heat release rate is 20 kW up to the time when it reaches 50 kW. During this period the fire growth rate was comparatively linear in most cases. The ninth column contains $q''_{\max}$ the maximum heat release rate per square exposed fuel surface area, i.e. $q''_{\max} = Q_{\max} / A_s$.

5.2 Gas temperatures

Test results related to the measured gas temperatures are shown in Table 3. The maximum ceiling temperature at distance X_f from the centre line of the fire source is shown in columns ten to seventeen. The values listed here are the maximum values measured by the thermocouple during one test. The identification and location of these thermocouples can be found in Figure 7.

5.3 Total heat flux

The total heat fluxes were registered by Schmidt-Boelter gages at floor level and different locations from the fire (identified as S18, S19 and S20 in Figure 7.). In the last two columns, the heat fluxes measured with heat flux meters, i.e. Max flux 1 and Max flux 2, are given in Table 3. Very low values of heat flux were measured by heat flux meter 3, so these have not been given. Note that the values given in Table 3 are the maximum total heat fluxes measured, which correspond well to the peak heat release rates. As the flux meters are cooled by water, they measure the total heat flux towards a surface which is colder than the surrounding walls (and glass). The measured value given in the column, Max flux 2, depends on the location of the flux meter. The flux meter was moved to different places during the performance of the test series. In tests 6-8 it was located 3.36 m downstream of the fire source. In other tests, it was moved to 0.7 m upstream of the fire source.

Table 3 Test results related to heat release rate, gas temperatures and heat flux.

Test Nr	V_{left}	V_{right}	$\dot{V}_{ex}$	$\dot{m}_{ex}$	$\dot{m}_{f,\max}$	$Q_{\max}$	$t_{\max}$	$\frac{\Delta Q}{\Delta t}$	$q''_{\max}$	$T_{1,max}$	$T_{2,max}$	$T_{3,max}$	$T_{4,max}$	$T_{5,max}$	$T_{6,max}$	$T_{11,max}$	$T_{12,max}$	*Max flux 1*	*Max flux 2*
	m/s	m/s	m^3/s	kg/s	kg/s	kW	min	kW/min	kW/m^2	ºC	ºC	ºC	ºC	ºC	ºC	ºC	ºC	kW/m^2	kW/m^2
X_f										-1.63m	-0.38m	0m	0.86m	2.1m	3.36m	4.6m	5.86m	0.86m	-0.7m
1[a]	0.61	1.0	0.15	0.16	0.0065	97.7	2.0	89.7	174.5	22.0	54.9	1056.9	672.8	443.6	307.2	246.9	21.0	NA	1.7
2	0.25	1.27	0.14	0.15	0.0043	65.1	3.1	27.5	116.3	178.6	762.3	860.2	656.5	21.2	21.5	21.5	21.0	14.7	5.4
3	0.73	0.26	0.09	0.15	0.0035	52.6	4.7	16.9	93.9	22.3	785.0	768.3	525.8	185.2	28.2	23.3	22.6	9.9	12.2
4	0.32	1.18	0.14	0.15	0.0057	86.6	2.6	42.9	77.3	174.2	676.4	1009.3	637.4	40.5	27.5	27.5	28.6	27.3	5.8
5	0.25	0.34	0.06	0.06	0.0038	57.6	3.3	23.3	102.9	134.5	845.5	939.3	582.3	66.0	23.2	22.8	22.6	14.3	13.9
6[a]	0.59	0.9	0.14	0.16	0.0056	83.9	2.7	50.0	149.8	24.0	60.5	1037.0	730.2	76.5	24.3	23.5	23.5	32.4	0.9
7[a]	0.57	1.05	0.14	0.17	0.0067	158.3	3.9	54.5	141.4	23.2	64.2	1004.5	807.8	865.5	543.0	409.7	26.2	46.0	16.5[d]
8[a]	0.58	0.94	0.14	0.15	0.0075	190.6	4.9	63.7	113.5	23.7	63.5	981.7	701.9	838.0	825.0	605.5	33.1	47.7	47.6[d]
9[b]	0.40	0.79	0.09	0.11	0.0034	51.4	3.7	22.2	91.8	95.6	848.6	1033.1	617.9	21.9	21.6	21.0	21.0	11.7	10.1
10[b]	0.52	0.99	0.14	0.16	0.0035	52.6	3.1	22.2	93.9	20.6	819.2	813.5	606.6	22.7	22.4	22.2	21.6	12.4	9.3
11[b]	0.36	0.81	0.09	0.10	0.0038	57.6	2.8	32.6	102.9	74.9	744.5	808.8	577.4	21.4	21.3	21.2	21.2	10.2	9.1
12[c]	0.38	1.3	0.14	0.16	0.0050	75.2	2.8	50.8	134.3	119.2	713.3	909.0	617.0	278.3	58.6	63.9	22.0	21.3	3.9

[a] forced longitudinal ventilation.
[b] two point extraction system.
[c] three points extraction system.
[d] measured 3.36 m downstream of the fire source.

5.4 Flame length

In Table 4, the results of flame lengths calculated by assuming a temperature at flame tips of 400°C and 500°C, respectively, are presented. In most of these experiments the flames extend to the extraction vents and spread into the vents, consequently, the flame tips located inside the extraction vent and the flame length is hard to estimate. We can only provide a lower limit here in these cases. Data from Test 1, 3, 5, 7 and 8 represent specific values, in all other case the flames extended to the extraction vent openings.

Table 4 Test results for temperature calculated flame lengths, L_f

Test Nr	Q	L_f	
		400°C	500°C
1	97.7	2.1	1.55
2	65.1	>0.85	>0.85
3	52.6	1.3	0.8
4	86.6	>0.85	>0.85
5	57.6	1.65	1.25
6	83.9	>0.85	>0.85
7	158.3	4.6	3.6
8	190.6	>5.1	4.8
9	51.4	>0.85	>0.85
10	52.6	>0.85	>0.85
11	57.6	>0.85	>0.85
12	75.2	>0.85	>0.85

“>” means that the flame in the test extends to the extraction vent.

5.5 Flame spread

In Table 5, detailed information concerning flame spread between wood cribs in six of the tests is given. Results from two former tests carried out by Ingason [4] are also listed here. Fire spread occurs in all the tests, with the exception of Test 11. The “ignition temperature” refers to the characteristic temperature below the ceiling and above the wood crib, when the wood crib is ignited, i.e. TC4 for Nr1 and TC5 for Nr2.

Table 5 Summary of tests for flame spread

Test no.	Arrangement of wood cribs	Flame spread	Ignited time (Ignited object)	Ignited temperature below ceiling	Incident heat flux[b]
			min : sec	(^oC)	(kW/m^2)
4	Nr1、Nr2	Yes	3 : 02 (Nr2)	584.2	14.9
7	Nr1、Nr2	Yes	1 : 47 (Nr2)	525.7	8.8
8	Nr1、Nr2、Nr3	Yes	1 : 49 (Nr2)	614.5	11.2
			2 : 47 (Nr3)	583.2	-
11	Nr1、Nr2	No	–	577.4	10.5
3[a]	Nr1、Nr2	Yes	1 : 44 (Nr2)	630.2	12.0
4[a]	Nr1、Nr2、Nr3	Yes	1 : 50 (Nr2)	613.6	10.5
			2 : 29 (Nr3)	648.3	-

[a] results of these two former tests carried out by Ingason [4].
[b] measured by Heat flux meter 1.

6 Discussion of results

The main focus of these tests is whether the point extraction system can control or confine the fire and smoke flow to an acceptable zone. In addition, many characteristic fire dynamics parameters, e.g., the maximum heat release rate and fire growth rate, maximum temperature below the ceiling, flame length, heat flux and fire spread were investigated. Note that in the analysis of these parameters, the data from tests no.9, 10 and 11 with two extraction vents opened are not used. The reason for the exclusion of these tests is that the flow pattern is significantly different and the longitudinal flow and flow across the fire site are unknown. Further, in tests 3 and 5, V_{right} was used instead of V_{left} as the longitudinal ventilation velocity (V).

6.1 Heat release rate

The wood cribs, tunnel ventilation, and tunnel geometry should all be taken into account for the analysis of the fire heat release rate.

According to Croce and Xin's experimental study of the wood crib fires [16], the porosity of a wood crib is very important for the heat release rate. The heat release rate increases with increasing porosity, and becomes a weak function of the porosity when the porosity is greater than 0.7. The porosity of a wood crib, P, is defined as [7]:

$$P = \frac{A_v}{A_s} s^{1/2} b^{1/2} \qquad (12)$$

where A_v is the total cross-sectional area of vertical crib shafts, A_s is the exposed surface area of the wood crib, s is the surface-to-surface spacing between adjacent sticks in a layer, and b is the stick thickness (with the same width and height).

In these model scale tests, the porosity of the wood crib was chosen as 0.94 mm for wood crib A and 1.24 mm for wood crib B respectively, to ignore the effect of the porosity on the heat release rate. This means that these wood cribs should not show any type of vitiated tendency during the tests.

The effect of the tunnel geometry and fire source was not investigated systematically. Only one cross-section was used in these experiments and two cross-sections were used in the former tests carried out by Ingason [4]. The heat release rate is not very sensitive to the geometry of the tunnel and fire source. The effect of the geometry of the tunnel and the fire source can be ignored in these tests because of the specific fire scenario of a HGV fire in a road tunnel. The main objective of the report is to investigate the fire characteristics and control of fire and smoke when the fires become relatively large, i.e. a HGV fire with heat release rate over 100 MW using different types of point extraction systems with a longitudinal ventilation system.

We will focus on the analysis of the relationship between the heat release rate and ventilation velocity. Different ventilation velocities and two model tunnels were used in these series of experiment.

Figure 9 shows the fuel mass loss rate per unit area fuel surface against the ventilation velocity across the fire source. Note that the fuel mass loss rate was measured for the first wood crib, even in tests involving several wood cribs. The stoichiometric fuel mass loss rate per unit fuel surface area is also given in Figure 9. According to the principles of

oxygen consumption, the stoichiometric fuel mass loss rate per fuel surface area can be expressed as:

$$\frac{\dot{m}_{f,stoi}}{A_s} = \frac{Q}{\chi \Delta H_c A_s} = 0.24 \frac{A}{A_s} V \qquad (13)$$

According to Equation (13), the fuel mass loss rate per unit fuel surface area should be expressed a function of AV/A_s. The reason why only one stoichimetric line is plotted here is that the ratio of the tunnel cross-sectional area to the fuel surface area for both wood crib A and wood crib B tests are almost of the same value, i.e. the relative error is 6.7%. However, it should still be kept it in mind that the tunnel area and the fuel surface area do have an effect on the ventilation controlled wood crib fire.

From Figure 9, it is shown that for a longitudinal ventilation velocity less than 0.35 m/s, the fuel mass loss rate per unit fuel surface area increases with the ventilation velocity, and follows the stoichiometric line. This indicates that the fire under these conditions is ventilation controlled. However, when the ventilation velocity rises to 0.35 m/s or more, the fire is not sensitive to the ventilation velocity. This indicates that the fire becomes fuel controlled. The upper limit of the fuel mass loss rate per unit fuel surface area is about 0.13 kg/(m^{2}s). Tewarson and Pion [17] found that the maximum burning rate per fuel surface area that wood (Douglas fir) could achieve is 0.13 kg/(m^{2}s), which correlates well with the experimental data. The value found by Tewarson and Pion is an ideal value based on the assumption that all heat losses were reduced to zero or exactly compensated by an imposed heat flux equal to the total heat losses from the fire source. Comparing data for wood crib A and B in the fuel-controlled region shows that the upper limit of the burning rate per fuel area for wood crib B is slightly higher than that for wood crib A. The reason for this increase may be that the wood crib is more susceptible to heat feedback when using wood crib B fire test due to the relatively lower tunnel ceiling.

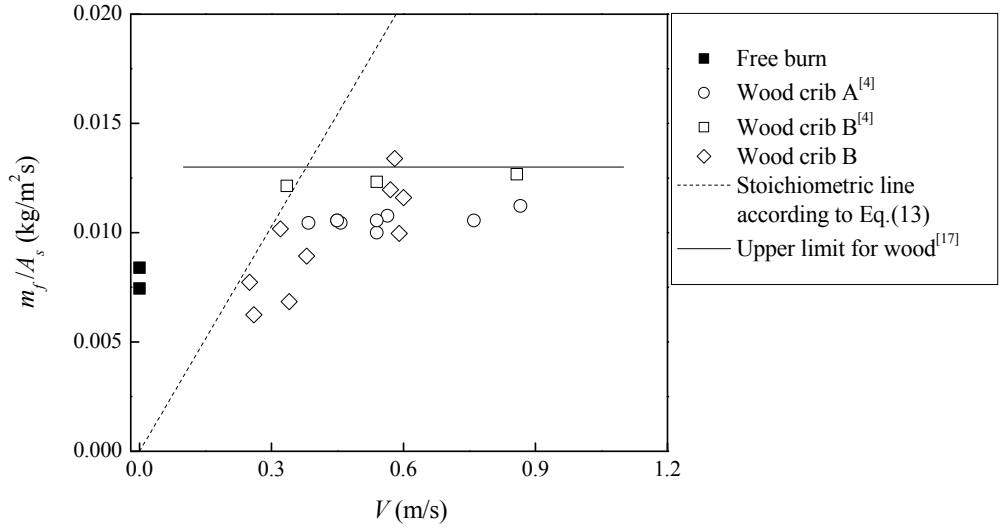

Figure 9 The maximum fuel mass loss rate per unit fuel surface area as a function of the ventilation velocity (first wood crib).

From Figure 9, it is also shown that in a large range of 0.35m/s to 0.9 m/s, the fuel mass loss rate per unit fuel surface area tends to be a constant. However, it can be expected that the fuel mass loss rate per unit fuel surface area will begin to decrease when the ventilation velocity is greater than a certain value due to the cooling effect of the ventilation. Comparing the data in tunnel fire tests and that in a free burn, shows that the

ratio of fuel mass loss rate per unit fuel surface area in a tunnel fire to that in a free burn is about 1.5 in the constant region (fuel-controlled), and that it can be less than 1 if the tunnel is not well ventilated.

For the two free burn tests (no wind) shown in Figure 9, it should be kept in mind that the ignition source was moved to the centre of the wood cribs whereas it was located upstream of the wood crib in the model tunnel tests. The original idea of doing this was to force the wood crib to be fully involved in flames, which is similar to the case for wood cribs burning in the model tunnels. After igniting one corner of the wood crib in a model tunnel, the ventilation and the heat feedback from tunnel walls forced the wood crib to be fully involved very quickly. As can be seen in Figure 9, the effects of the ventilation and the proximity of the walls clearly increase the maximum heat release rate for the wood cribs tested.

The above analysis is based on the data of fuel mass loss rate of the first wood crib. In some tests, several wood cribs were burnt together and the total heat release rate was measured using oxygen calorimetry technique in the exhaust vent rather than the weighing platform.

Figure 10 shows the maximum heat release rate per unit fuel surface area as a function of the ventilation velocity. The stoichiometric heat release rate per fuel surface area was plotted. For a fire with several wood cribs, the total fuel surface area of these wood cribs was used. According to the principles of oxygen consumption, the stoichiometric heat release rate per fuel surface area can be expressed as:

$$q''_{stoi} = \frac{Q}{A_s} = 3600 \frac{A}{A_s} V \qquad (12)$$

From Figure 10, it is seen that the same trend as Figure 9 is present, although the data does not correlates as well. The reason is that in a test with several wood cribs, all surfaces of these wood cribs are not burnt at the same time. When a maximum heat release rate occurs, part of the first wood crib has started to decay. As a consequence, the maximum heat release rate divided by the total fuel surface area is slightly lower for the case with several wood cribs compared to that with a single crib.

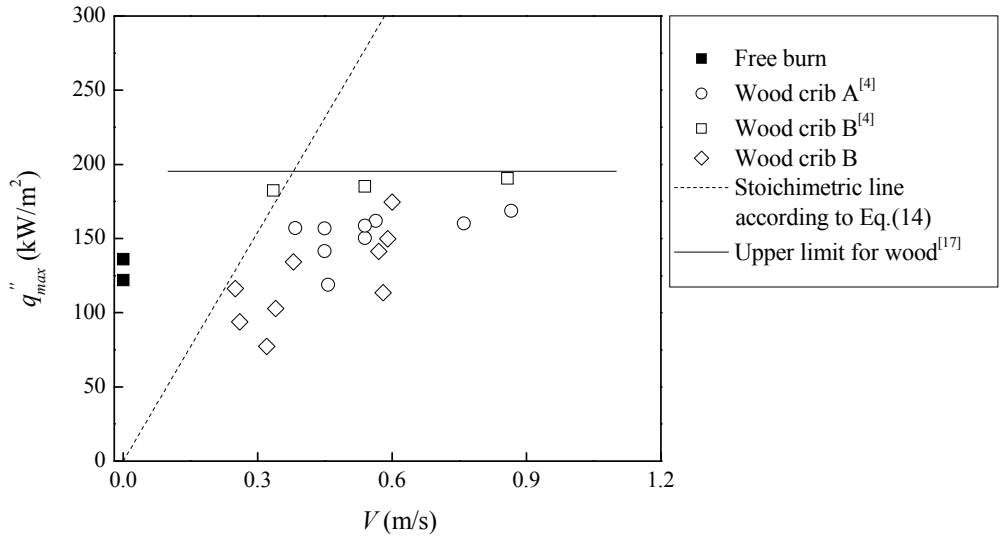

Figure 10 The maximum heat release rate per unit fuel surface area as a function of the ventilation velocity.

The fire growth rate for the wood cribs against the average ventilation velocity is given in Figure 11. The fire growth rate is calculated based on the data at the heat release rate ranges from 20 kW to 5 kW in these experiments. Clearly, it shows that the fire growth rate increases linearly with the ventilation velocity. The experimental data can be correlated well using the following equation:

$$\frac{\Delta Q}{\Delta t} = 133V \qquad (13)$$

A correction coefficient of 0.932 was found for Equation (15). This shows that the fire growth rate is nearly 3 times larger than that in a free burn test, when the ventilation velocity equals 1 m/s (4.8 m/s in large scale). This means that the ventilation velocity plays a very important role in the fire development.

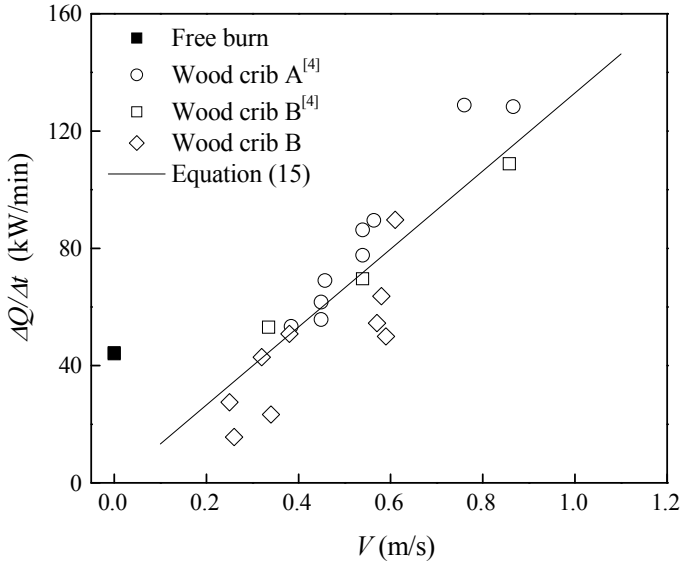

Figure 11 The fire growth rate for the wood cribs tested as a function of the ventilation rate across the fire source.

From figure 11, it is also clearly shown that the fire growth rate for a ventilation velocity of 0.3 m/s equals that in a free burn test, however, it is obviously lower for ventilation velocities below 0.3 m/s. There can be two possible explanations to this behaviour. One reason is that the fire can entrain more air in a free burn than that in a tunnel fire if the longitudinal flow is very low and the fire is completely ventilation controlled. The other is that the centre location of the ignition source for ignition in a free burn makes the fire development more rapidly.

6.2 Maximum gas temperature rise below the ceiling

Figure 12 shows the dimensionless maximum temperature rise below the ceiling in model scale tests with point extraction ventilation combined with longitudinal and natural ventilation. The dimensionless maximum temperature rise lies mainly in a range of 2.9 to 3.75, corresponding to the maximum temperature rise of 850 °C to 1100 °C. It seems that the maximum gas temperature beneath the tunnel ceiling is a weak function of the heat

release rate and the ventilation velocity for large fires with heat release rates more than 100 MW in large scale.

According to the data for the flame lengths listed in Table 4, it can be concluded that in all the tests the continuous flame zone extended to the ceiling at its maximum heat release rate. Consequently, the temperature below the ceiling in these cases represents the continuous flame zone temperature. Based on McCaffrey's fire plume theory, the maximum temperature rise in the continuous flame zone is nearly constant. In his tests it lies mainly in a range of 700 °C to 900 °C. As an average value McCafferey used a maximum temperature rise corresponding to 800 °C [18]. Consequently, one would expect that for a large fire in a tunnel, the maximum temperature rise beneath the tunnel ceiling should also be a constant if the continuous flame extends to the ceiling height, regardless of heat release rate and ventilation velocity.

However, the experimental data obtained here of the maximum temperature rise beneath the tunnel ceiling is slightly higher than the 800 °C proposed by McCaffrey. In Kurioka *et al.*'s model scale tunnel fire experiments, 800 °C was also found for maximum temperature rise below tunnel ceiling [19]. However, gas temperatures over 1000 °C were measured below tunnel ceiling in many large scale tests [2][20]. The reason for this increase could be the presence of soot that hinders radiation loss and absorbs the heat.

Above all, the temperature below the ceiling in these experiments represents the temperature in the continuous flame zone, and it lies mainly in a range of 850-1100°C, which fit the data from the large scale tests well.

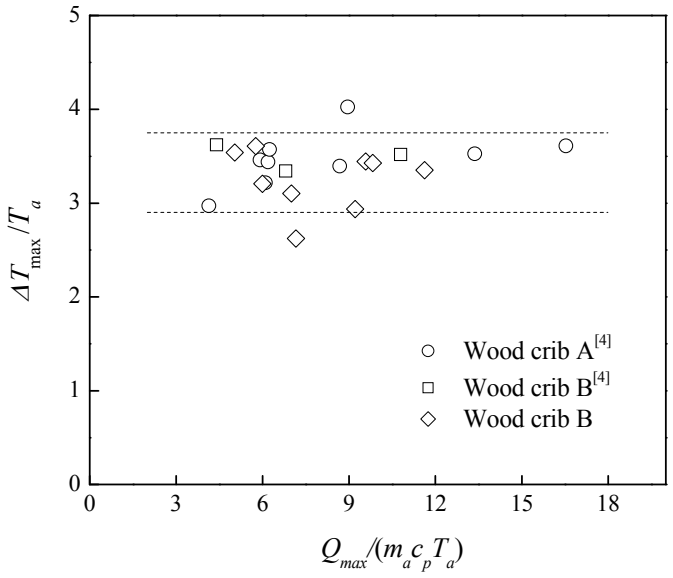

Figure 12 The dimensionless maximum temperature rise below the ceiling as a function of the dimensionless heat flow parameter.

6.3 Flame length

Few applicable data concerning flame lengths were obtained due to the arrangement of the point extraction ventilation systems. In most cases the flames extend to the extraction vents and beyond. As a consequence, it is difficult to estimate the flame length. In other words, the extraction vent confines the flame zone, and the evacuation environment near the fire site is safer. The flame length discussed here is defined as the horizontal distance from the fire source centre to the flame tip, as shown in Figure 13.

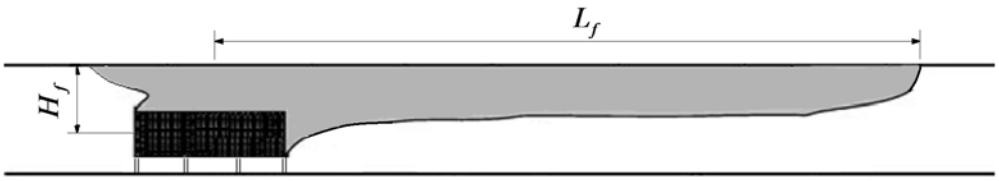

Figure 13 The schematic diagram of the flame length for a HGV fire

The effect of ventilation velocity on the flame length is hard to estimate, regardless of the heat release rate here. On the one side, the longitudinal flow increases the air entrainment into the flame zone, which reduces the flame length. On the other hand, a longitudinal flow forces the combustible gases away from the fire source, which increases the flame length. According to our analysis of experimental data and data from large scale tests, it is found that the flame length is only a weak function of the ventilation velocity.

To normalize the results, a dimensionless flame length was defined:

$$L_f^* = \frac{L_f}{H} \qquad (14)$$

and a dimensionless heat release rate was defined as follows:

$$Q_f^* = \frac{Q}{\rho_o c_p T_o g^{1/2} A H_f^{1/2}} \qquad (15)$$

The parameter, H_f, defined in Equation (17) is the vertical distance between the fire source center and the ceiling height. This fire source center is defined as the geometrical center of a fire. For a wood crib fire, the geometrical center is at the half wood crib height, as shown in Figure 13.

Figure 14 plot the dimensionless flame length as a function of the dimensionless heat release rate. Data from model scale tests with extraction ventilation and longitudinal ventilation are all plotted here. Ingason [4] compared the flame length from longitudinal ventilation tests based on observation with that based on the ceiling temperature, and found that a temperature rise of the flame tip of about 400 ^oC is the best fit value for these model scale tests. A correlation coefficient of 0.930 was found for the regression line. It is shown that the experimental data for flame length correlate well with the regression line, although the experimental data for flame lengths at low heat release rates are slightly higher than the proposed line. It can be concluded that experimental data of the flame length can be correlated well with the dimensionless heat release rate, as defined in Equation (17).

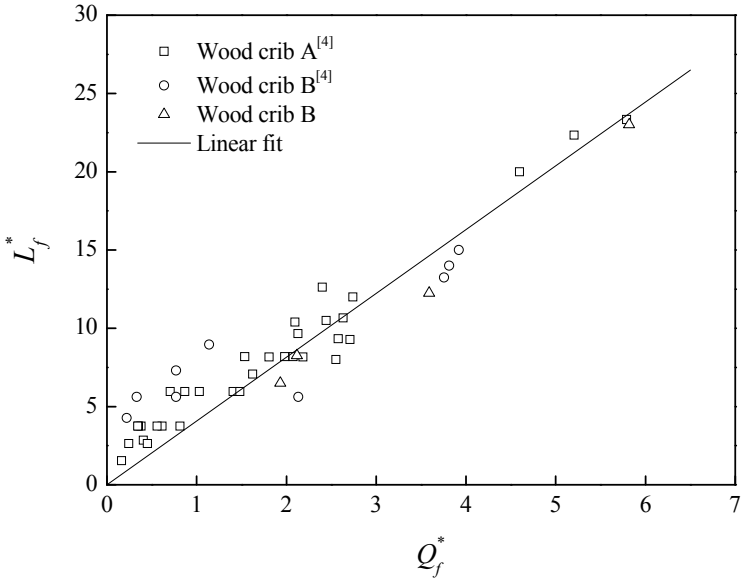

Figure 14 Flame lengths from model scale tests with extraction ventilation and longitudinal ventilation as a function of Q_f^*.

Comparison of experimental data from these model scale tests with results from some large scale tests was also made to validate the correlation. These large scale tests included in this comparison were the Runehamar tunnel tests [1-3], Eureka 499 Programme [21] and Memorial tunnel fire tests [20].

The Runehamar tunnel fire tests [1-3] were carried out in the de-commissioned Runehamar Tunnel in Norway with a length of 1600 m and a slope varying between 0.5 % uphill and 1% downhill. The cross-section of the tunnel near the fire source is 5 m high and 7.1 m wide. These tests were performed with a fire simulating a HGV-trailer. Different commodities, i.e. wood pallets, plastic pallets, polystyrene cups in compartmented cardboard cartons and polyurethane mattresses, were used as fuel. The heat release rates were measured using the oxygen calorimetery. Two mobile fans were used to create a longitudinal flow inside the tunnel. The heat release rates were obtained by the oxygen calorimeter method.

The Eureka 499 Programme [21] was performed in the abandoned Repparfjord Tunnel with a length of 2.3 km and a gradient of <1 % in northern Norway. The tunnel is approximately 5.3 to 7.0 m wide with a maximum height in the center between 4.8 m and 5.5 m. An average value of 5.15 m and 6.15 m was used as the tunnel height and width, respectively, in the analysis conducted here as a bias for the comparison. The HGV trailers was 2.4 m wide, 2.5 m high, and 12.5 m long. Nominally the level of a HGV trailer is about 1 m above the floor. The total fire load consisted of three parts, i.e. the furnishing material inside the cab, the furniture placed in the trailer and th combustible materials used in the construction of the trailer and attached to the chassis.

The Memorial tunnel fire tests [20] with longitudinal ventialiton were conducted in the Memorial Tunnel with a length of 853 m length, a height of 7.9 m and a grade of 3.2 % in West Virginia, USA. Jet fans installed in groups of three were used to evaluate the ability of the longitudinal ventilation system to control the direction of smoke and heat spread, and a variety of parameters, including fire heat release rate, fan response time, and the number of fans operated, were taken into account in these tests. The fire sources, set at 762 mm above the tunnel floor, consisted of four fuel pans and were used to vary the heat release rate from 10 MW to 100 MW.

Table 6 Summary of results of flame length from Runehamar tunnel tests (H=5 m, W=7.1 m, A=32.1 m^2).

Q	V	L_f	Q	V	L_f
kW	m/s	m	kW	m/s	m
3000	3	0	80000	2.8	20
5000	3	6.75	90000	6.8	23
6000	3	0	93000	2.4	42
11000	3	10	100000	2	70
9000	3.3	0	104000	2.2	57.95
14840	3.2	10	106000	2.8	30
17000	2.3	20	118000	2	76.38
19000	2.4	10	118600	2.2	65.54
27000	2.75	20	112000	2.8	38
30000	2.25	40	112500	2.4	55.31
38000	2.75	20	120000	1.8	72.87
43000	2.7	40	120000	2	30
50700	2.1	22	120000	2.8	37
51000	2.8	20	125000	2.2	75.81
51000	6.8	10	130000	2.1	78.11
54000	2.5	40	133000	2.1	83.59
60000	2.25	70	141000	2.2	70
63000	6.8	20	147000	2	85.76
72000	2.8	10	156630	2.4	80.47
73500	1.9	42	166000	2.2	85.54
78500	2.7	40	187000	2.3	94.68
79000	2.4	22	201890	2.2	88.19

Table 7 Summary of results of flame length from Eureka 499 (H=5.15m, W=6.15m, A=33.8m^2).

Q	V	L_f	Q	V	L_f
kW	m/s	m	kW	m/s	m
51000	6.8	10	106000	2.8	30
63000	6.8	20	112000	2.8	38
72000	2.8	10	120000	2.0	30
80000	2.8	20	120000	2.8	37
90000	6.8	23			

Table 8 Summary of results of flame length from Memorial tunnel tests (H=7,9m, W=8,75m, A=60m^2).

Q	V	L_f
kW	m/s	m
50000	1.2	24
50000	2.2	21
100000	2.4	63

Figure 15 gives the dimensionless flame length as a function of the dimensionless heat release rate defined in Equation (17). All the data from series of model scale tests and large scale tests are plotted here. It is shown that the dimensionless heat release rate can correlate well with all the data in both scales. The proposed line in Figure 15 can be expressed as:

$$L_f^* = 4.3Q_f^* \qquad (16)$$

A correlation coefficient of 0.882 was found for Equation (18).

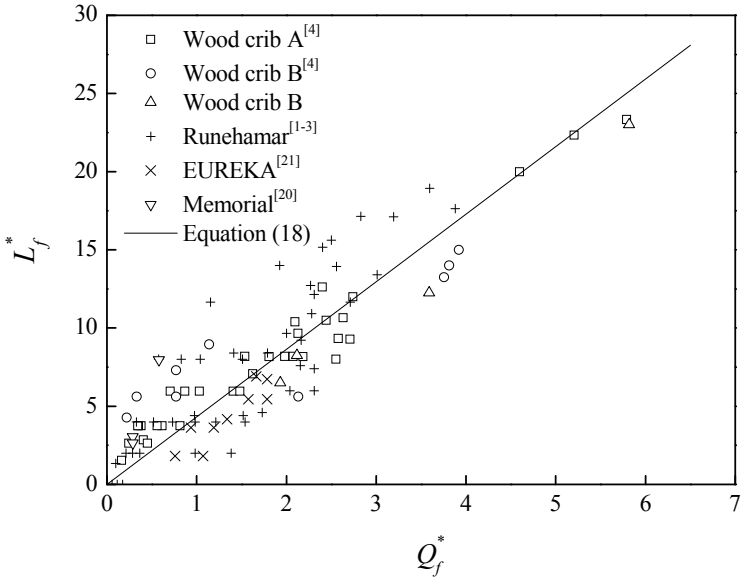

Figure 15 Flame lengths from series of model scale tests and large scale tests are plotted as a function of dimensionless heat release rate Q_f^*.

The good correlation shown in Figure 15 suggests that it is reasonable to ignore the effect of ventilation on the flame length. This in turn leads us to the conclusion that the flame length is a weak function of the ventilation velocity for large tunnel fires.

In addition, according to the analysis of flame length, we know that in many tests with extraction vents, the flames extend to the extraction vent. Obviously, the extraction system removes fire and smoke efficiently. This can reduce the risk of fire spread and provides a safer evacuation environment.

6.4 Total Heat flux

The following equation can be used to estimate the total heat flux [13]:

$$q''_{flux} = h_c(T_g - T_a) + F\varepsilon\sigma(T_{avg}^4 - T_a^4) \qquad (19)$$

where h_c is the convective heat transfer coefficient, in kW/(m^2 K), F is the view factor, ε is the emissivity, σ is the Stefan-Boltzmann constant of 5.67 x 10^{-11} kW/m^2 K^4. Note that the temperature T_g and T_a must be expressed in degrees Kelvin for this equation to be valid.

The average temperature can be obtained by the measurement of vertical temperature distribution at thermocouple pile A. In tests 6, 7 and 8, the heat fluxes were measured here. The peak total heat flux can be plotted using Equation (19). Note that the heat fluxes were set at the floor level, and so the convective heat transfer is very low compared to the radiation heat transfer. The convective heat loss coefficient, h_c, was set to be equal to 0.005 kW/m^2 K. The view factor F in Equation (19) was assumed to be one. The

emissivity, ε, in Equation (19) was assumed to be equal to 0.8. The experimental data fitted the measured data well, as shown in Figure 16. The framed graph in Figure 16 is a zoom of the data closest to origin.

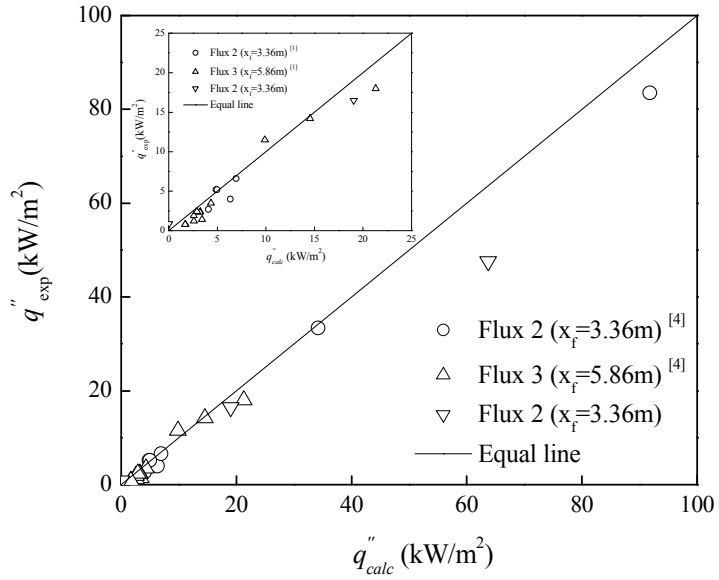

Figure 16 The measured total heat flux as a function of the calculated heat flux using Equation (19). A zoom of the data closest to the origin is given as well in the enclosed graph.

There are also some data of heat flux left out as it cannot be estimated from the average temperature based on the measured temperature distribution. Therefore, a simpler method to predict the total heat flux at the floor level is proposed here. Due to small effect of convection on total heat flux at the floor level, the convection is neglected here. Then Equation (16) can be transformed into:

$$q''_{flux} = F\varepsilon\sigma(T_f^4 - T_a^4) \qquad (20)$$

The view factor F in equation (17) is assumed to be equal to one. The emissivity, ε, was determined based on the experimental data, as shown in Figure 17. The emissivity, ε, equals to the slope of the fit line, which is determined as 0.68. Then Equation (20) can be transformed into:

$$q''_{flux} = 0.68\sigma(T_f^4 - T_a^4) \qquad (17)$$

A correction coefficient of 0.950 was obtained for Equation (21). In Ingason's model scale test, there is one data point with a heat flux of 203.5 kW/m^2 (see Figure 15). This data point was ignored as it would create a large error in the curve fitting of the main data. According to Equation (21), a heat flux of 171.4 kW/m^2 is predicted for this test.

Equation (19) can be used to estimate the total heat flux at floor level in a tunnel fire if the average temperature across a tunnel cross-section is known, or Equation (21) can be used if the temperature beneath the tunnel ceiling is known. It should be pointed out here that all the data for the total heat flux represent the peak total heat fluxes measured by the

heat flux meters during the tests. The time of peak total heat flux correlates well with that of peak heat release rate. This implies the heat flux meter responds rapidly.

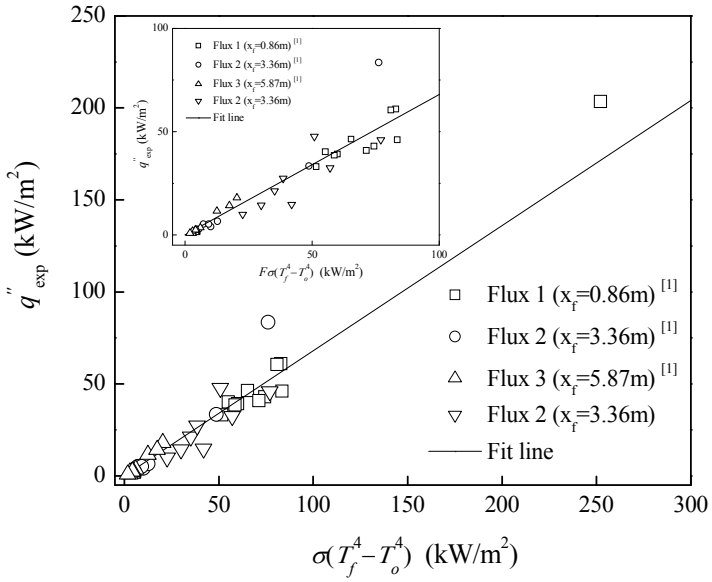

Figure 17 Determination of the emissivity defined in Equation (20).

6.5 Fire spread

The wood crib will be ignited when the heat flux towards the surface of the wood crib reaches a certain critical value or gas temperature.

Figure 18 shows the gas temperature beneath the ceiling when the wood crib was ignited. It is shown that the wood crib was ignited when the gas temperature beneath the ceiling and above the wood crib is in a range of 520 - 650 °C. An average value of 600 °C was found for the critical gas temperature beneath the ceiling for all the tests involving fire spread. Based on this information, it is easy to determine whether the wood crib is going to ignite or not. According to Equation (21), a critical heat flux of 22.1 kW/m^2 was also found. This value does not correlated well with the value measured by the heat flux meter, the reason could be that Equation (21) uses experimental data under peak condition (both gas temperature and heat flux), while the heat flux meter has a lag.

Data from Test 16 without ignition was also given for comparison in Figure 18. Note that in test 16, although the gas temperature above the wood crib rose up to 577.4 °C, the wood crib did not ignite. However, it is observed in this experiment that one corner of the wood crib towards the extraction vent was charred, and the wood crib can be regarded as beginning to burn, so it is a critical case.

It is observed that in the tests involving fire spread that the wood crib was ignited soon after the flame crawled above this wood crib. This indicates there is a close relationship between the fire length and fire spread. According to the above analysis, a critical temperature of about 600 ^{o}C above the wood crib is required to ignite it. It is also known that temperature of the flame tip is in the range of 400 to 600 ^{o}C. Obviously, fire spread will not occur if the flame length does not reach this position, i.e. the fire is not above the

wood crib. In other words, the fire spread only occurs after the flame is found above the wood crib.

From Table 5, it is clear that in tests with longitudinal flow adjacent to the fire and wood cribs, the second wood crib will catch fire in about 1 minute and 47 seconds on average, and the third wood crib in about 2 minute and 38 seconds. This implies that a vehicle 15 m behind a (simulated) burning HGV will catch fire in about eight and a half minute, and a third vehicle a further 15 m behind the second vehicle in only about three more minutes, due to the accumulated heat from the first vehicle. These numbers should only be used as an indication of the phenomena rather than actual values for a real scale scenario. The properties of radiation and ignition of the involved materials do not scale properly in the model scale tests.

In these model scale tests, the main reason for this rapid development is the fire development in the first wood crib. In most of the tests, the first wood crib takes about 3 minutes to reach its peak heat release rate. Before this, the heat release rate increases almost linearly. At about 1 minute and 47 seconds after ignition, the flame tip reaches above the second wood crib, and consequently ignites it. Although the second wood crib is not the main reason responsible for the fire spread to the third wood crib, it may be mainly responsible for a possible fourth wood crib, and the second wood crib may also be responsible for the fire spread of the third wood crib if the peak HHR of the first wood crib is not large enough, i.e. the flame length cannot extend to above the position of the third wood crib.

Ignition time of the second wood crib in Test 4 was delayed, comparing with that in Tests 7 and 8, and in former Test 3 and 4 carried by Ingason [4]. Note that the second wood crib is located beside the Nr 2 vent. In Test4, the opened extraction vent (Nr2) removes the flame and smoke directly, which reduces the temperature beside the second wood crib, consequently, the wood crib was ignited only when the fire grows sufficiently large. This shows that the extraction system can suppress the fire development, i.e. delay the ignition time of secondary objects in the tunnel. The ignition time in Test 4 is about 3 minutes, corresponding to the peak heat release rate of the first wood crib, which suggests that the fire spread can be suppressed with a single extraction system if the peak heat release rate is less than the value in this test.

Comparing data from Test 4 and Test 11, indicates that the two point extraction ventilation system seems to be more effective in suppressing the fire spread than the single extraction system, although the flame lies between the two extraction vents and the zone of not fulfilling the tenability criteria gets larger. However, it should be pointed out that the fire and smoke can be controlled by both systems. Further, the fire spread in a single extraction system will not occur if the second wood crib (vehicle) lies further away from the extraction vent.

Note that in an extraction system, the incoming air flow from both sides flows towards the fire source, which means that it is very difficult for the fire to spread beyond the extraction vent. This is the main reason for the ability of the system to control the fire and smoke flow between the fire source and extraction vent in a single point extraction system, or between two extraction vents in a two point extraction system.

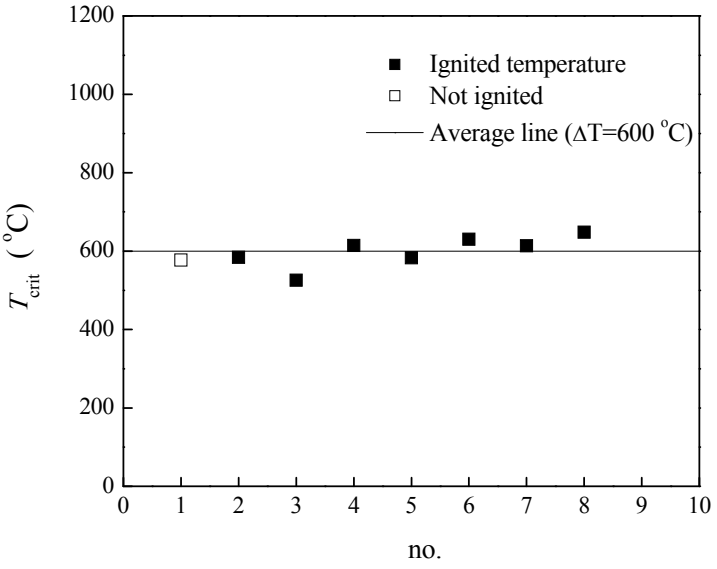

Figure 18 Critical gas temperature beneath the tunnel ceiling when the neighbouring wood crib was ignited.

The distribution of the maximum gas temperatures below the ceiling in the Tests 1, 7 and 8 are given in Figure 19. Only extraction vent Nr 4 was open in these tests. The figure shows that in these tests the flame and smoke upstream of the fire site is controlled, and the temperature distribution downstream of the fire source is different due to the fire spread. The temperature is above 600 °C in a range of 0 ~ 1 m in Test 1, 0 ~ 3 m to Test 7, and 0 ~ 4 m in Test 8. The reason for this variation is that one wood crib in Test 1, two wood cribs in Test 7 and three wood cribs in Test 8. The result of the fire spread is that the zone between the fire source and the extraction vent with high temperature expands thereby extending the area with a dangerous environment for tunnel occupants trying to evacuate from the fire scene. However, the extraction system with the longitudinal ventilation system can confine the fire and smoke between the fire source and the extraction vent efficiently.

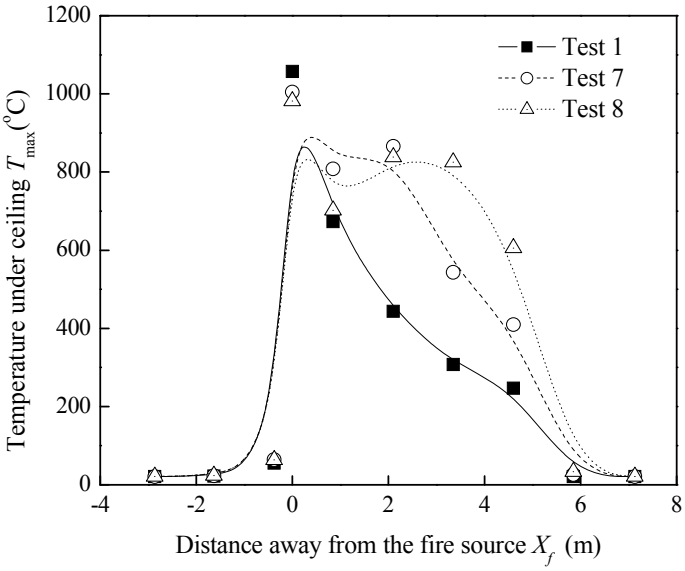

Figure 19 Distribution of the maximum temperature below the ceiling along the model tunnel (Test1, 7 and 8).

6.6 Single point extraction system

In a single point extraction system, as shown in Figure 20, the exhaust volumetric flow rate through the extraction vent is a very important parameter. However, the exhaust volumetric flow rate varies significantly with the gas temperature of the smoke flow. This implies that different exhaust volumetric flow rates will be present at different locations relative to the extraction vent, especially for a large fire which produces smoke flow with very high gas temperatures. Therefore, it is more appropriate to use the exhaust mass flow rate as a characteristic parameter of the extraction vent, rather than the exhaust volumetric flow rate. According to the law of mass conservation, the exhaust mass flow rate can be determined if the ventilation velocities on both sides are known. Here the focus is on the longitudinal ventilation velocities required to prevent the smoke flow on both sides, and not on the exhaust mass flow rate or the exhaust volumetric flow rate.

The principle of an effective single point extraction system is expected to be that sufficient fresh air is supplied from both sides. Consequently, the fire and smoke in the zone between the fire source and the extraction vent point is constrained. The minimum ventilation velocity for each side is defined as the critical longitudinal ventilation velocity upstream of the fire source and the critical longitudinal ventilation velocity downstream of the extraction vent respectively. If the ventilation velocity is smaller than the critical velocity, the phenomenon of back-layering occurs. The distance between the fire source and the smoke front on the left-hand side is defined as the back-layering length upstream of the fire source, L_{us}, and the distance between the extraction vent and the smoke front on the right-hand side is defined as the back-layering length downstream of the extraction vent, L_{ds}, as shown in Figure 20.

The ventilation velocity upstream the fire source, V_{us}, should not be smaller than the critical velocity in a longitudinally ventilated tunnel, due to the fact that there is a little difference between this system and the longitudinal ventilation system upstream of the fire source (on the left hand side). However, the phenomenon of control of smoke flow downstream of the fire source (on the right hand side) is quite different.

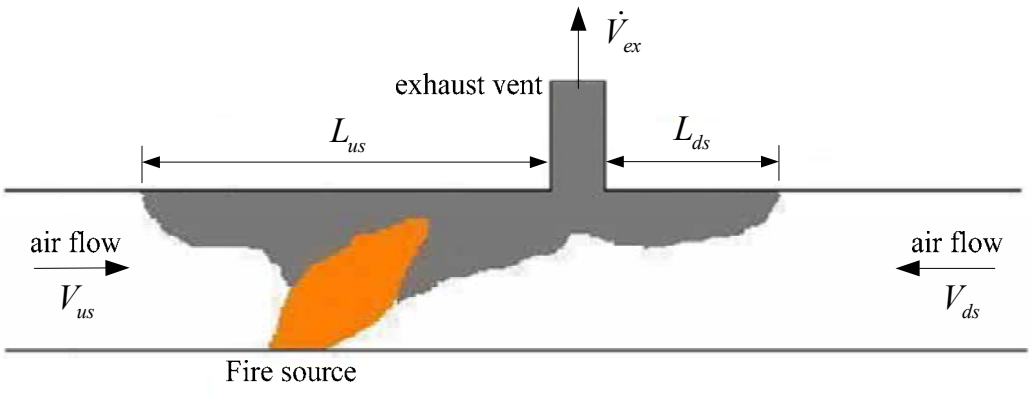

Figure 20 Schematic diagram of single point extraction system.

Eight tests were conducted with a single point extraction system. The heat release rate in these tests was in the range of 52.6 kW to 190.6 kW, corresponding to 133 MW to 484 MW in large scale. The volumetric flow rate is strongly dependent on the temperature due to the linear correlation between the volumetric flow rate and density. The mass flow rate of the extraction vent should be a more reasonable parameter for an extraction system. The mass flow rate of the extraction vent is in a range of 0.06 kg/s to 0.16 kg/s, corresponding to 152 kg/s to 406 kg/s in large scale, or volumetric flow rate of 127 m^3/s

to 338 m^3/s for fresh air. According to the experiment carried out by Lacroix et al [22], the geometry of the extraction vents has little effect on the performance of the extraction ventilation system. The effect of the geometry of an extraction vent is therefore not discussed here.

Figure 21 gives the gas temperature distribution below the ceiling. It is shown that in all the tests the gas temperature near the exits of the model tunnel is nearly equivalent to the ambient temperature. This means the fire and smoke are controlled or confined inside the model tunnel, as observed during the tests. According to analysis of the gas temperature distribution below the ceiling, whether a fire and smoke flow was controlled or not and the range in which the back-layering disappears can be given. The data concerning back-layering length upstream of the fire source and downstream of the extraction vent are given in Table 9.

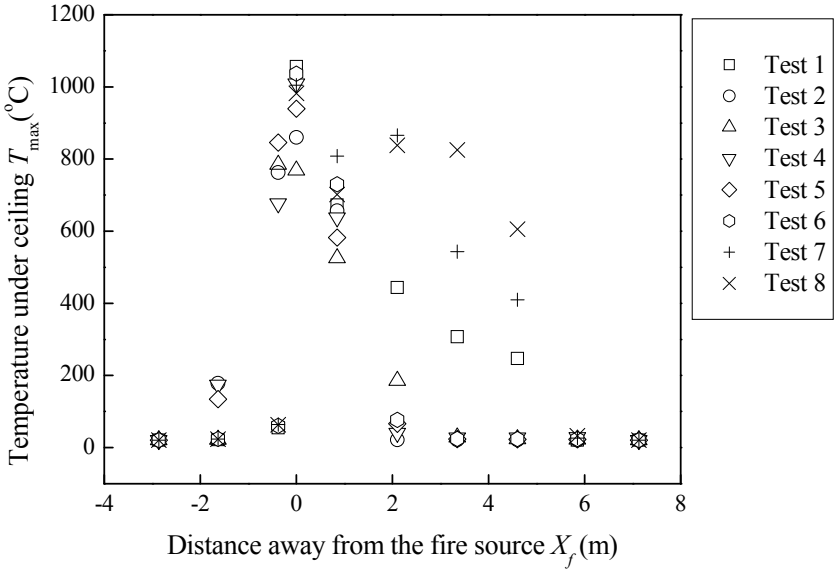

Figure 21 Distribution of maximum gas temperature below the ceiling along the model tunnel (Test1~8)

Firstly, we consider whether there is a critical total mass flow rate or total volumetric flow rate for the extraction vent for control of fire and smoke in an acceptable zone, and secondly whether we simply need to obtain a critical total flow rate, regardless of the longitudinal ventilation velocities on both sides. From Table 9, it is clearly shown that test 5, with an exhaust mass flow rate of 0.06 kg/s, is the worst case. Test 2, 3, and 4 are not optimal either, although the total mass flow rate in the exhaust tube is up to 0.1 kg/s, even 0.15 kg/s. The reason is that the longitudinal ventilation velocities upstream of the fire source in Test 2 and Test 4 are too slow, smaller than 0.4 m/s. The longitudinal ventilation velocities on the both sides are dependent on the ventilation system of the whole tunnel, and the longitudinal ventilation velocity on one side may be very low even though the total flow rate is large. Consequently, we cannot just control the total volumetric flow rate in an extraction vent, regardless of the ventilation velocities on both sides. The incoming air flows with a high enough ventilation velocity on both sides should be supplied to control the smoke from flowing upstream and downstream of the fire source, respectively.

Table 9 The back-layering lengths upstream of the fire source and downstream of the extraction vent.

Test Nr	HRR	Upstream		Downstream		Extraction vent	
	Q_{max}	V_{us}	L_{us}	V_{ds}	L_{ds}	$\dot{V}_{ex}$	$\dot{m}_{ex}$
	kW	m/s	m	m/s	m	m^3/s	kg/s
1	97.7	0.61	<0.38	1.01	<0.5	0.15	0.16
2	65.1	0.25	1.63~2.87	1.27	0*	0.14	0.15
3	52.6	0.26	2.1~3.35	0.73	<0.53	0.09	0.10
4	86.6	0.32	1.63~2.87	1.18	<1.1	0.14	0.15
5	57.6	0.34	1.0~2.1	0.25	0.53~1.77	0.056	0.06
6	83.9	0.59	<0.38	0.90	<1.1	0.14	0.16
7	158.3	0.57	<0.38	1.05	<0.5	0.14	0.17
8	190.6	0.58	<0.38	0.94	<0.5	0.14	0.15

* no back-layering observed during the test.

6.6.1 Upstream of the fire source

From Table 9, it is shown that in Test 2– 5, The longitudinal ventilation velocities upstream of the fire source were about 0.3 m/s, which is about half the critical velocity in a longitudinally ventilated tunnel, and the back-layering lengths are in the range of 5*H*– 15*H*, corresponding to a range of 115 m– 385 m in large scale. In Tests 1, 6, 7, and 8, with longitudinal ventilation velocities of about 0.6 m/s upstream of the fire source and of 0.90 m/s– 1.05 m/s downstream of the extraction vent, the fire and smoke flow can be considered as being controlled completely on both sides. The corresponding exhaust mass flow rate is about 0.15 kg/s, corresponding to 317 kg/s in large scale and maximum heat release rate in these tests is up to 190.6 kW, corresponding to 484 MW in large scale.

We propose that the phenomenon of back-layering upstream of the fire source is the same as the longitudinal ventilation system. In the following, this hypothesis is discussed and evaluated.

Figure 22 shows the back-layering length as a function of the longitudinal ventilation velocity upstream of the fire source for the single point extraction ventilation. In this figure, “smoke” means that the back-layering was observed, and “no smoke” implies no observed smoke at this position, for a given longitudinal ventilation velocity. Consequently, the actual back-layering length should lie between data point for “smoke” and data point for “no smoke”. The data for different heat release rates can be correlated into a single form, as shown in Figure 22. The reason for this is that for a very large fire the back-layering length upstream of the fire source is independent of the heat release rate, i.e. the dimensionless heat release rate is over 0.15 [23]. For a very large fire, the combustion near the fire source is confined due to the tunnel geometry, and the temperature of smoke flow is almost constant. This means that the critical velocity is only a weak function of the fire heat release rate. It is shown in Figure 22 that the back-layering length decreases with the ventilation velocity, and the critical velocity can be considered as about 0.6 m/s for this model tunnel. This value corresponds to 2.9 m/s in large scale.

Further, we can compare the data in Figure 22 to experimental data from model scale tests with longitudinal ventilation for wood crib B [4], as shown in Figure 23. In this

figure, two experimental data indicate that the back-layering length is zero. This implies that there is no back-layering observed in these experiments. These experimental data correlate well with each other.

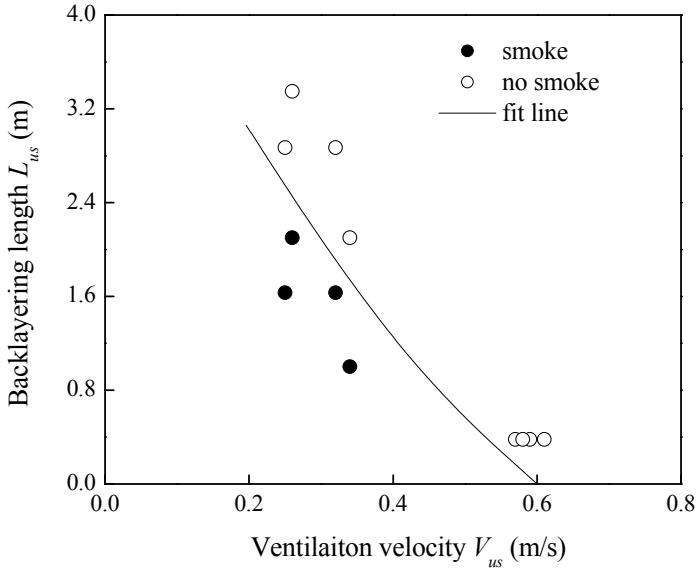

Figure 22 Back-layering length and ventilation velocity upstream of the fire source in model scale tests with single point extraction ventilation.

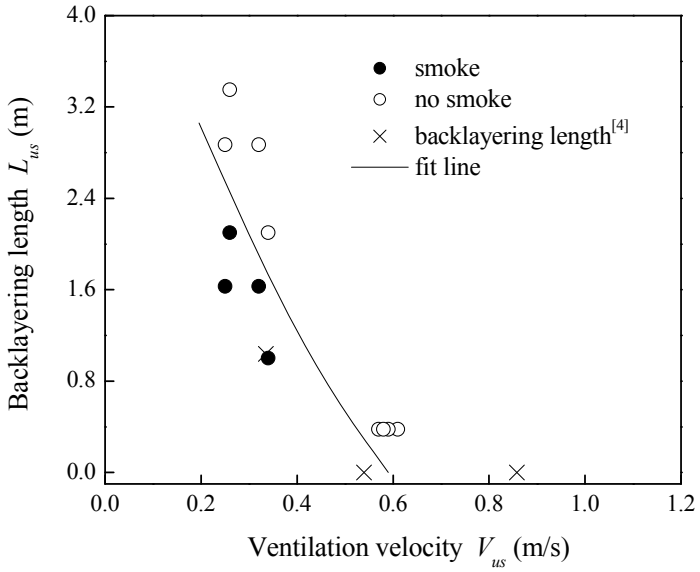

Figure 23 Comparison of experimental data with that from longitudinal ventilation tests.

To compare the data from extraction ventilation tests with all data from longitudinal ventilation tests, the dimensionless ventilation velocity and dimensionless back-layering length are used here [23], due to differences in the geometry of these model tunnels. These two terms are defined as:

$$L_{us}^{*} = \frac{L_{us}}{H} \qquad (18)$$

and

$$V_{us}^{*} = \frac{V_{us}}{\sqrt{gH}} \qquad (19)$$

Figure 24 shows the dimensionless back-layering length as a function of the dimensionless heat release rate upstream of the fire source. Clearly, data form these two tests can be correlated reasonably well with the proposed line. This confirms that there is little difference between this system and the longitudinal ventilation system upstream of the fire source (on the left hand side). The proposed line can be expressed as:

$$L_{us}^{*} = 16.5 \ln(0.39 / V_{us}^{*}) \qquad (20)$$

According to Equation (24), the critical velocity can be easily determined by forcing the dimensionless back-layering length to be zero. Equation (24) has a similar form with the correlation proposed by Li *et al.* [23] but with little different coefficients. The dimensionless critical velocity is 0.39 according to Equation (24) and 0.43 for Li *et al.*'s correlation. The reason for the little lower value is that in Li et al's experiments is that the fire source was set at floor level which was not the case in these experiments.

In order to control the smoke flow between the fire source and the point extraction vent in a single point extraction system, the smoke back-layering has to be prevented. Until now we have known how to control the smoke flow upstream of fire source. Alternatively, it may be better to confine the smoke flow to an acceptable zone, which can reduce the capacity of the exhaust fans and preserve smoke stratification well. This means that only a ventilation velocity smaller that the critical velocity, which is called confinement velocity, is required to be supplied to suppress the back-layering upstream of the fire source. From Figure 24, it is shown that the ventilation velocity can be reduced to half the critical velocity upstream of the fire source if a back-layering length of about 12 times the tunnel height is permitted, and 75 % of critical velocity if a back-layering length of about 5 times the tunnel height is permitted. This can efficiently reduce the capability of the exhaust fans and the size of the extraction vent. NFPA 130 [24] states that the application of tenability criteria at the perimeter of a fire is impractical. The zone of tenability should be defined to apply outside a boundary a certain value away from the perimeter of the fire. This distance should be dependent on the fire heat release rate and could be as much as 30 m. The reason for the instigation of this perimeter is that the environment near the fire site is difficult to keep tenable due to high heat radiation from the fire source. This means that the back-layering lengths of about 4– 5 times the tunnel height can be allowed in most practical cases.

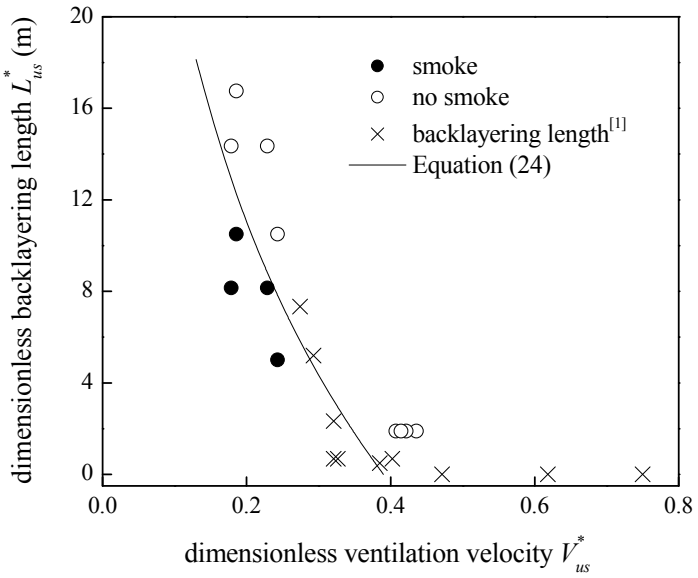

Figure 24 Comparison of experimental data from model scale tests with single point extraction system with that with longitudinal ventilation system.

6.6.2 Downstream of the extraction vent

From Table 9, it is shown that most of experimental data indicate that the back-layering lengths downstream of the extraction vent are <0.5 m. This suggests the smoke flow downstream of the fire source was controlled completely or confined to an acceptable zone in the tests. The corresponding ventilation velocity downstream of the fire source lies mainly in a range of 0.73 m/s to 1.27 m/s.

It also seems to be that the back-layering length downstream of the fire source is independent of the heat release rate for a very large fire in a tunnel. The back-layering lengths are plotted as a function of the ventilation velocity downstream of the extraction vent, as shown in Figure 25. If the back-layering length is <0.5 m, we can roughly regard the smoke flow as being controlled completely. From Figure 25, it is shown that the critical velocity for smoke control downstream of the fire source (or downstream of the extraction vent) when the back-layering disappears was in a range of 0.7 m/s– 1.0 m/s. A value of 0.8 m/s should be sufficient to prevent the smoke flow downstream of the extraction vent. Note that this value is about 1.3 times the critical velocity in a longitudinally ventilated tunnel.

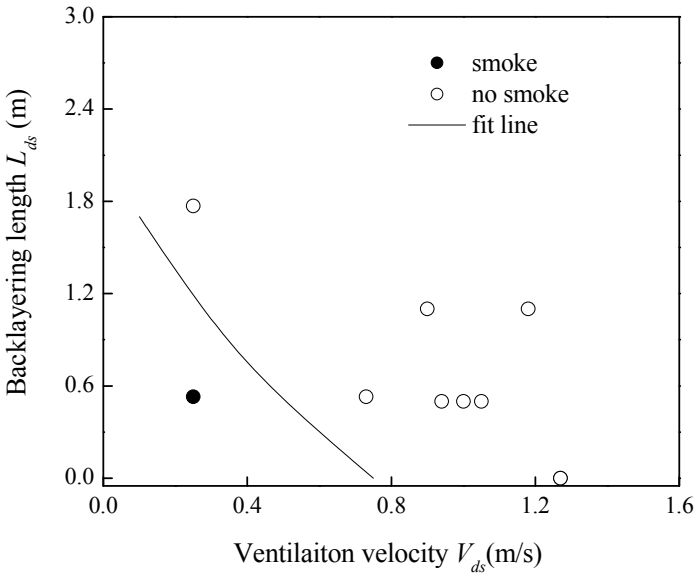

Figure 25 Back-layering length and ventilation velocity downstream of the fire source in model scale tests with single point extraction ventilation.

Based on the above analysis, it can be concluded that in a single point extraction system, fire and smoke flows upstream and downstream of the fire source can be fully controlled, if the ventilation velocity upstream of the fire source is up to 0.6 m/s (2.9 m/s in large scale), and the ventilation downstream of the extraction vent is above about 0.8 m/s (3.8 m/s in large scale), for a HGV fire or even several HGVs with heat release rate up to 484 MW. Under these conditions, the mass flow rate through the extraction vent is about 0.134 kg/s, corresponding to 340 kg/s in large scale, i.e. a volumetric flow rate of 284 m^3/s for fresh air in large scale. This indicates that there is a critical mass flow rate of the extraction vent or a critical total volumetric flow rate of the incoming air flows from both sides, however, above all, the ventilation velocities on both sides should fulfil the requirements for control of fire and smoke flow between the fire source and the extraction vent. Note that the critical velocity required to prevent smoke back flow upstream of the fire source is nearly equal to the critical velocity in a longitudinally ventilated tunnel, and the critical velocity downstream of the extraction vent can be regarded as 1.3 times the critical velocity in a longitudinally ventilated tunnel.

Further, smaller ventilation velocities on both sides can be used for just confining the fire and smoke flow in acceptable zones. This can efficiently reduce the capacity of the extraction vent and the geometry of the extraction vent. However, the ventilation velocity cannot be too small, i.e. not be smaller than 0.75 times the dimensionless ventilation velocity to prevent the fire and smoke flow upstream of the fire source from spreading to a distance of about 5 times the tunnel height.

Data from tests with different vent geometries show that the fire and smoke flow in tests with a vent geometry of 0.26 m × 0.1 m can also be controlled or confined to an acceptable zone for a single point extraction system. However, the vent geometry of 0.26 m × 0.2 m is recommended, corresponding to 6 m × 4.6 m in large scale, since it is easier to keep the ventilation velocity through the vent at a low level.

6.7 Two point extraction system

Figure 26 gives a schematic diagram of a two point extraction system. It is designed to be capable of producing a dual inward flow to control the fire and smoke flow. The ventilation velocity across the fire source is dependent on the ventilation system of the specific tunnel. In most cases the system is not symmetrical, and there is always a longitudinal flow across the fire source. In that case the fire source leans toward one side, as shown in Figure 26. In the zone between the two extraction vents, smoke stratification is preserved well if the ventilation velocity across the fire source is very small compared to the critical velocity in a longitudinal flow for a certain heat release rate. Of course, the gas temperature in this zone is very high. However, the dangerous region can be confined by reducing the spacing distance between two extraction vents, and the environment in the near-field region of the fire site is not the focal point. Here we focus on how to control of the fire and smoke flow on both sides. Three model scale tests with this system were carried out.

For a two point extraction system, as shown in Figure 26, the back-layering length on the left-hand side is defined as the distance between the smoke front and the left extraction vent. In a similar way the definition of the back-layering length on the right-hand side can be made.

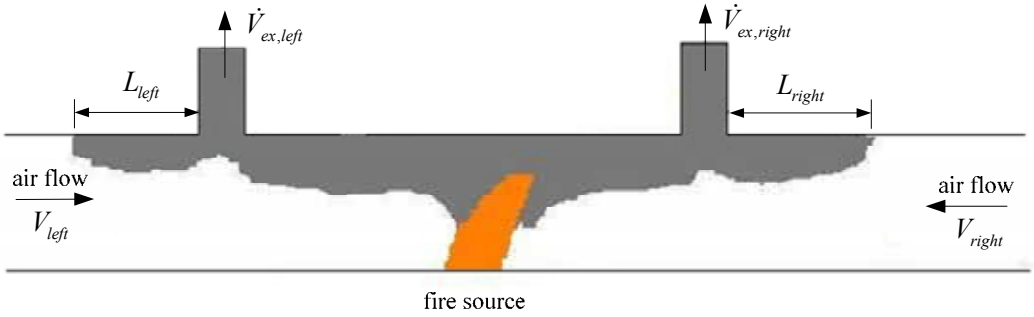

Figure 26 Schematic diagram of a two point extraction system.

Figure 27 shows the distribution of the maximum gas temperature below the ceiling along the model tunnel in these tests with two point extraction ventilation system. According to the gas temperature distribution, the back-layering lengths on both sides of the tunnel can be given, as shown in Table 10. During these tests, only the total mass flow rate and total volumetric flow rate of the extraction vents are measured.

The ventilation velocity of the air flow near the fire site (between the fire source and the exhaust vents) is hard to measure due to its low value. However, according to the observation during these tests, the fire plume did not lean toward any side, which suggests that the fires are nearly symmetrical. This means that the ventilation flow should be symmetrical too. The scenario is similar to a fire in a tunnel with natural ventilation or an enclosure with large windows and roof extraction vents. The fresh air is introduced from both portals by the extraction system and the fire, and it flows towards the fire in the lower layer. A characteristic of this system is the lower heat release rate due to the absence of forced ventilation. It can be seen from Table 10 that the heat release rates are close to each other, i.e. about 54 kW, corresponding to 137 MW in large scale, for these tests with a two point extraction system.

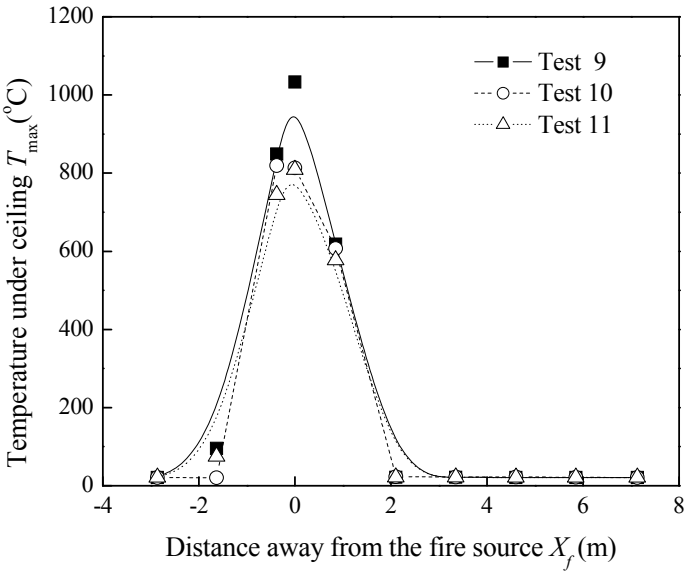

Figure 27 Distribution of maximum temperature below the ceiling along the model tunnel (Test 9, 10 and 11)

Due to the symmetry of the scenario in these tests, data for both sides can be plotted in a single form. Figure 28 shows the back-layering length as a function of the ventilation velocity in the model scale tests with two point extraction ventilation. It can be concluded that the ventilation velocity on each side of the vents should be greater than about 0.6 m/s, corresponding to 2.9 m/s in large scale, to completely confine the fire and smoke flow in the zone between two extraction vents. Note that this value is almost equal to the critical velocity in a longitudinally ventilated tunnel. Of course, it is more reasonable to simply confine the fire and smoke to an acceptable zone, i.e. to permit back-layering to some extend. It is also shown that a value of 0.52 m/s, corresponding to 2.5 m/s in large scale, can prevent the fire and smoke flow from spreading to a distance of 3 times the tunnel height.

Table 10 Back-layering length on both sides of the tunnel.

Test Nr	HRR	Left		Right		Extraction vent	
	Q_{max}	V_{left}	L_{left}	V_{right}	L_{right}	$\dot{V}_{ex,total}$	$\dot{m}_{ex,total}$
	kW	m/s	m	m/s	m	m^3/s	kg/s
11	51.4	0.40	0.53~1.77	0.79	<1.1	0.09	0.11
12	52.6	0.52	<0.53	0.99	<1.1	0.14	0.16
16	57.6	0.36	0.53~1.77	0.81	<1.1	0.09	0.10

If the same intervals between the extraction vents are used in a tunnel, obviously, the smoke zone of a two point extraction system will inherently wider, compared with a single point extraction system. Extraction vents for a single point extraction system can be arranged with larger intervals and larger geometry.

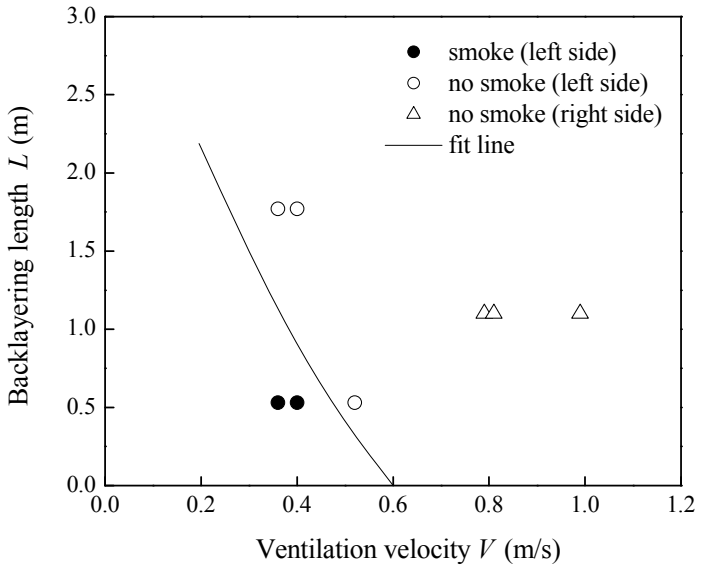

Figure 28 Back-layering length and ventilation velocity in model scale tests with two point extraction ventilation.

7 Conclusions

Fire tests were carried out in a 1:23 model scale tunnel. Fire loads corresponding to a HGV trailer were simulated using wood cribs of two different sizes. Point extraction ventilation system were tested under different fire conditions. The parameter tested were the number of wood cribs, the longitudinal ventilation velocity, ceiling height and the arrangement of the exhaust openings and the exhaust capacity. The fire spread between wood cribs with a free distance corresponding to 15 m in large scale was tested. In these tests, the heat release rate, the fire growth rate, fire spread, flame length, and gas temperatures beneath tunnel ceiling were also tested.

The model scale trials show that extraction vents at ceiling level provides very effective control of smoke in a large fire in a tunnel. The extraction vent flows and the inward air flows that are thereby produced in the tunnel will constrain the smoke within the zone between the extraction vent and the fire source in a single extraction system, or between the two opened extraction vents in a two point extraction system. This suggests an encouraging fact that even a very large fire, i.e. a HGV fire, can be controlled by appropriate extraction ventilation system.

An effective extraction system has been shown to be established when sufficient fresh air flows are supplied from both sides, to confine the fire and smoke to the zone between the fire source and the extraction vent for a single point extraction ventilation system, or between two extraction vents for a two point extraction ventilation system. The fire and smoke flow could not be confined if only the flow rate in the extraction vents were controlled, regardless of the ventilation velocities on both sides. In a single extraction system, fire and smoke flows upstream and downstream of the fire source can be fully controlled, if the ventilation velocity upstream of the fire source is up to 0.6 m/s (2.9 m/s in large scale), and the ventilation downstream of the extraction vent is above about 0.8 m/s (3.8 m/s in large scale), for a HGV fire or even several HGVs with heat release rate up to about 500 MW. Under these conditions, the mass flow rate through the extraction vent is about 0.134 kg/s, corresponding to 340 kg/s in large scale, i.e. the volumetric flow rate of 284 m^3/s for fresh air in large scale. In a two point extraction system, the longitudinal ventilation velocity on the each side should be greater than about 0.6 m/s, corresponding to 2.9 m/s in large scale, to completely confine the fire and smoke flow in the zone between the two extraction vents.

The extraction system will also significantly reduce the risk of the fire spreading outside the fire and smoke zone, as a result of removing the flame and heat of the fire from the tunne. However, in the near proximity of the fire site, the fire spread cannot be prevented. Fire spread to a neighbouring wood crib occurs when the gas temperature below the ceiling and above the wood crib rises to about 600 °C. Experimental data suggest that in a real tunnel, a vehicle 15 m behind a (simulated) burning HGV would catch fire in about nine minutes, and a third vehicle 15 m further behind the second vehicle would catch fire in about three more minutes, mainly due to heat from the first vehicle. The trials clearly show the snowball effect resulting from HGVs close to each other. The fire spread rate is in quite good agreement with the Runehamar tunnel trials, where 'targets' were placed 15 m from the fire in order to simulate the effects of possible spread of the fire.

The heat release rate, the fire growth rate, the maximum gas temperature rise beneath the ceiling, the flame length and the heat flux were also investigated. A stoichiometric line correlates well with the experimental data of the fuel mass loss rate per unit fuel surface area when the ventilation velocity is less than 0.35 m/s. The fuel mass loss rate per unit fuel surface area is not sensitive to the ventilation velocity for higher ventilation velocity. This means there is an upper limit of about 0.13 $kg/(m^2s)$ for the wood cribs used here,

which correlates well with the ideal value found by Tewarson and Pion based on the assumption that all heat losses were reduced to zero.The fire growth rate increases linearly with the ventilation velocity. The fire growth rate is nearly 3 times larger than that in free burn tests, when the longitudinal ventilation velocity equals to 1 m/s, corresponding to 4.8 m/s in large scale. The dimensionless maximum temperature rise lies mainly in a range of 2.9– 3.75, corresponding to the maximum temperature rise of 850 °C– 1100 °C. It seems that the maximum gas temperature beneath the tunnel ceiling is a weak function of the heat release rate and the ventilation velocity for a HGV fire with heat release rate more than 100 MW. The flame length is a weak function of the ventilation velocity, and the experimental data are correlated well with the dimensionless heat release rate defined in Equation (17). The total heat flux can be estimated well using average temperature, and another correlation using the gas temperature beneath the tunnel ceiling is also presented.

8 References

1. Ingason, H. and Lönnermark A., *Heat Release Rates from Heavy Goods Vehicle Trailers in Tunnels.* Fire Safety Journal, 2005. **40**: p. 646-668.
2. Lönnermark, A. and Ingason H., *Gas Temperatures in Heavy Goods Vehicle Fires in Tunnels.* Fire Safety Journal, 2005. **40**: p. 506-527.
3. Lönnermark, A. and Ingason H., *Fire Spread and Flame Length in Large-Scale Tunnel Fires.* Fire Technology, (in press).
4. Ingason, H., *Model Scale Tunnel Fire Tests - Longitudinal ventilation*. 2005, SP Swedish National Testing and Research Institute: Borås, Sweden.
5. Vauquelin, O. and Telle, D., *Definition and experimental evaluation of the smoke "confinement velocity" in tunnel fires*. Fire Safety Journal, 2005. 40: p. 320-330.
6. Vauquelin, O. and Mégret, O., Smoke extraction experiments in case of fire in a tunnel. Fire Safety Journal, 2002. 37: p. 525-533.
7. Heskestad, G. *Modeling of Enclosure Fires*. in *Proceedings of the Fourteenth Symposium (International) on Combustion*. 1972. The Pennsylvania State University, USA: The Combustion Institute.
8. Quintiere, J. G., *Scaling Applications in Fire Research.* Fire Safety Journal, 1989. **15**: p. 3-29.
9. Heskestad, G., *Physical Modeling of Fire.* Journal of Fire & Flammability, 1975. **6**: p. p. 253 - 273.
10. Saito, N., Yamada, T., Sekizawa, A., Yanai, E., Watanabe, Y., and Miyazaki, S., *"Experimental Study on Fire Behavior in a Wind Tunnel with a Reduced Scale Model"*, *Second International Conference on Safety in Road and Rail Tunnels*, 303-310, Granada, Spain, 3-6 April, 1995.
11. Tewarson, A., *Generation of Heat and Chemical Compounds in Fires*, in *The SFPE Handbook of Fire Protection Engineering*, P.J. DiNenno, et al., Editors. 2002, National Fire Protection Association: Quincy, MA, USA. p. 3-82 -- 3-161.
12. Janssens, M. and W.J. Parker, *Oxygen Consumption Calorimetry*, in *Heat Release in Fires*, V. Babrauskas and T.J. Grayson, Editors. 1995, E & FN Spon: London, UK. p. 31-59.
13. Ingason, H., *Fire Dynamics in Tunnels*, in *The Handbook of Tunnel Fire Safety*, R.O. Carvel and A.N. Beard, Editors. 2005, Thomas Telford Publishing: London. p. 231-266.
14 Hermann Schlichting. *Boundary-layer theory* (6th edition). McGraw hill. New York. 1987. p. 596-600.
15. McCaffrey, B. J. and G. Heskestad, *Brief Communications: A Robust Bidirectional Low-Velocity Probe for Flame and Fire Application.* Combustion and Flame, 1976. **26**: p. 125-127.
16. Croce, P. A., and Xin, Y., *Scale modeling of quasi-steady wood crib fires inenclosures*, Fire Safety Journal. 2005, **40,** 245-266.
17. Tewardson A., Pion, R. F. *Flammability of plastics*. I. Burning intensity. Combustion and Flame. 1976, 26,85-103.
18. McCaffrey B. J. *Purely buoyant diffusion fames: some experimental results*. National Bureau of Standards. NBSIR. 1979; 79-1910.
19. Kurioka H., Oka Y., Satoh H., Sugawa O. *Fire properties in near field of square fire source with longitudinal ventilation in tunnels*. Fire Safety Journal. 2003,38: 319-340.
20. *Memorial Tunnel Fire Ventilation Test Program-Test Report*, Massachusetts Highway Department and Federal Highway Administration, 1995.
21. *Fires in Transport Tunnels: Report on Full-Scale Tests*. 1995, edited by Studiensgesellschaft Stahlanwendung e. V. : Düsseldorf, Germany.

22. Lacroix, D., Chasse, P. and Muller T. *Small scale study of smoke trap door system*. The 8th International symposium on aerodynamics and ventilation of vehicle tunnels. BHR Group. Liverpool, UK, 1994. p. 409-438.
23. Li Y. Z., Lei B. and Ingason H. *Study of critical velocity and backlyaering length in longitudinally ventilated tunnel fires*. Fire Safety Journal, 2009 (Submitted).
24. NFPA130. *Standard for fixed guideway transit and passenger rail system*. National Fire Protection Association. Quincy, MA. 2009.

Appendix A Test Results – Extraction ventilation

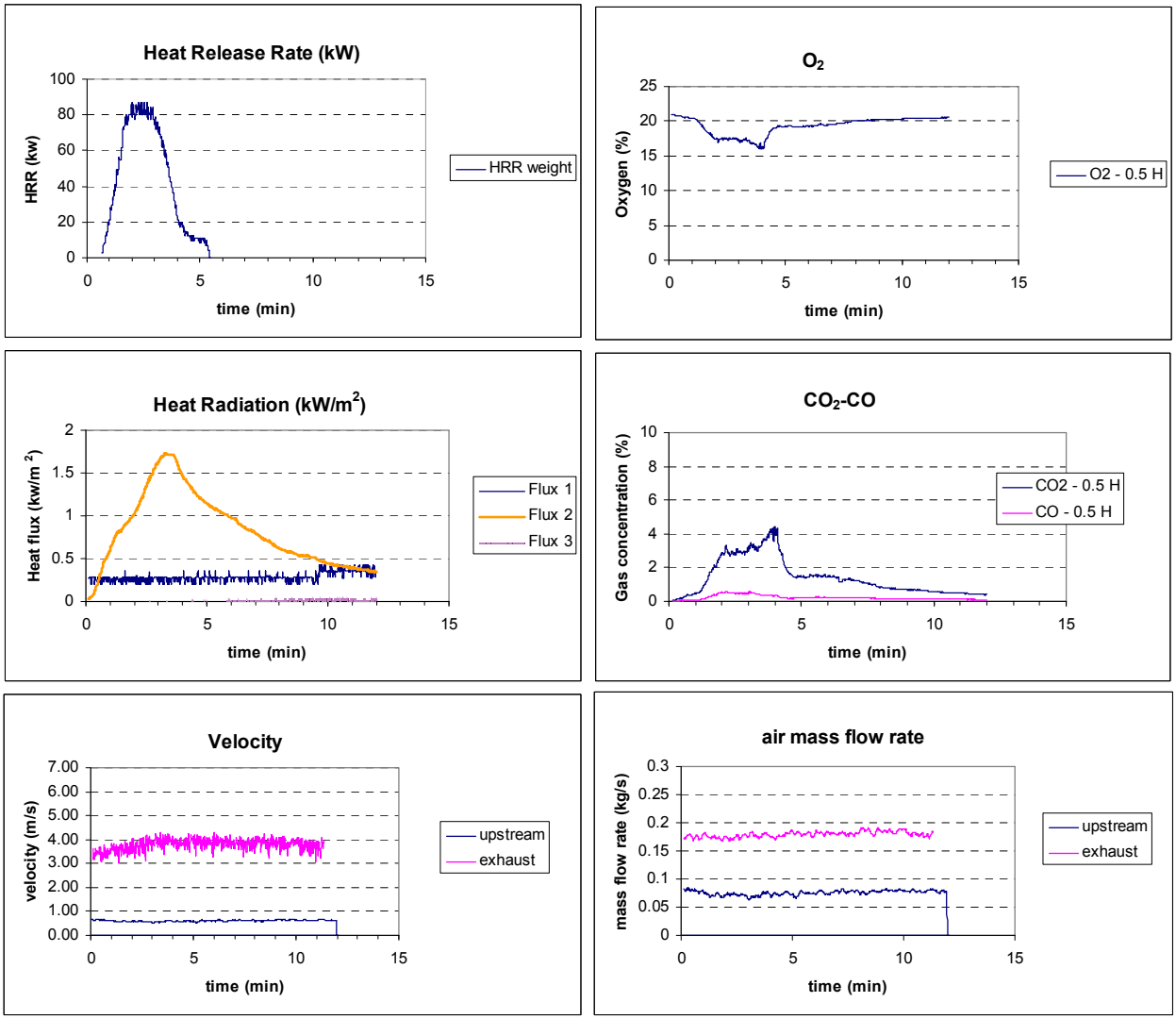

Figure A1 Measured energy released of the initial wood crib, gas concentrations, heat fluxes and air flow in Test 1.

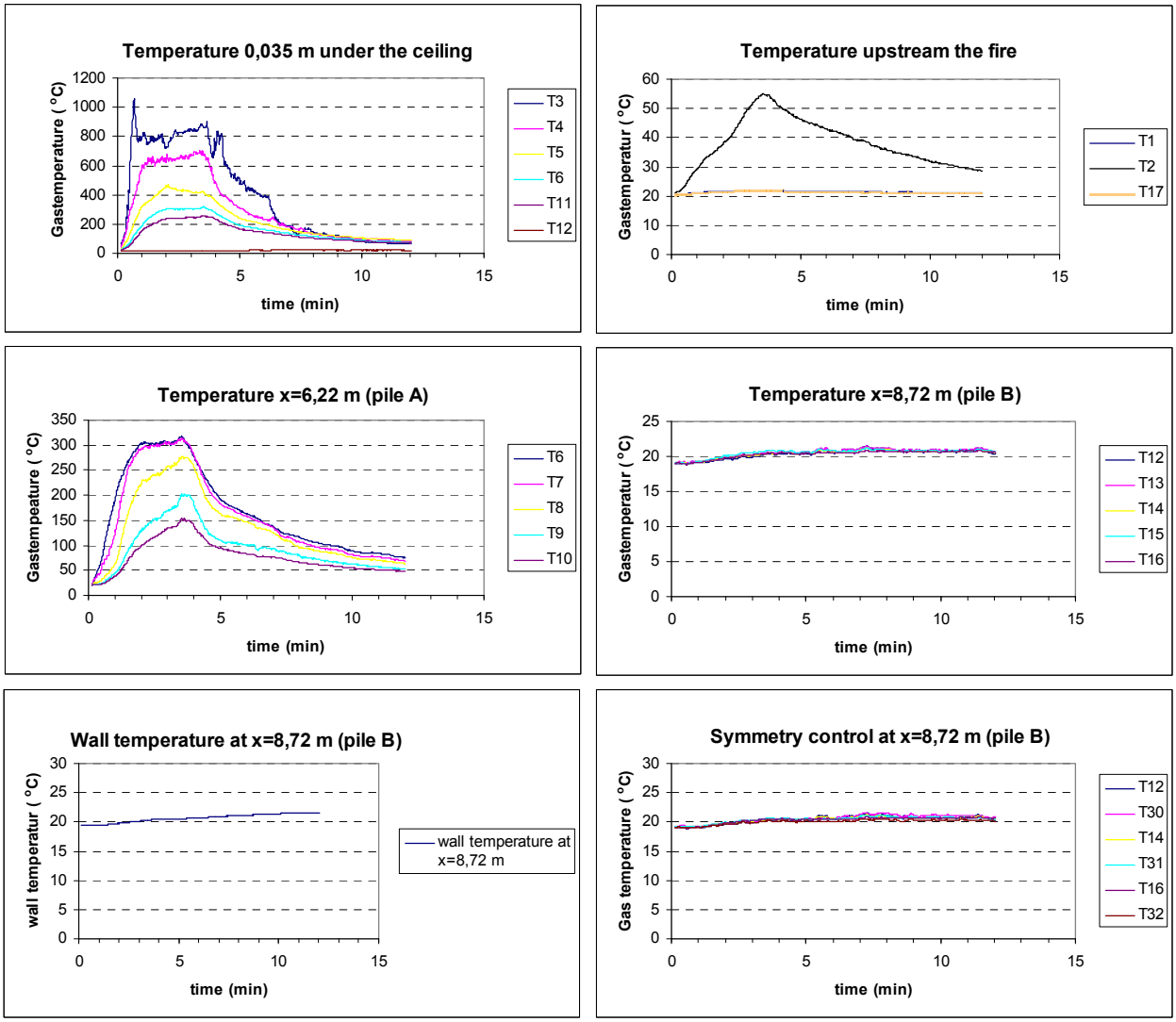

Figure A2 Measured temperatures in Test 1.

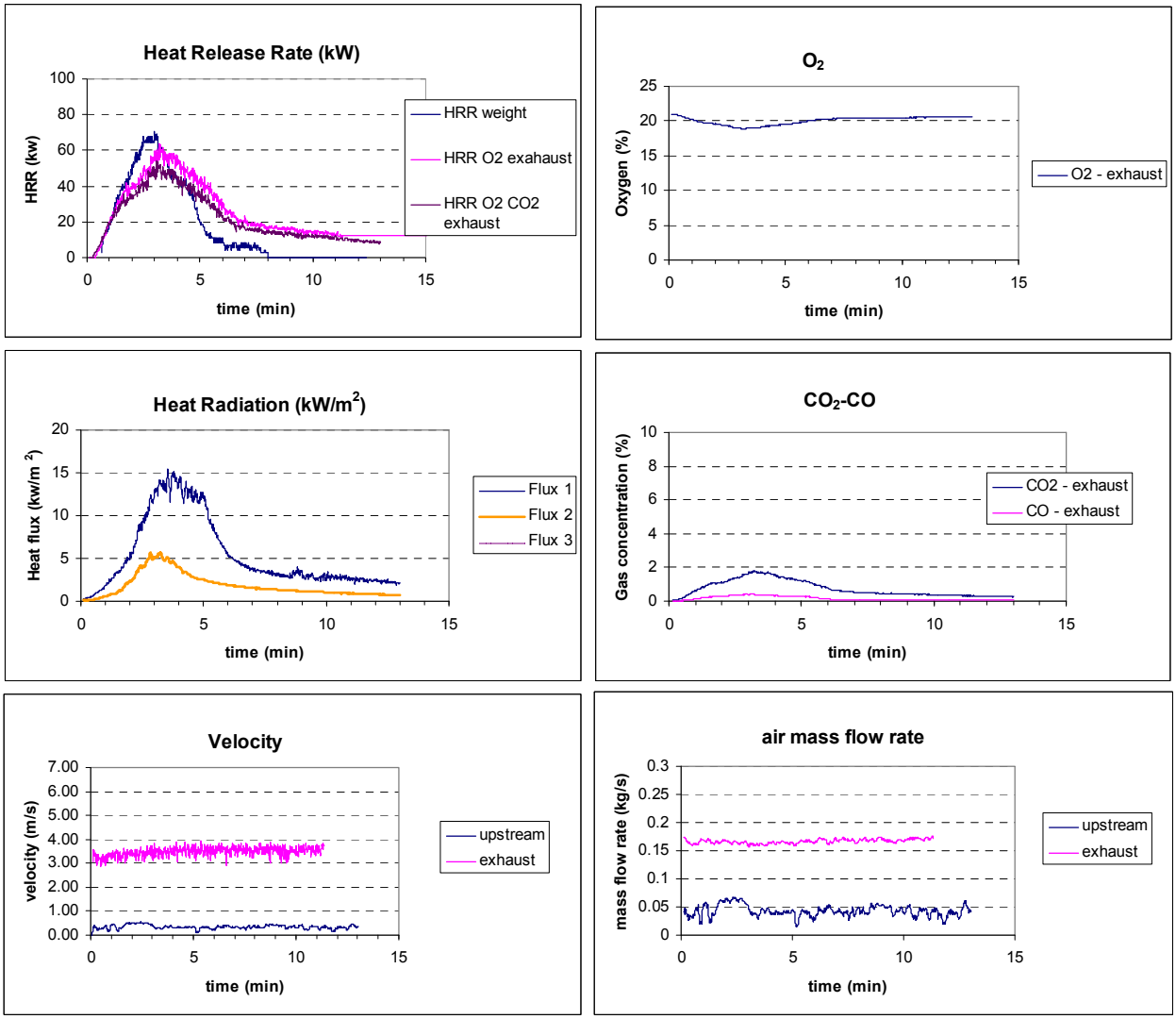

Figure A3 *Measured energy released of the initial wood crib, gas concentrations, heat fluxes and air flow in Test 2.*

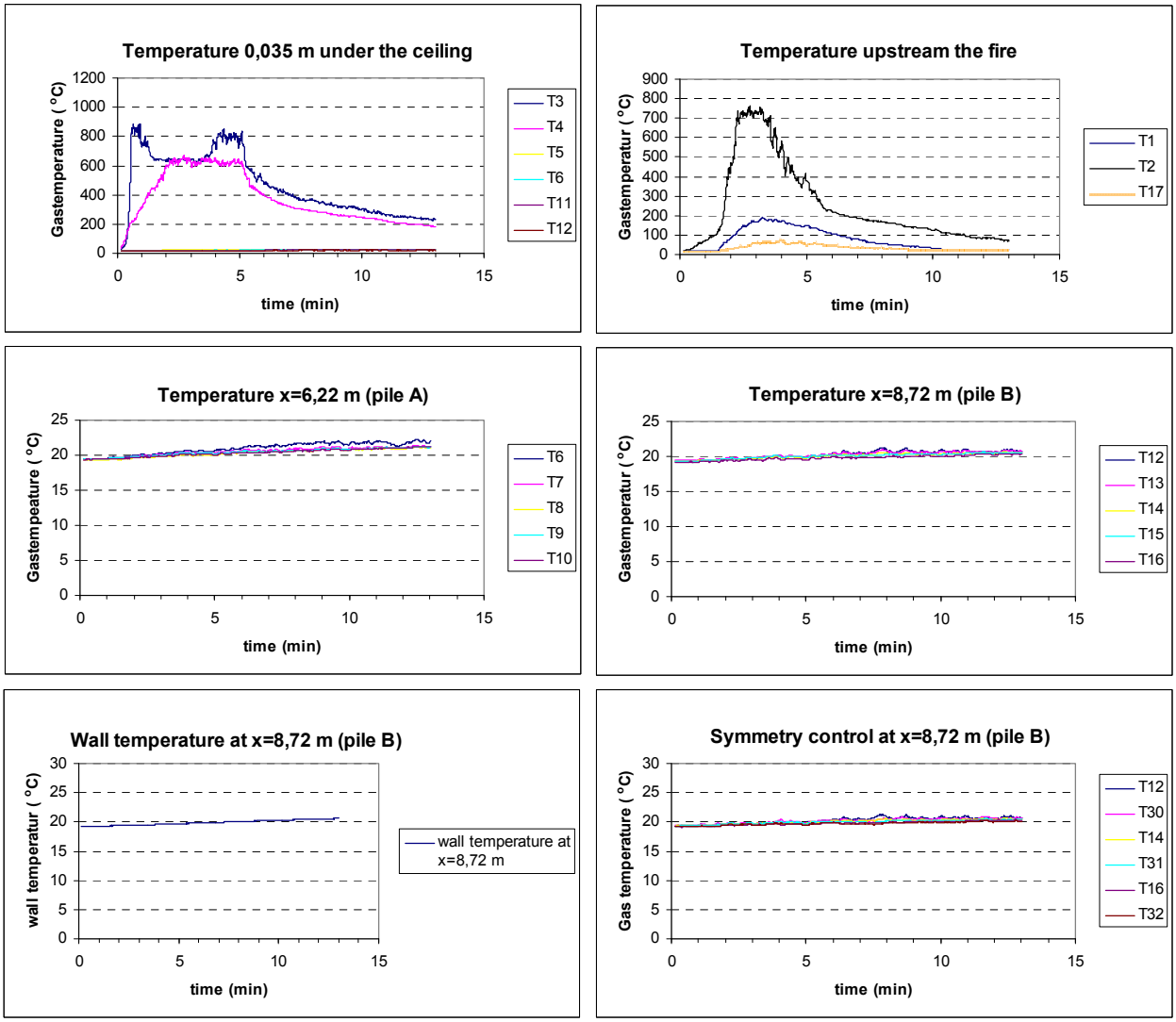

Figure A4 Measured temperatures in Test 2.

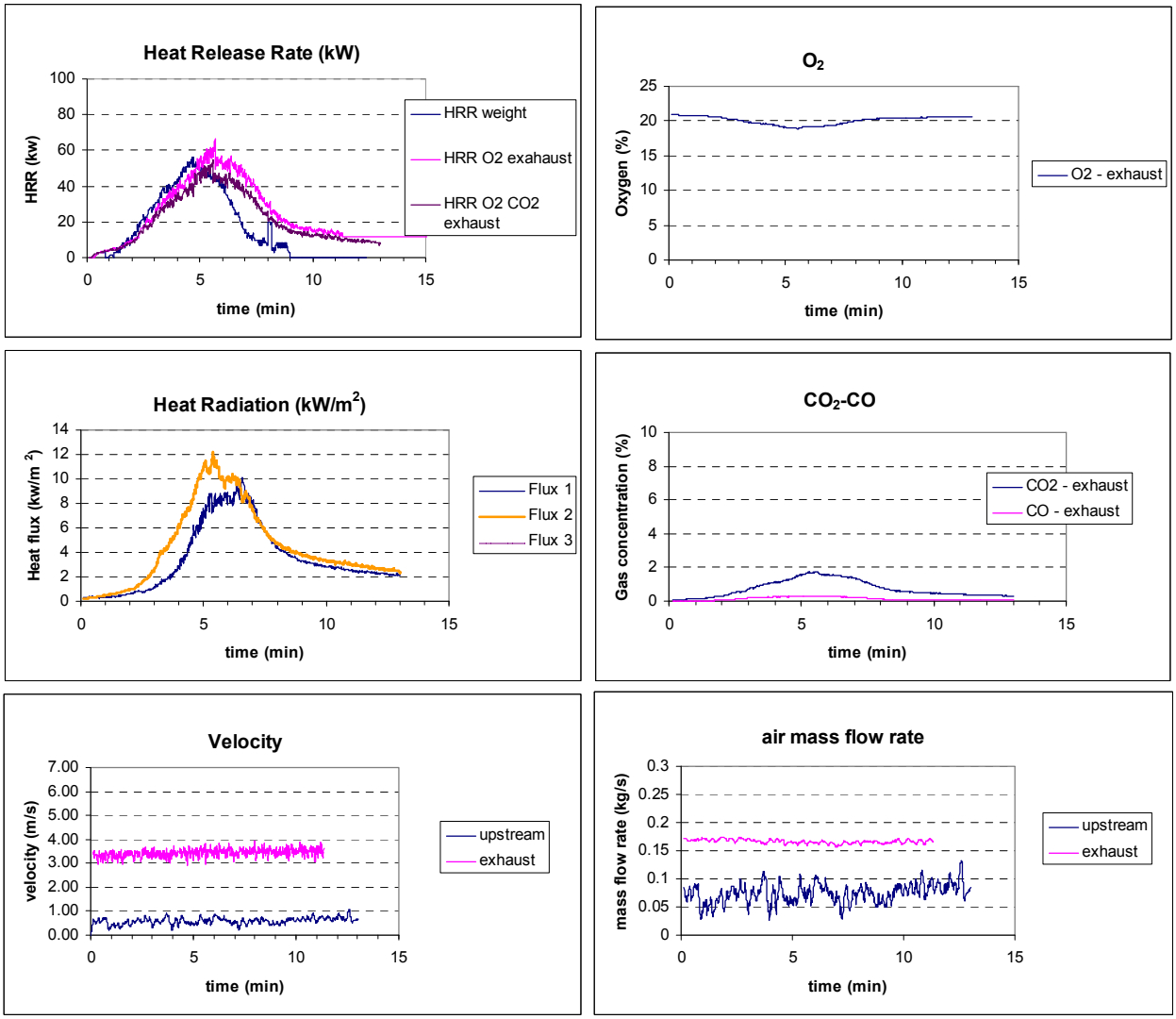

Figure A5 *Measured energy released of the initial wood crib, gas concentrations, heat fluxes and air flow in Test 3.*

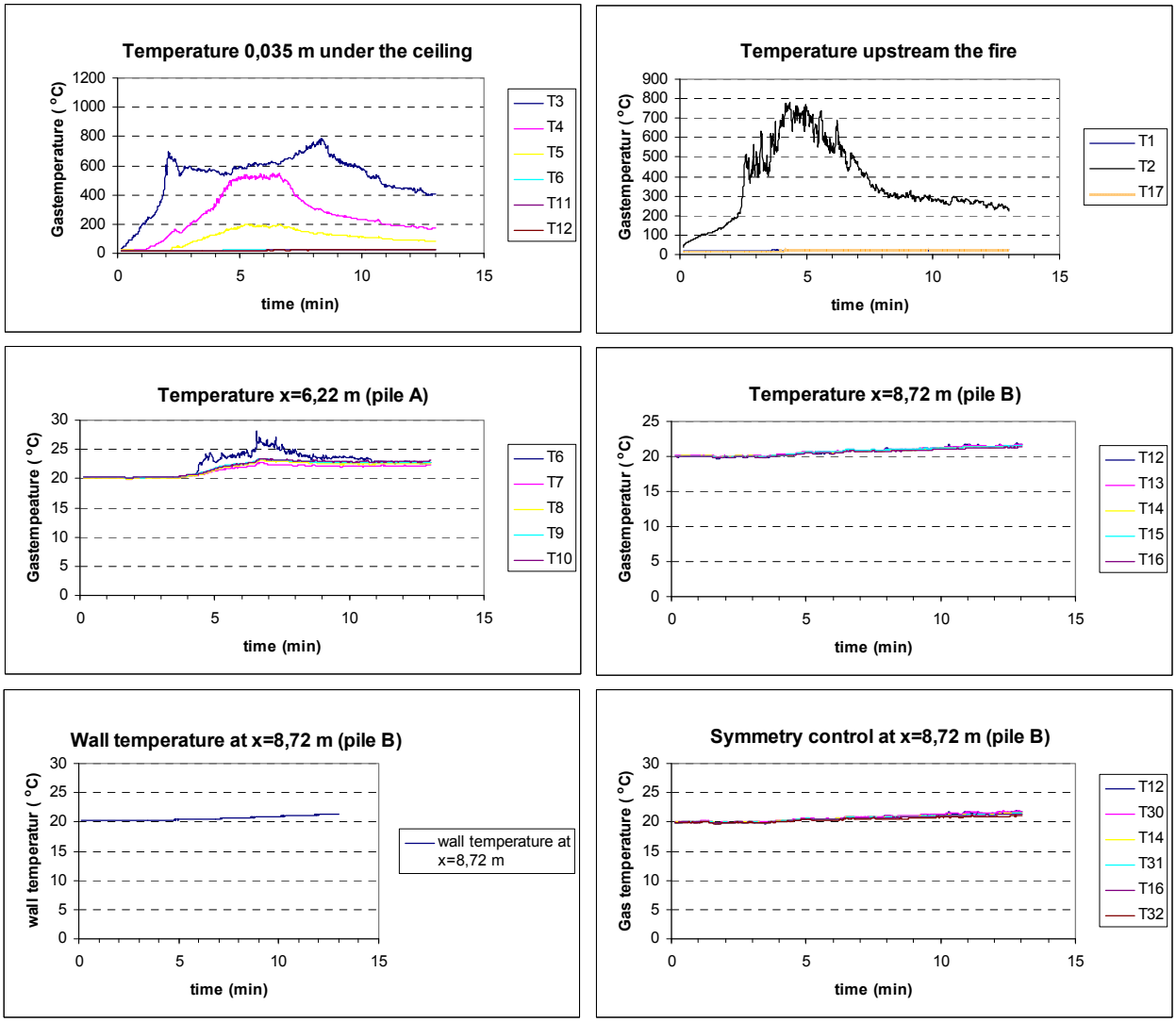

Figure A6 Measured temperatures in Test 3.

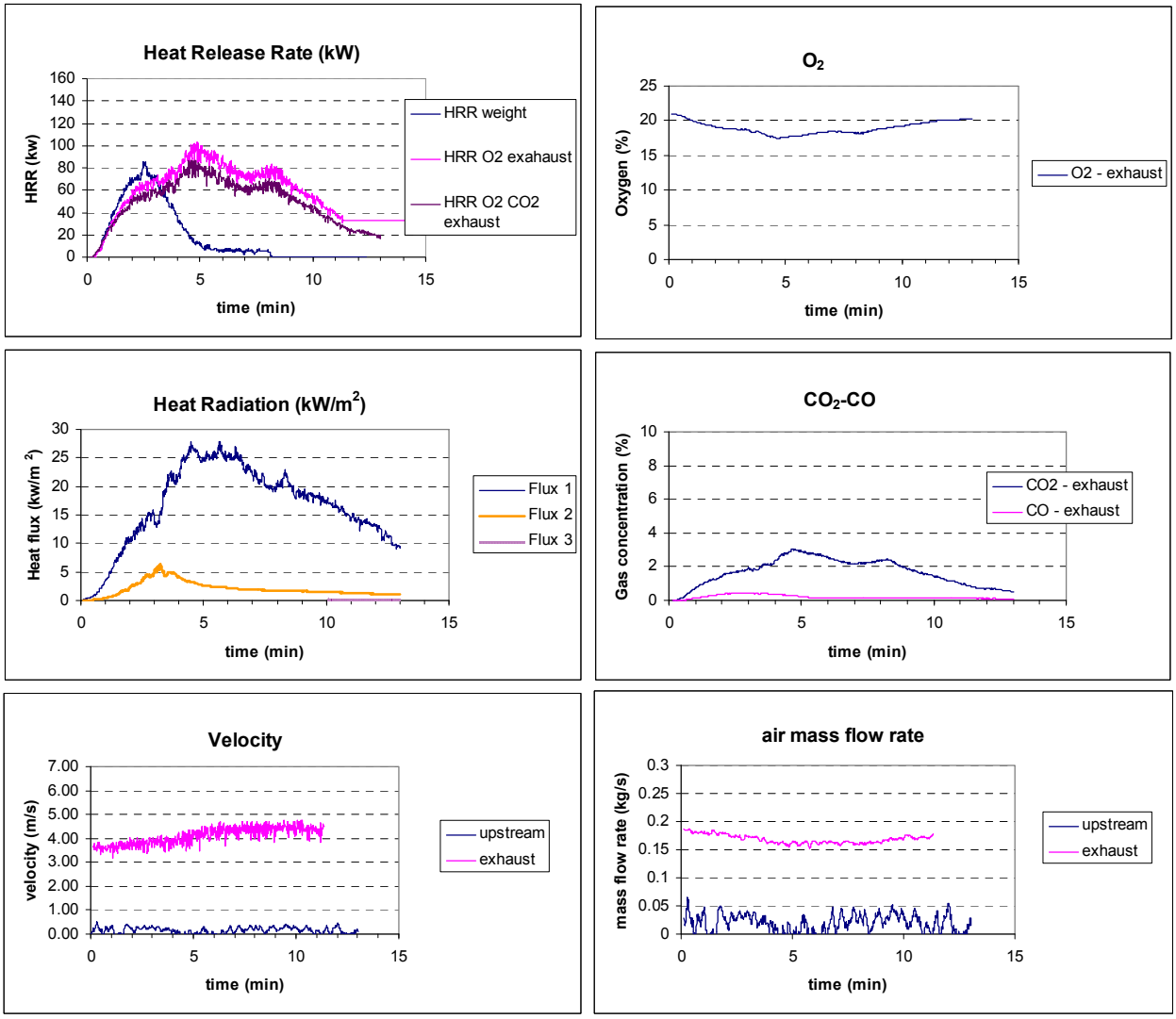

Figure A7 *Measured energy released of the initial wood crib, gas concentrations, heat fluxes and air flow in Test 4.*

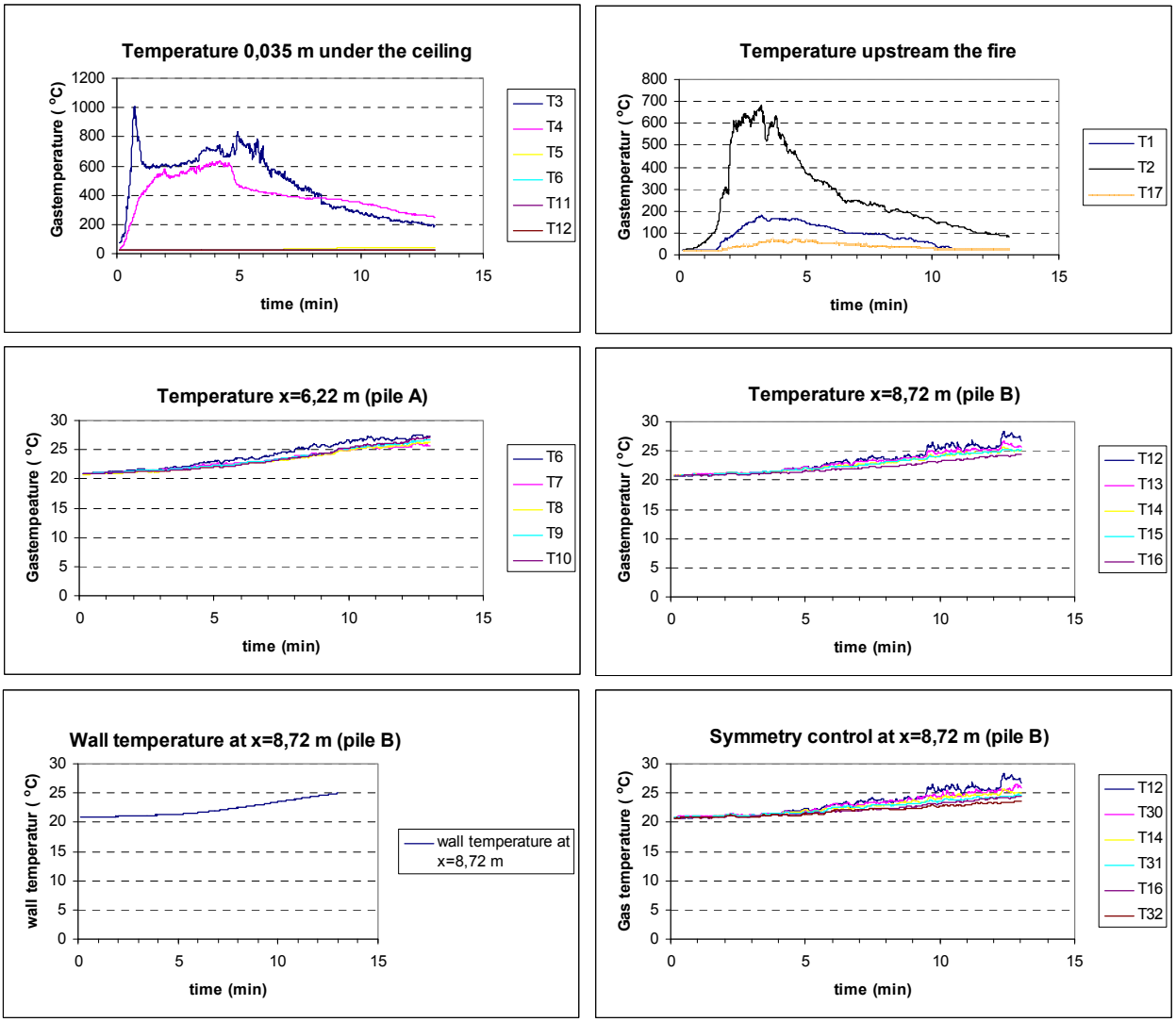

Figure A8 Measured temperatures in Test 4.

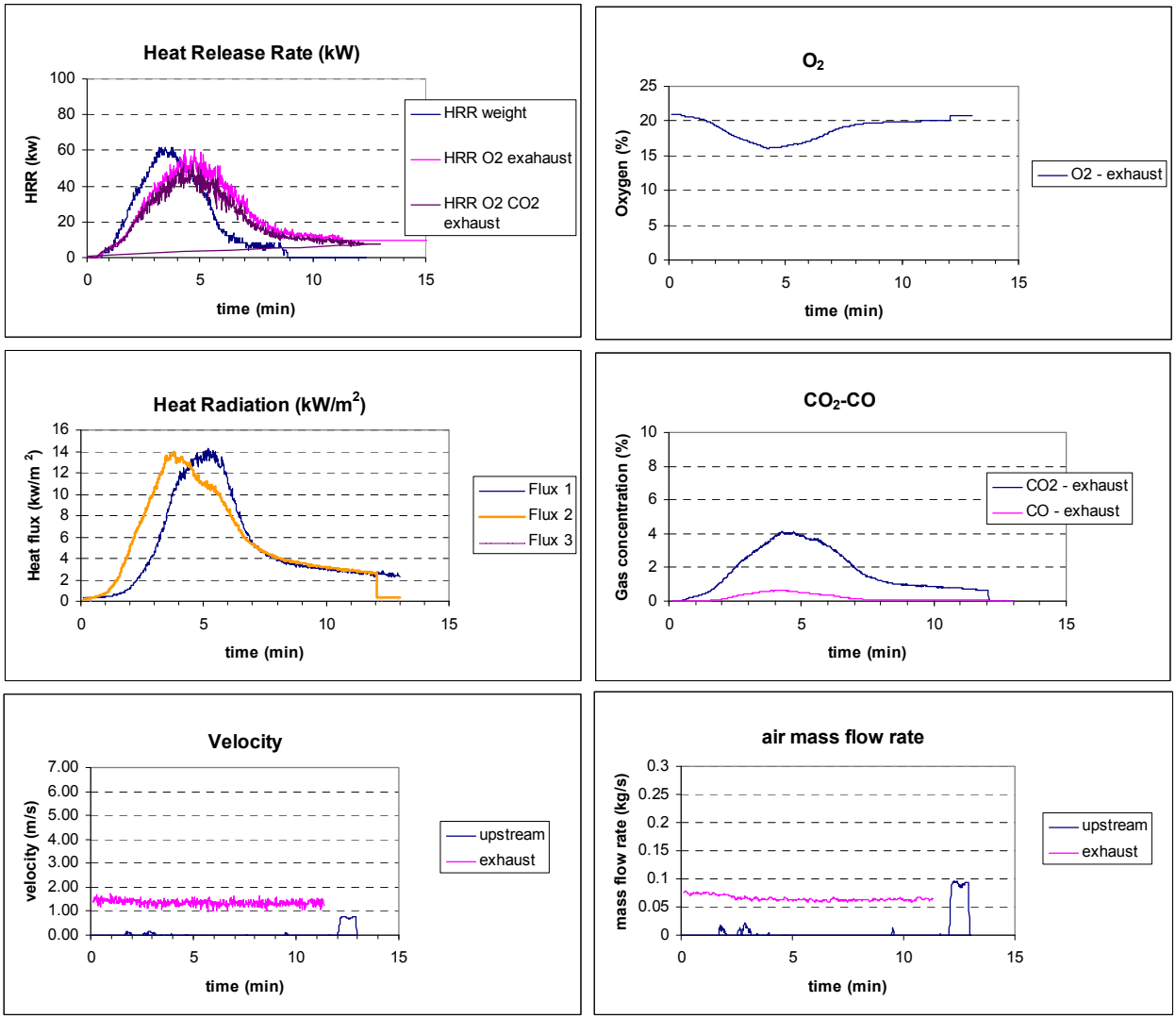

Figure A9 *Measured energy released of the initial wood crib, gas concentrations, heat fluxes and air flow in Test 5.*

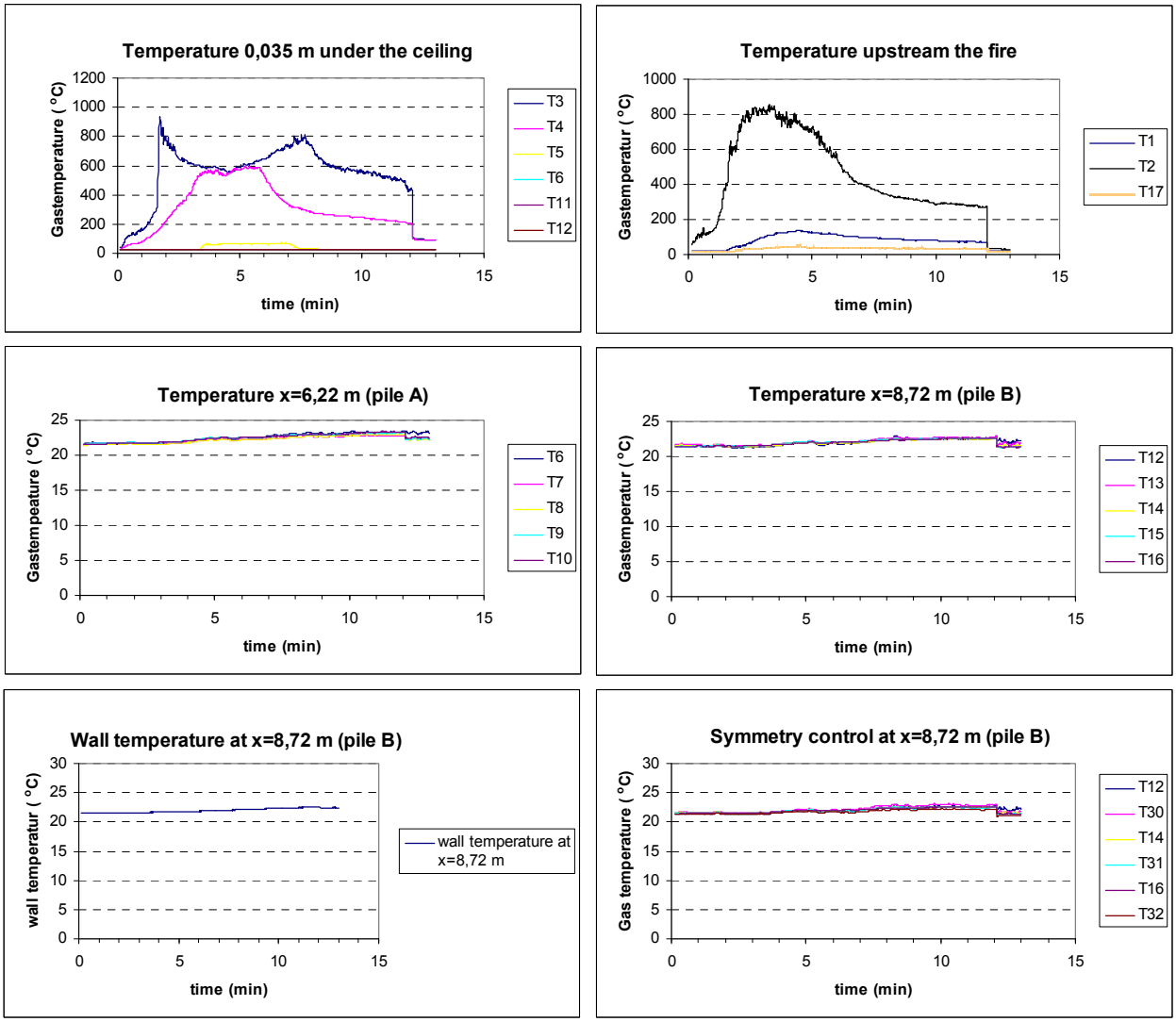

Figure A10 Measured temperatures in Test 5.

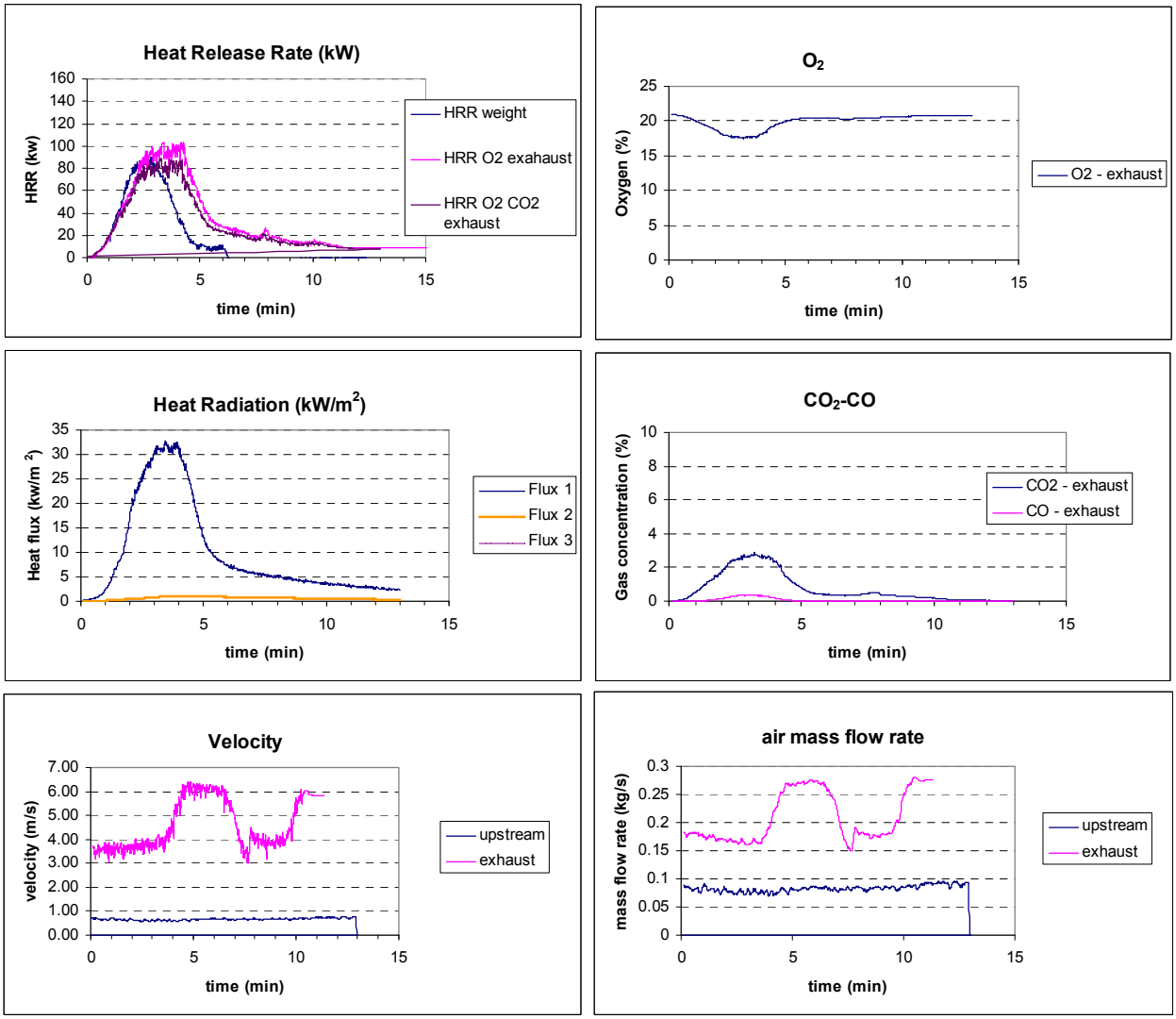

Figure A11 Measured energy released of the initial wood crib, gas concentrations, heat fluxes and air flow in Test 6.

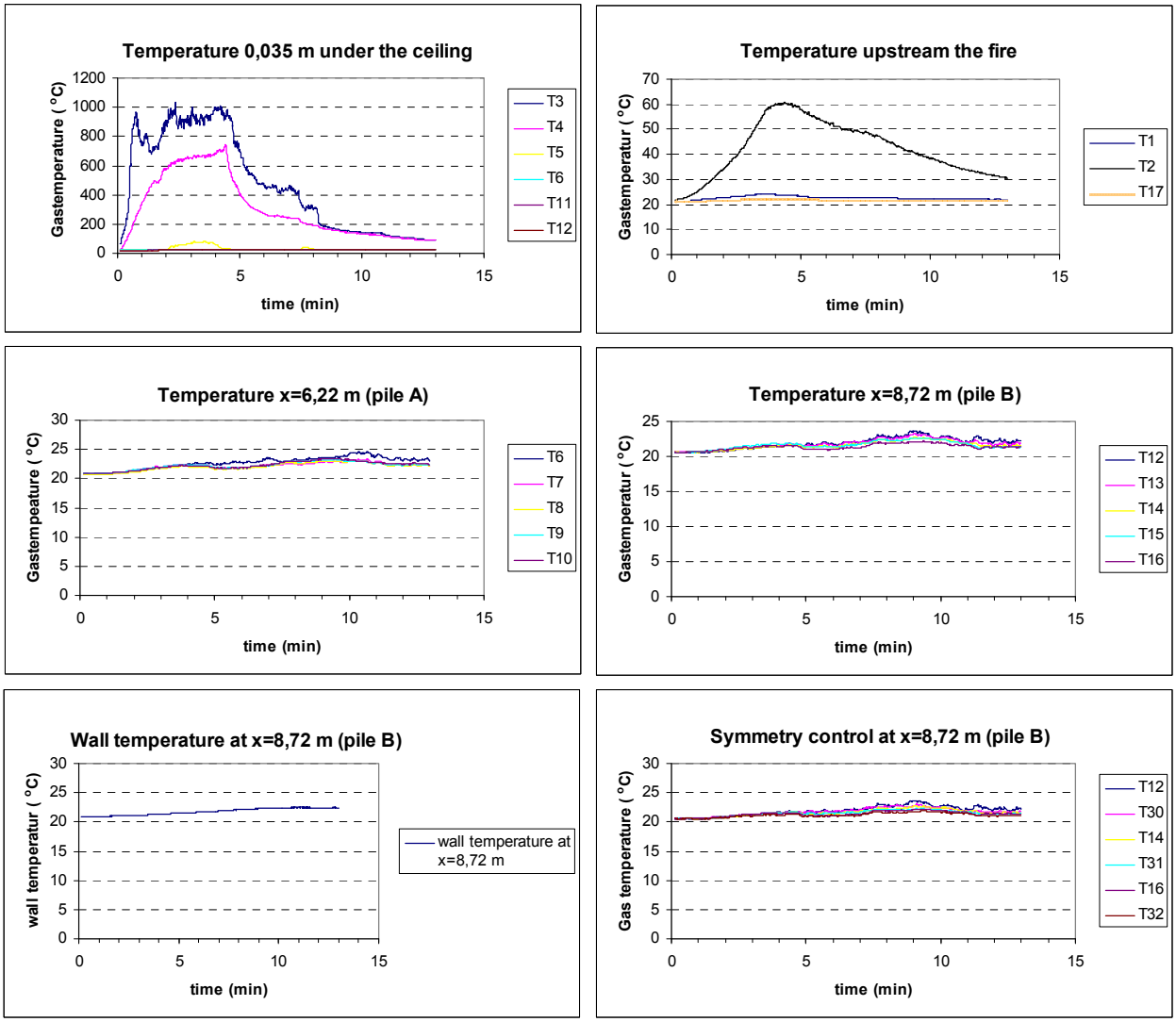

Figure A12 Measured temperatures in Test 6.

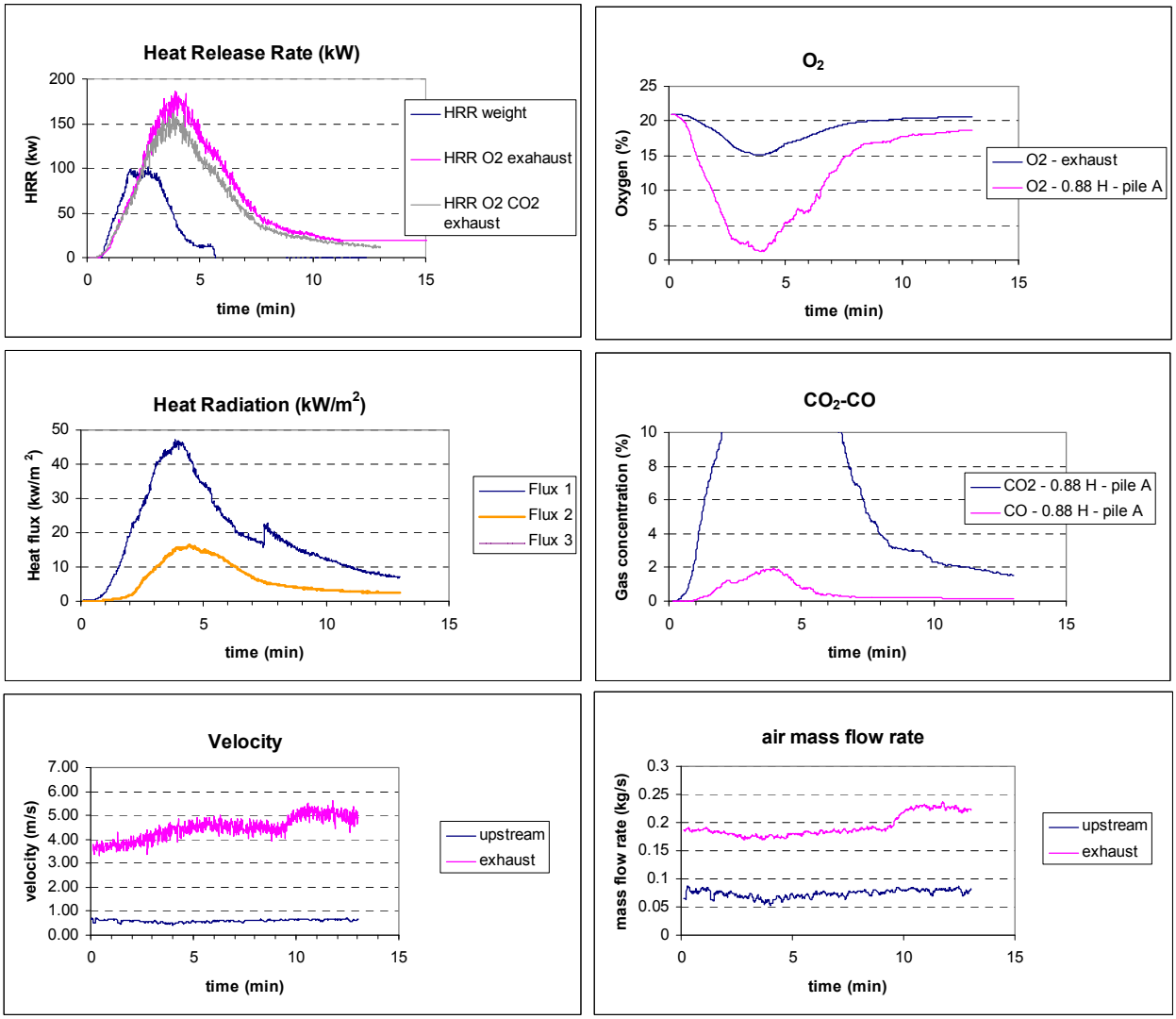

Figure A13 Measured energy released of the initial wood crib, gas concentrations, heat fluxes and air flow in Test 7.

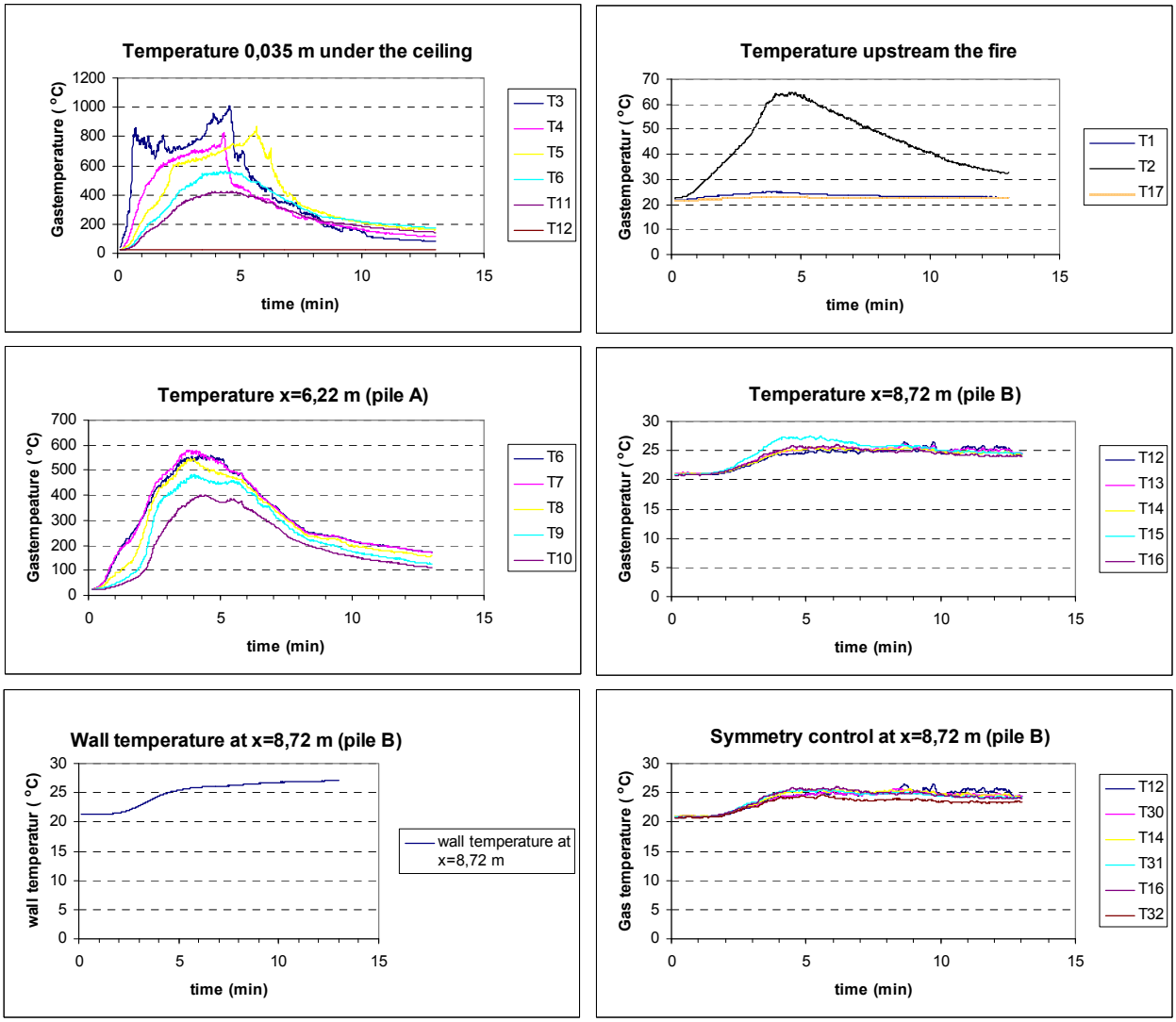

Figure A14 Measured temperatures in Test 7.

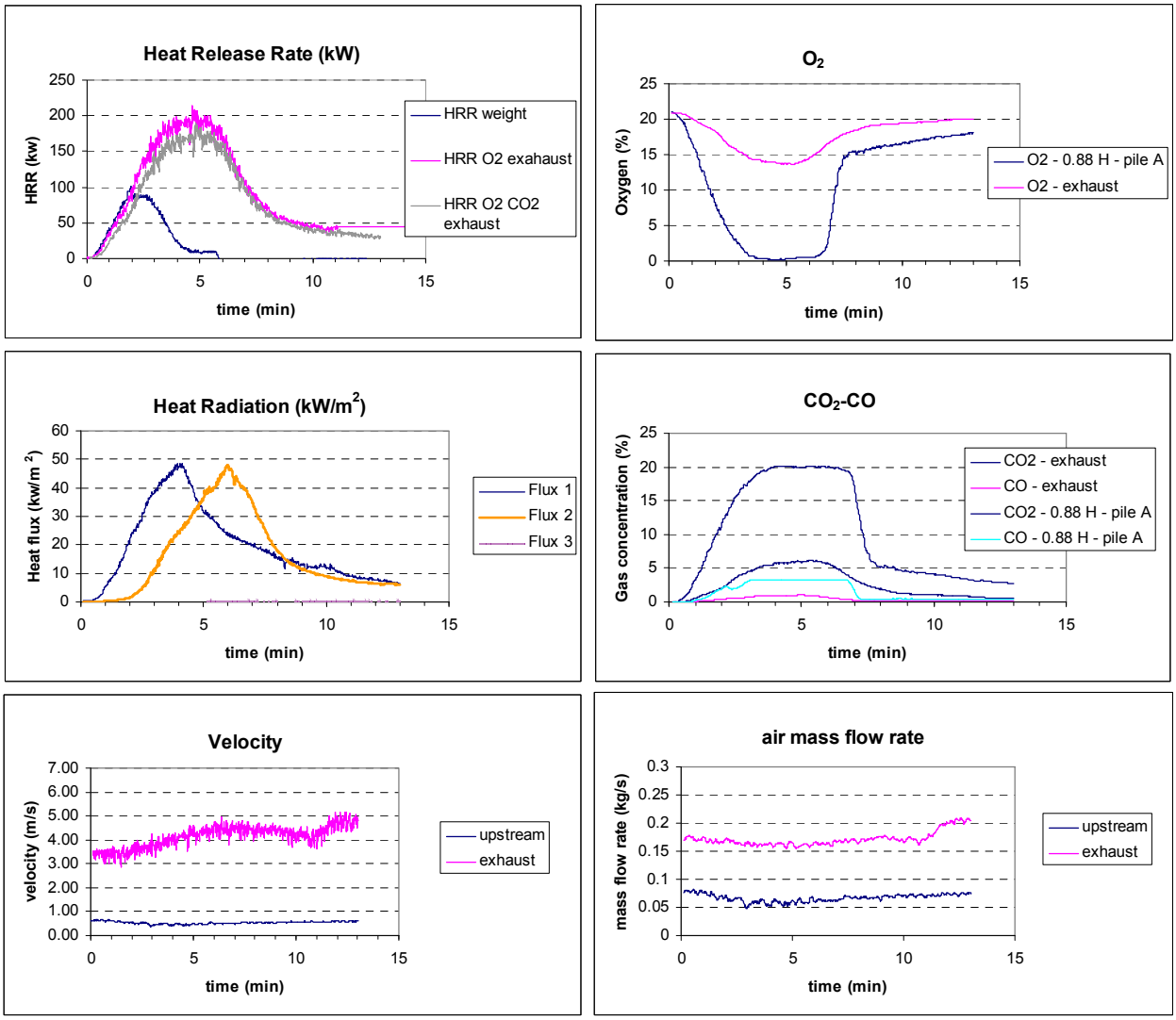

Figure A15 Measured energy released of the initial wood crib, gas concentrations, heat fluxes and air flow in Test 8.

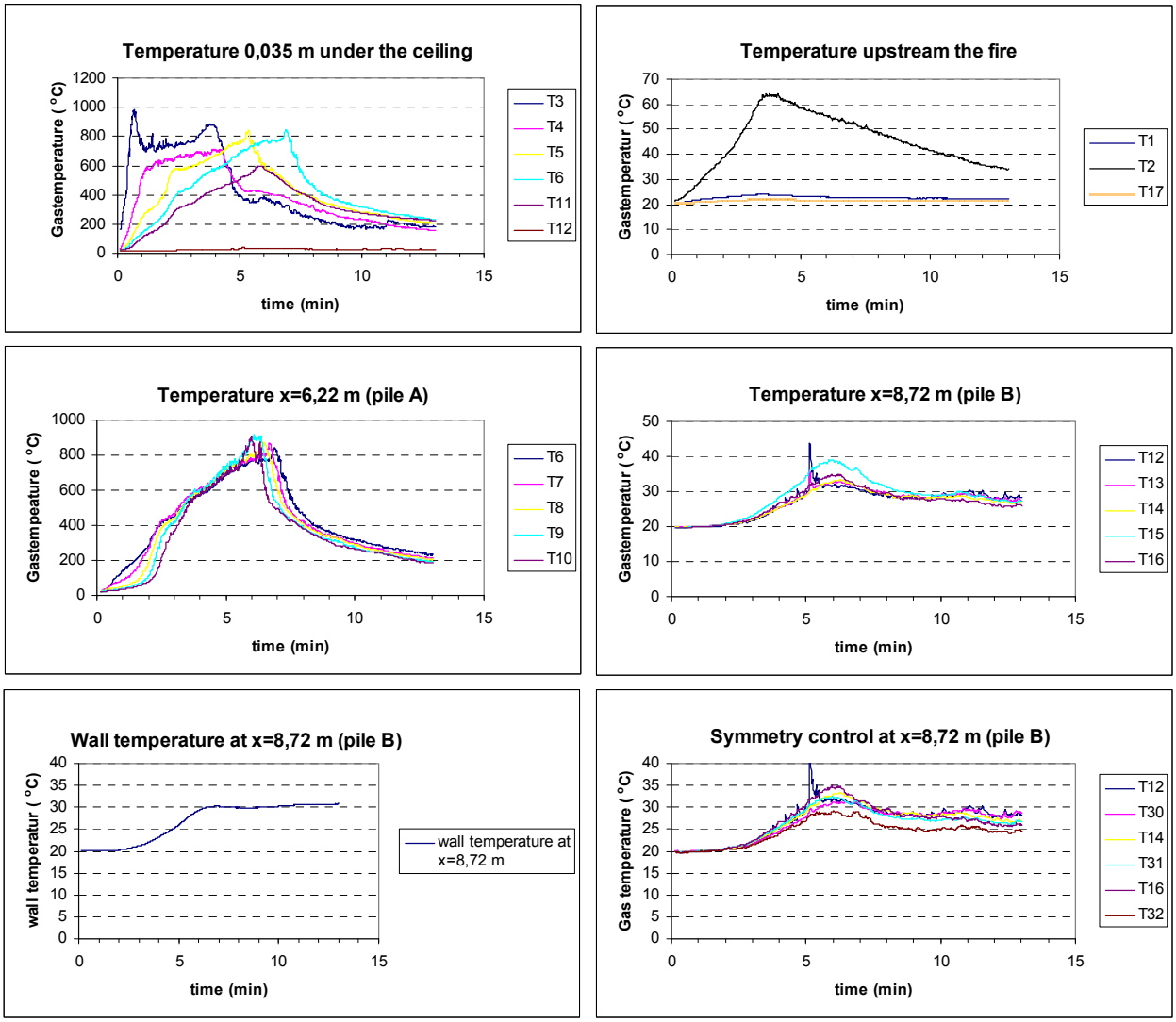

Figure A16 Measured temperatures in Test 8.

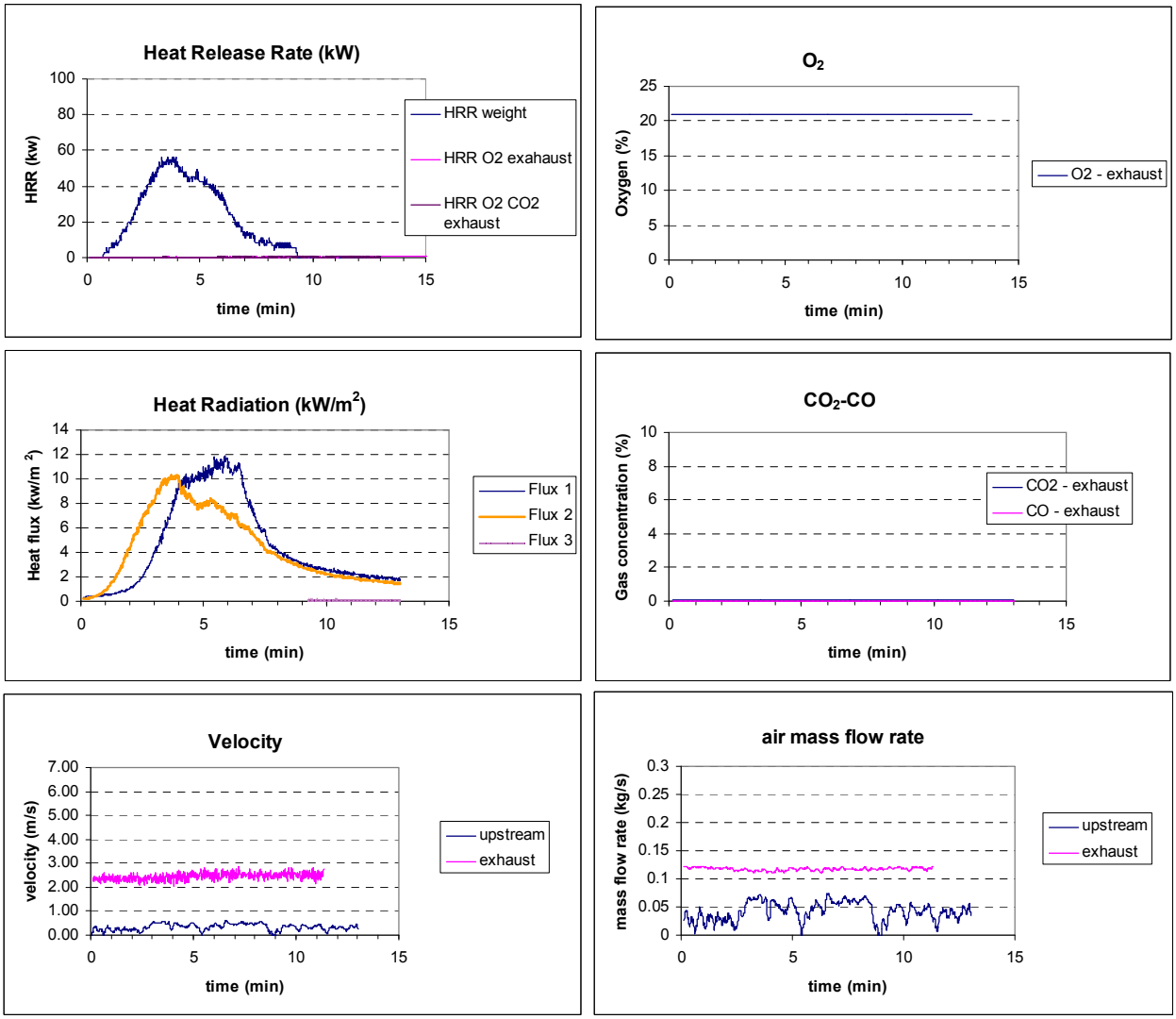

Figure A17 Measured energy released of the initial wood crib, gas concentrations, heat fluxes and air flow in Test 9.

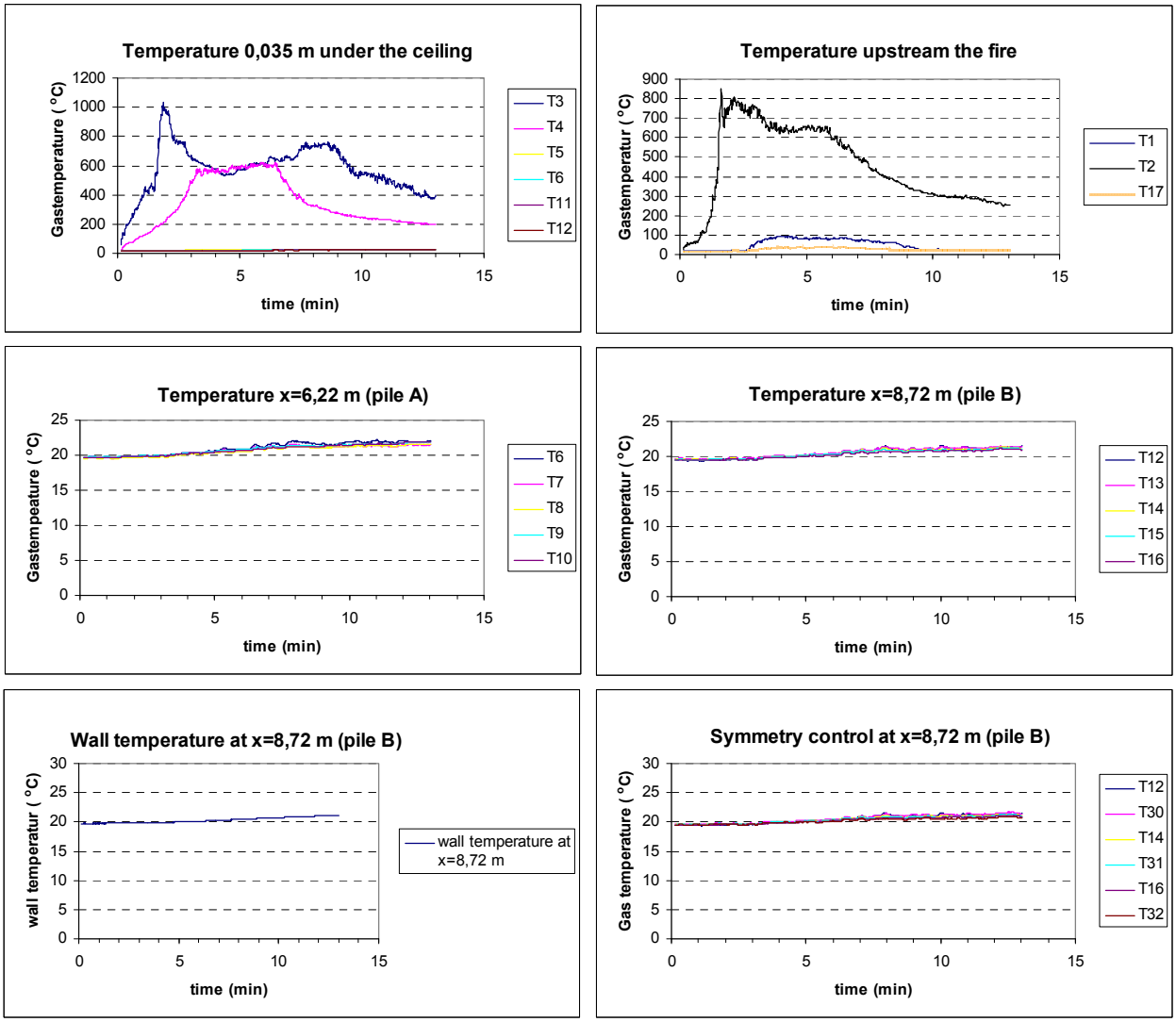

Figure A18 Measured temperatures in Test 9.

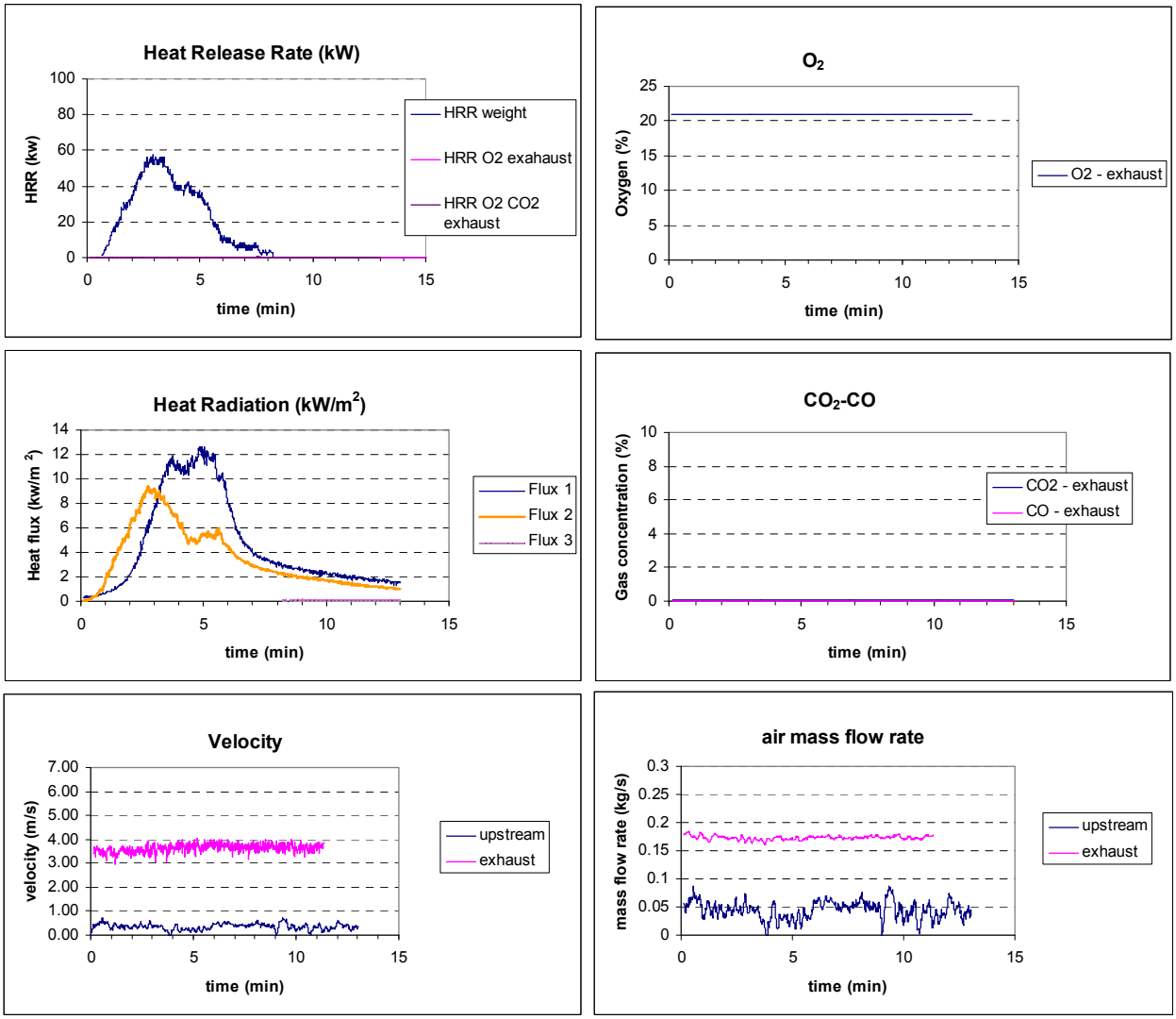

Figure A19 Measured energy released of the initial wood crib, gas concentrations, heat fluxes and air flow in Test 10.

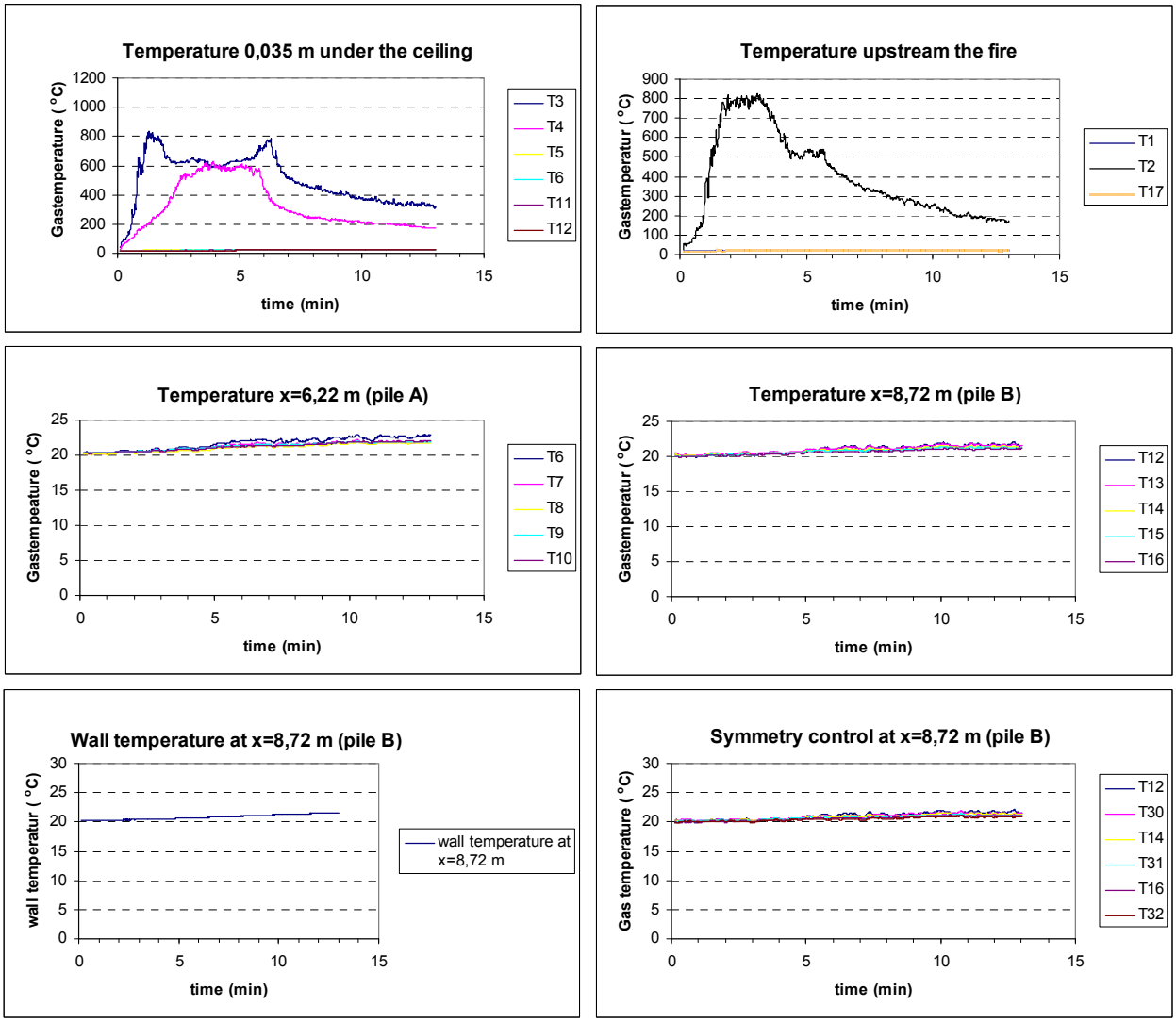

Figure A20 Measured temperatures in Test 10.

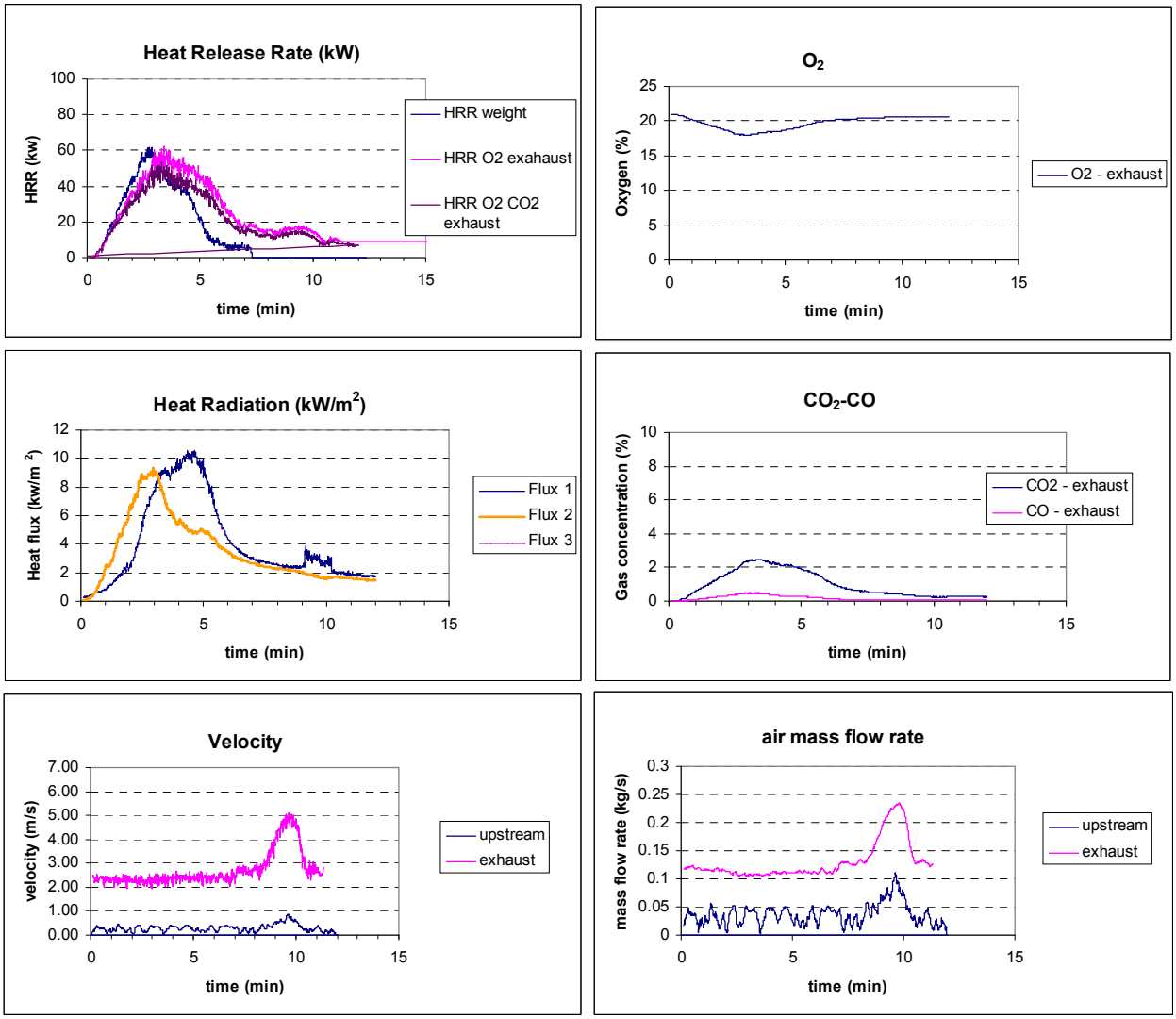

Figure A21 Measured energy released of the initial wood crib, gas concentrations, heat fluxes and air flow in Test 11.

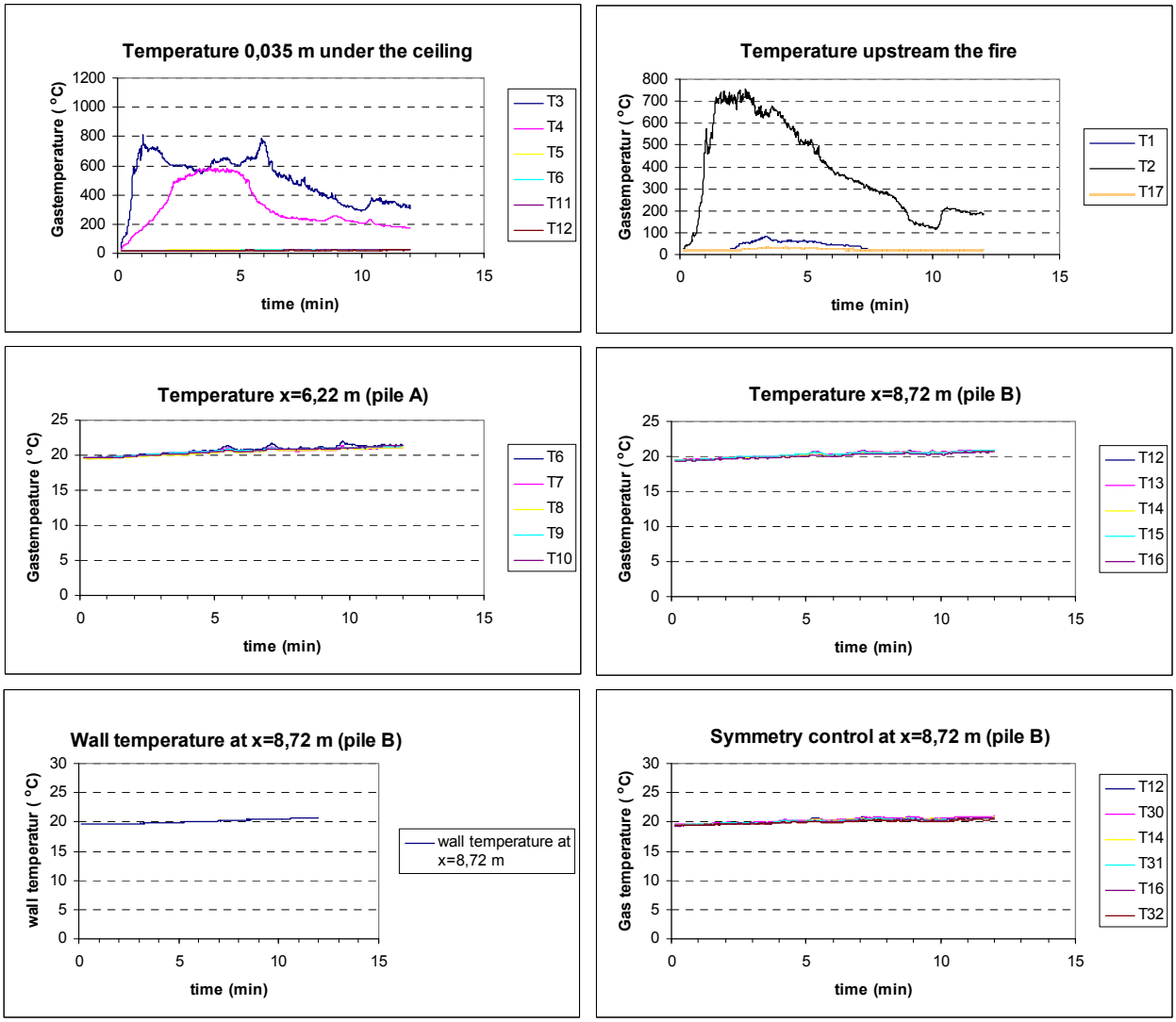

Figure A22 Measured temperatures in Test 11.

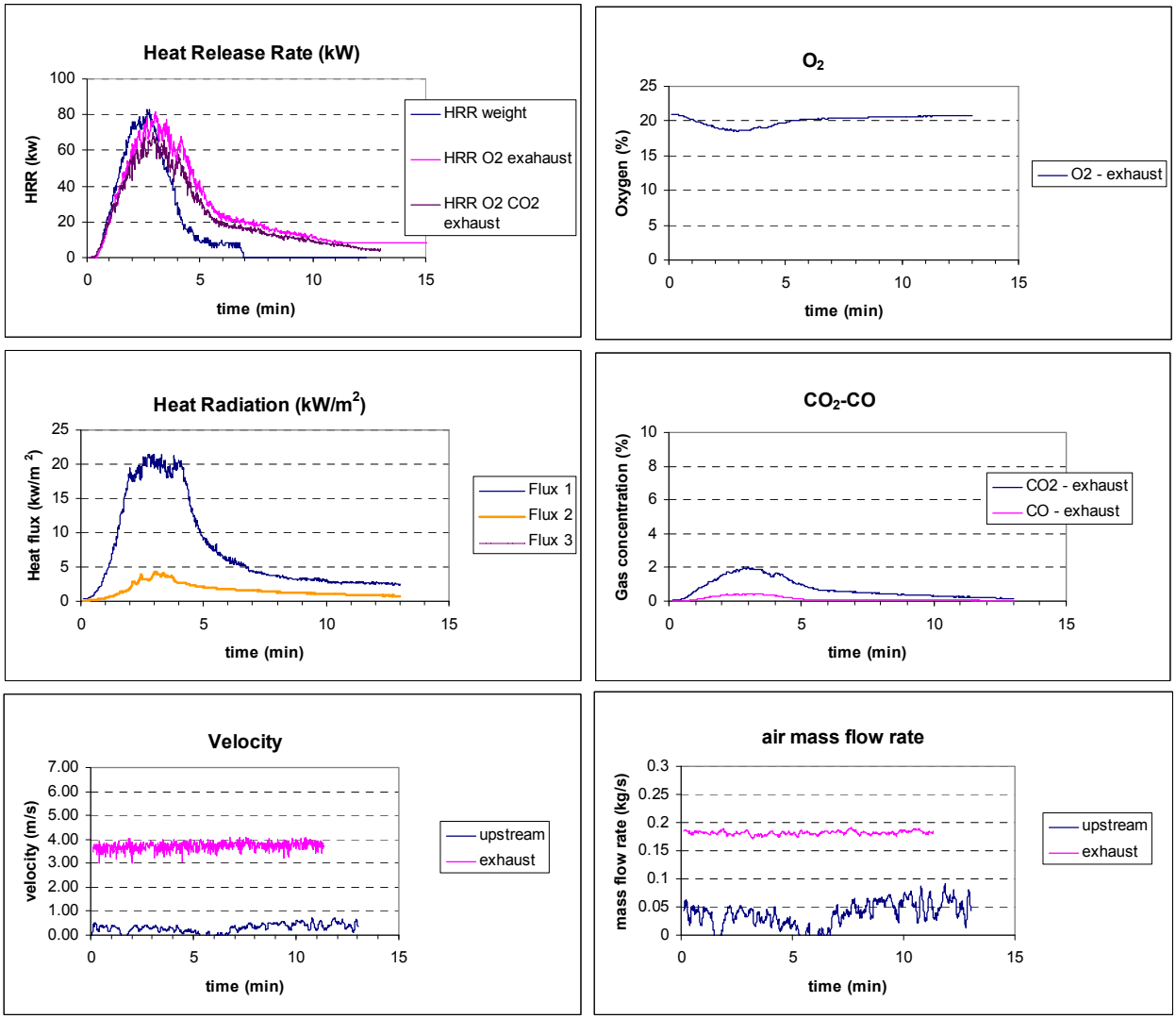

Figure A23 Measured energy released of the initial wood crib, gas concentrations, heat fluxes and air flow in Test 12.

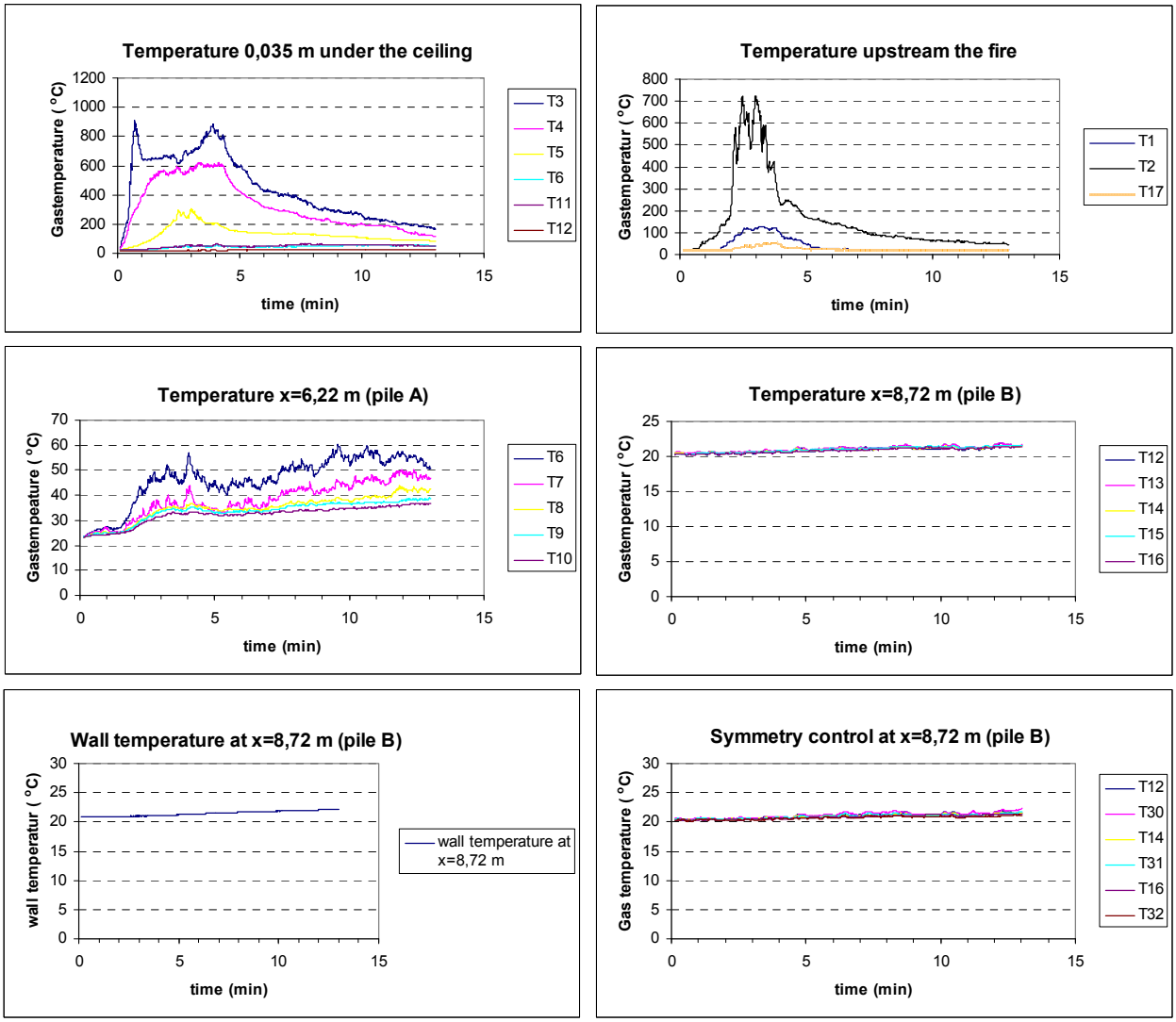

Figure A24 Measured temperatures in Test 12.

SP Technical Research Institute of Sweden develops and transfers technology for improving competitiveness and quality in industry, and for safety, conservation of resources and good environment in society as a whole. With Sweden's widest and most sophisticated range of equipment and expertise for technical investigation, measurement, testing and certification, we perform research and development in close liaison with universities, institutes of technology and international partners.

SP is a EU-notified body and accredited test laboratory. Our headquarters are in Borås, in the west part of Sweden.

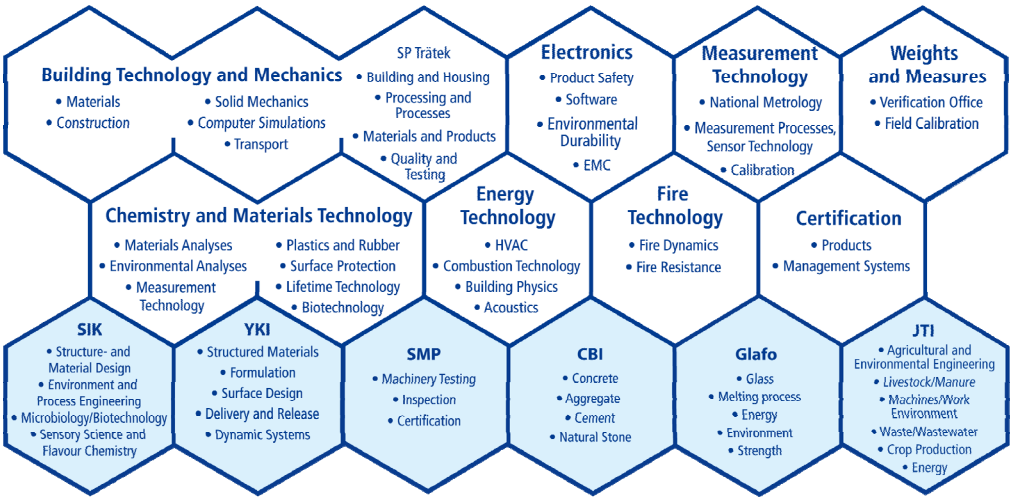

SP consists of eight technology units and six subsidiary companies. Three of the companies, CBI, Glafo and JTI are each 60 % owned by SP and 40 % by their respective industries.

SP Technical Research Institute of Sweden
Box 857, SE-501 15 BORÅS, SWEDEN
Telephone: +46 10 516 50 00, Telefax: +46 33 13 55 02
E-mail: info@sp.se, Internet: www.sp.se
www.sp.se

Fire Technology
SP Report 2010:03
ISBN 978-91-86319-38-0
ISSN 0284-5172